

Lunar Telescope Facility

Final Design Report

Mark S. Avnet
Gautier Brunet
Justin M. Colson
Phillip M. Cunio
Tamer Elkholy
Bryan Gardner
Takuto Ishimatsu
Richard Jones

Jim Keller
Zahra Khan
Ryan Odegard
Jeff Pasqual
Jaime Ramirez
Timothy Sutherland
Chris Tracy
Chris Williams

Table of Contents

TABLE OF CONTENTS	0
LIST OF FIGURES.....	2
LIST OF TABLES.....	6
ABSTRACT	8
1. INTRODUCTION	9
1.1 THE LUNAR ENVIRONMENT	9
1.2 OTHER CONSIDERATIONS	12
2. EXISTING AND PROPOSED TELESCOPES	14
2.1 EXISTING MAJOR SPACE TELESCOPE DESIGNS	14
2.2 PROPOSED LUNAR SURFACE TELESCOPE CONCEPTS.....	17
2.3 PROPOSED FREE-SPACE TELESCOPE CONCEPTS.....	20
3. STAKEHOLDER ANALYSIS	21
3.1 STAKEHOLDER IDENTIFICATION	21
3.2 N ² REPRESENTATION OF STAKEHOLDER FLOWS	22
3.3 ESTIMATES OF RESOURCE FLOWS.....	23
3.4 STAKEHOLDER VALUE DELIVERY NETWORK MODEL.....	25
3.5 IMPORTANT LOOPS IN THE STAKEHOLDER VALUE DELIVERY NETWORK	26
4. SCIENCE GOALS	28
4.1 NEEDS AND GOALS	28
4.2 CANDIDATE SCIENTIFIC PROGRAMS	28
4.3 RANKING OF SCIENCE OBJECTIVES	29
5. BROAD SYSTEM REQUIREMENTS.....	35
6. CONCEPT DEVELOPMENT METHODOLOGY.....	38
6.1 INITIAL FORMULATION OF CONCEPT SPACE	38
6.2 OBJECT-PROCESS METHODOLOGY DIAGRAM AND CONCEPT SPACE MATRIX	39
6.3 EXISTING CONCEPT INVESTIGATIONS	45
6.4 CONCEPT DOWNSELECTION CYCLES	46
7. LUNAR INTERFEROMETRIC RADIO ARRAY (LIRA).....	48
7.1 APPROACH AND ASSUMPTIONS.....	48
7.2 INSTRUMENTATION AND RADIO ARRAY	56
7.3 ELECTRONICS SUBSYSTEM	61
7.4 POWER SUBSYSTEM.....	62
7.5 CLUSTER STRUCTURE SUBSYSTEM	65
7.6 COMMUNICATIONS SUBSYSTEM.....	67
7.7 TRANSPORTATION SUBSYSTEM.....	74
7.8 DEPLOYMENT SUBSYSTEM	76
7.9 TRADE STUDY AND OPTIMIZATION.....	82
8. LUNAR INFRARED MODULAR INTERFEROMETRIC TELESCOPE (LIMIT).....	86
8.1 APPROACH AND ASSUMPTIONS.....	86

8.2 INSTRUMENTATION AND INTERFEROMETRIC ARRAY	93
8.3 ELECTRONICS SUBSYSTEM	100
8.4 POWER SUBSYSTEM.....	101
8.5 STRUCTURE SUBSYSTEM.....	103
8.6 THERMAL CONTROL SUBSYSTEM	106
8.7 COMMUNICATIONS SUBSYSTEM.....	115
8.8 TRANSPORTATION, DEPLOYMENT, AND SERVICING SUBSYSTEMS	117
8.9 DUST MITIGATION	126
9. COST ESTIMATION AND SPREADING	130
9.1 TELESCOPE COST ESTIMATION	130
9.2 LIRA COST ESTIMATION	130
9.3 LIMIT COST ESTIMATION	133
9.4 SOFTWARE AND GROUND SEGMENT DEVELOPMENT COST.....	137
9.5 ARES V TRANSPORTATION COSTS	137
9.6 OPERATING COSTS.....	138
9.7 COST SPREADING.....	138
9.8 CUMULATIVE COST SPREADING	141
10. FUTURE WORK.....	143
10.1 FURTHER DESIGN TRADES	143
10.2 OTHER FUTURE DEVELOPMENT.....	145
11. CONCLUSION	146
ACKNOWLEDGMENTS.....	147
REFERENCES	148
APPENDICES.....	153
APPENDIX A: CONTRIBUTORS OF NEW MATERIAL BY SECTION	153
APPENDIX B: AN ANALYSIS OF TEAM INTERACTIONS	154

List of Figures

Figure 1. Earth as seen from the lunar surface.....	9
Figure 2. Earth’s atmospheric opacity for different wavelengths.....	11
Figure 3. The Hubble Space Telescope	14
Figure 4. The James Webb Space Telescope.....	15
Figure 5. The Spitzer Space Telescope.....	15
Figure 6. The Herschel Space Telescope.....	16
Figure 7. The SAFIR observatory.....	16
Figure 8. The Terrestrial Planet Finder telescope.....	17
Figure 9. Conceptual design for the Large Lunar Telescope.....	18
Figure 10. Artist’s rendition of a liquid mirror telescope on the Moon.....	19
Figure 11. A lunar interferometer concept.....	19
Figure 12. A radio telescope on the Moon uses a crater to support its large primary dish.....	20
Figure 13. Major stakeholders in the design and development of a lunar telescope.	21
Figure 14. N ² diagram indicating the types of flows between stakeholders.	22
Figure 15. N ² diagram indicating the importance of each flow between stakeholders.....	23
Figure 16. Rate of publication of papers using Hubble data.....	24
Figure 17. Cost and speed of observation for instruments on the Hubble Space Telescope	25
Figure 18. Stakeholder value delivery network model.	26
Figure 19. The most important loop in the stakeholder value delivery network.	27
Figure 20. Public outreach flows.	27
Figure 21. Relative strength of six candidate science programs.....	33
Figure 22. Concept development process.	38
Figure 23. Object-Process Methodology description of telescope design.....	40
Figure 24. Concept tree for segmented reflecting telescopes.	46
Figure 25. Exemplar Pugh matrix for Far-IR telescopes.....	47
Figure 26. N ² diagram of the major relationships between parameters	48
Figure 27. All important technical parameters in the LIRA telescope design.....	49

Figure 28. Lunar noise attenuation from the lunar far side.....	52
Figure 29. Lunar polar sunlight illumination fraction	53
Figure 30. Noise attenuation utility.	54
Figure 31. Illumination and utility versus angle.	54
Figure 32. Angular resolution utility.	54
Figure 33. Component masses.	55
Figure 34. Utility versus angular resolution.	56
Figure 35. Folded LIRA cluster.	66
Figure 36. Deployed LIRA cluster.....	66
Figure 37. LIRA communications systems cost and size scaling	68
Figure 38. Interior communications system arrangement.....	70
Figure 39. Relay subsystem.	70
Figure 40. Total system view.....	71
Figure 41. Storable mode, front and top views	72
Figure 42. Partially-deployed standing mode.	72
Figure 43. Fully-deployed relay.....	73
Figure 44. Relay optical package.....	73
Figure 45. Artist’s conception of the Ares V launch vehicle.....	74
Figure 46. Artist’s conception of NASA’s Lunar Surface Access Module.....	75
Figure 47. NASA’s unpressurized rover concept	76
Figure 48. Notional view of array deployment.....	78
Figure 49. Notional view of communications relay deployment.....	79
Figure 50: Scientific Figure Of Merit/Cost trade study surface.	83
Figure 51. Sensitivity of LIRA.	84
Figure 52. Angular resolution of LIRA.	85
Figure 53: Hybrid IR telescope design.	86
Figure 54. Stars with exoplanets seen by Spitzer.	91
Figure 55. Star with an exoplanet.	91
Figure 56. Baseline configuration for LIMIT concept.....	94

Figure 57: The final layout of the ARGOS optical train	95
Figure 58: Beam combining layout for LIMIT beam combiner.....	95
Figure 59: A sparse-aperture telescope implemented with twelve separate focal telescopes feeding a common beam combiner	96
Figure 60. Existing telescope comparison of angular resolution.....	96
Figure 61. Point Spread Function for a Golay-3 configuration.	97
Figure 62. Point Spread Function for a Golay-9 configuration.	98
Figure 63. Comparison of SNR to a single telescope of equivalent diameter	98
Figure 64. Required increase in imaging time for a sparse array.	99
Figure 65. Conceptual design of LIMIT unit telescope.....	103
Figure 66. Mount concept consisting of hollow aluminum honeycomb	104
Figure 67. Simplified mount structure for analysis.	105
Figure 68. Finite element von Mises stress analysis.....	106
Figure 69. Surface temperature for lunar craters at three latitudes;.....	109
Figure 70. Mirror temperature and longest observed wavelength	110
Figure 71. Radiation model for emissivity relationship to temperature.	111
Figure 72. Temperature variation with effective MLI	112
Figure 73. Model to determine the time required	113
Figure 74. Transient results for radiative cooling to sky.	113
Figure 75. Helium cooling concept for initial deployment of telescopes.	113
Figure 76. Transient temperature of He-cooled temperature and amount of He required.....	114
Figure 77. Cost versus downlink data rate.....	116
Figure 78. Cost versus distance from human base.....	116
Figure 79. Communications system overview.....	117
Figure 80. Moon base at the lunar south pole.	118
Figure 81. Telescope location.	119
Figure 82. Ares V (CaLV).	119
Figure 83. Lunar Surface Access Module (LSAM).....	120
Figure 84. Crew/rover-assisted deployment.	120

Figure 85. ATHLETE rover.....	121
Figure 86. Deployment process.	123
Figure 87. Repair process.	125
Figure 88. Lunar dust grain.....	126
Figure 89. Transient temperature of dust grain incident on a LIMIT telescope mirror.....	128
Figure 90. Smoothed surface of sintered lunar dust.	129
Figure 91. Concept for lunar lawn mower for microwave regolith sintering.	129
Figure 92. Effect of number of dipoles on total system cost	132
Figure 93. Effect of number of telescope elements on total system cost.....	136
Figure 94. Spreading of the \$1.987 billion development cost for LIRA.	139
Figure 95. Spreading of the \$1.631 billion development cost for LIMIT	140
Figure 96. Cumulative cost spreading of \$1.987 billion development cost for LIRA.....	141
Figure 97. Cumulative cost spreading of \$1.631 billion development cost for LIMIT.....	142

List of Tables

Table 1. Estimated Vehicle Parameters for Telescope.	12
Table 2. Importance of each stakeholder.	22
Table 3. Example of stakeholder value metrics for NASA and the media.	30
Table 4. Derived stakeholder utility scores for each science objective.	31
Table 5. Expected level of strength for each stakeholder value loop.	32
Table 6. Expected strength of each stakeholder value loop for science objective AGN.	33
Table 7. Level 0 and Level 1 requirements.	35
Table 8. Detailed concept space matrix.	40
Table 9. Requirements for LIRA.	49
Table 10. Optimal value ranges.	56
Table 11. Command & data handling parameters for LIRA.	62
Table 12. Power subsystem constants.	63
Table 13. Final power subsystems design values (solar-powered).	65
Table 14. High-flow and low-flow data systems.	69
Table 15. Relay properties.	74
Table 16. Rover energy requirements and battery mass.	81
Table 17. Requirements for IR interferometer.	87
Table 18. Optical parameters of Optical Units.	93
Table 19. Metrics for LIMIT power system.	101
Table 20. Space IR telescope wavelengths and temperatures.	110
Table 21. System components to be transported.	122
Table 22. Deployment time estimate.	124
Table 23. Typical human activities and maximum ranges.	128
Table 24. Subsystem mass and cost breakdown for the LIRA concept.	130
Table 25. Total transportation cost for the LIRA concept.	131
Table 26. Subsystem mass and cost breakdown for the LIMIT.	133
Table 27. Total transportation cost for the LIMIT concept.	133

Table 28. Research and development cost multipliers for various LIMIT telescope subsystems.135

Abstract

The National Aeronautics and Space Administration (NASA) has outlined plans to return humans to the Moon by the year 2020. Because of the inherent advantages to performing astronomy from the lunar surface, the Moon has long been envisioned as a possible site for a space telescope. With the most recent lunar plans serving as a motivation and basis for re-consideration of the Moon as the location of an astronomical observatory, this report provides a thorough investigation into the design of a lunar telescope facility.

An overview of features of the lunar surface relevant to a telescope is provided. A literature review gives the context in which a lunar telescope facility is considered. This context includes previous ideas for telescopes on the Moon and concepts for other space telescopes (both existing and planned).

Using the 2001 National Research Council Astronomy and Astrophysics Decadal Survey as a principal reference, the science goals for the next generation of space telescopes are enumerated and ranked based on an analysis of the relevant stakeholders. This methodology develops a value delivery network model and ranks the relative importance of the key stakeholders and key flows in the network. Features of the network, such as the historical values of important flows and the role of the media in key loops, are also noted. The stakeholder value delivery network is then used to perform a utility analysis of the six candidate broad science objectives. This analysis informs the subsequent telescope concept enumeration and downselection.

A methodology developed for concept downselection consists of: 1) elucidating the full concept space via the use of a design space matrix, 2) narrowing the concepts down via a tree method of isolating attractive options from the design space matrix, and 3) selecting the best of these concepts using the quantitative ranking techniques of Pugh analysis, with the results of the stakeholder analysis informing the downselection process. Through this methodology, a comprehensive architecture space of 6048 possible concepts is narrowed to just two, which are then developed in detail for use as reference designs.

Specific trades emerge as the two reference designs are matured, and detailed investigations lead to development of the subsystems. The subsystems analyzed include instrumentation, electronics, power, structures, thermal, communications, and transportation/deployment. Cost, mass, and power figures for all these systems are calculated, as are subsystem and overall costs for each design. Recommendations are also made to help identify the areas that should require further study and research.

The results of this study show how two potential space telescope concepts are uniquely enabled by returning to the Moon, both of which would provide scientific output beyond anything that has before been possible. The Lunar Interferometric Radio Array (LIRA), is a large array of radio-frequency dipoles located on the far side of the Moon, where shielding from radio noise created by Earth would allow unsurpassed sensitivity to regions of the radio spectrum never observed. The Lunar Infrared Modular Interferometric Telescope (LIMIT), is an interferometric array of 85-cm infrared (IR) apertures located in the cold Shackleton Crater at the lunar south pole. The long and stable baselines of this array would achieve an angular resolution better than any existing or proposed IR telescopes. Both of these telescope designs would greatly benefit from, and provide scientific motivation for, returning to the Moon, and they would serve to look at our universe at wavelengths that until now have had only limited study.

1. Introduction

This study into a lunar telescope facility was conducted by members of the Space Systems Engineering class (16.89/ESD.352) at the Massachusetts Institute of Technology in the spring of 2007. The challenge of the class was to design a lunar telescope facility that would deliver the most scientific value, while leveraging the proposed crewed lunar transportation architecture and ensuring both technical and budgetary feasibility. The approach to this challenge is outlined in this report, and two final design proposals are presented that meet these goals.

The initial specification for the proposed Lunar Telescope Facility was to create a lunar telescope, with consideration of location including points on the surface of the Moon, as well as points in space near the Moon, or at a Lagrange point between the Earth and the Moon or the Earth and the Sun. Due to the need for new telescopes to advance the state of the art beyond previous designs, telescopes in Low Earth Orbit (LEO) were initially discounted as possible design goals, although they provide a useful context for later phases of the design.

1.1 The Lunar Environment

Although the Moon was one of the first objects at which Galileo pointed his early telescopes, it was not until the middle of the 20th century that the idea of putting a telescope on the Moon was conceived. While some of the earliest ideas of the time required people to build and run the observatory (even manually changing on the photographic plates and looking through the eyepiece), many advantages of the lunar surface remain the same for more modern telescope concepts [1].

The results of a literature search illustrate the major features of the lunar surface, and their potential as arguments for and against the development and deployment of a lunar telescope. The discussion draws heavily upon a comprehensive discussion put forth by Lester et al. [2].



Figure 1. Earth as seen from the lunar surface.

1.1.1 Advantages and disadvantages of a lunar surface location

The major features of the lunar surface are detailed here, with relevant information for telescopes given. Potential advantages and disadvantages are also noted.

- Feature: Low temperatures
Cold temperatures are reached on the Moon, particularly the lunar poles where limited incident light arrives from the Earth and the Sun. Crater floors at the poles with no direct line-of-sight to either body could potentially create a naturally cold environment, with ambient temperatures around 40-50 K. This is optimal for IR telescopes, which otherwise must be actively cooled.
- Feature: Radio quiet
The far side of the lunar surface is shielded from terrestrial radio interference, both man-made and naturally occurring. On Earth, the ionosphere also blocks much of the radiation coming in at radio frequencies of interest. Modern radio interference mitigation techniques, which can be implemented at lunar distances in free space, deliver similar levels of shielding from interference effects, although the costs are higher.
- Feature: Lifetime
The lunar surface is a stable location that carries no inherent cost for maintaining telescope position and orientation once deployed. This is opposed to free-space telescopes, which have finite levels of cryogenics for active cooling and a limited amount of propellant for station-keeping.
- Feature: Solid surface
The lunar surface provides a stable foundation for deploying interferometers with a range of baselines. Free-space interferometers have been conceived, but precise formation flying at large baseline distances has not yet been demonstrated in space, and the truss structure required for formation flying at smaller baseline distances may be prohibitive. A possible drawback of the lunar surface is the presence of dust. Lunar dust presents a contamination hazard for optics and could impede mechanical system performance. See Section 8.9 for a discussion of possible means for mitigation of lunar dust issues.
- Feature: Gravity
Lunar gravity enables the design and deployment of liquid mirror telescopes, which offer huge collecting areas for zenith surveys (large liquid mirrors cannot be achieved on Earth due to wind effects on the surface). A disadvantage of telescopes on the Moon is they would require a more substantial structure to withstand the gravitational forces. Working on a solid surface where parts do not float away, however, would be of benefit to astronauts doing deployment or maintenance work.
- Feature: Slow sidereal rate
Slow motion of celestial sphere about lunar sky enables long-duration surveys with less precise guiding.
- Feature: Stable thermal environment
Slower motion of the Sun across the lunar sky creates longer periods of thermal equilibrium, which yields more consistent optical performance. Telescopes in low Earth orbit (LEO) undergo cycles of thermal expansion due

to heating and cooling each orbital period, but free-space telescopes at long distances from Earth (i.e. Lagrange points) are not susceptible to these effects.

- Feature: Absence of substantial atmosphere, magnetic field, orbital debris
Like other free-space telescopes, viewing from outside the Earth's atmosphere opens up regions of the electromagnetic spectrum that are inaccessible from the ground. Absorption of incoming radiation or emission from the atmosphere prevents astronomical observations at certain wavelengths in the IR and RF bands (see Figure 2).

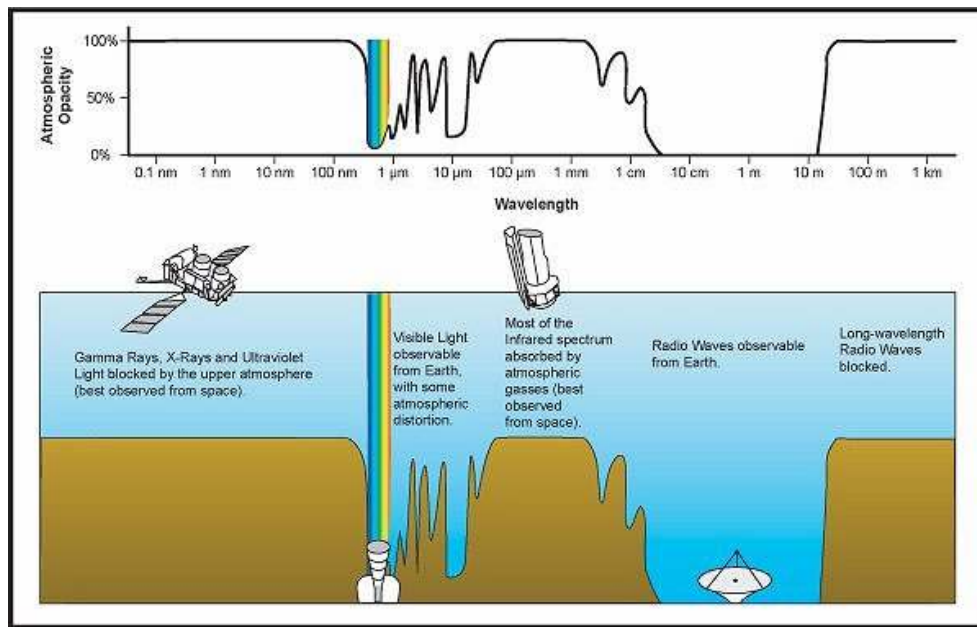


Figure 2. Earth's atmospheric opacity for different wavelengths [3].

1.1.2 Discussion of a lunar surface location

Most of the features of the lunar surface offer equal performance or distinct performance advantages over other possible locations, such as in free space, in Low Earth Orbit, or on the surface of the Earth. However, some disadvantages are inherent in the lunar surface properties already described in Section 1.1.1. Access to crater floors at the lunar poles and structural needs under gravity conditions present challenges for system designers. In addition, lunar dust presents a challenge. Lunar dust issues are not important for free-space locations, although similar issues exist (and have been largely mitigated) on Earth-surface locations. There is also the impact on cost of needing to land mass on the Moon. This, in general, requires more expenditure of propellant than if a telescope remains in free space. Also, provisions would need to be made to ensure the telescope could endure a soft landing on the Moon. A returned human presence on the Moon, however, would supply further impetus and opportunity to capitalize on the advantages of the lunar surface environment.

1.2 Other Considerations

1.2.1 Human spacecraft servicing

Human servicing of spacecraft has proven tremendously successful when viewed in the context of the Hubble Space Telescope (HST) and the International Space Station (ISS).

For the HST, the most important and visible servicing mission was to correct the optics, which were found to be manufactured incorrectly after the HST was initially put in orbit. The successful repair has been one of the most notable achievements in the history of space telescopes. Completed extravehicular activity (EVA) tasks have included installing new scientific instruments and replacing spacecraft components that have failed. In addition to installing new instruments, astronauts have replaced, or are planning to replace, solar panels, control moment gyros, and batteries, which degrade over continuous operations in the Low Earth Orbit environment. The net effect of this servicing has been to increase the on-orbit lifetime of the HST while continually upgrading its scientific capability [4].

While ISS astronauts have occasionally installed scientific experiments during EVA, the bulk of the spacewalks have been devoted to construction and maintenance of the ISS. During construction of the space station, astronauts installed fluid, electrical and structural connections between station elements during their activation. Automated features to perform these functions were ruled out due to envelope restrictions of the launch vehicle and cost considerations [5].

These spacecraft servicing efforts have shown how beneficial human servicing can be for the success of a space project, especially one involving the construction, upgrade, and repair of complex space systems. This should be considered in terms of the proposed long-term presence of humans on the Moon.

1.2.2 Robotic spacecraft servicing

In the aftermath of the Columbia tragedy, the final shuttle servicing mission to the HST was canceled and a number of teams performed studies on the possibility of robotically performing the mission requirements. The University of Maryland developed a concept using mostly developed flight hardware. It utilized a rebuilt propulsion module designed for ISS station-keeping and a robotic servicing module largely built from existing hardware. The propulsion module was flown to perform propulsion, rendezvous, communications power generation, and station-keeping during repair. To perform all the requirements of the last servicing mission, the vehicle parameters shown in

Table 1 were estimated [6].

Table 1. Estimated Vehicle Parameters for Telescope.

Propulsion Module Dry Mass	3000 kg
Robotic Module and Hubble Component Mass	4900 kg
Total Servicing Craft Wet Mass	8500 kg
Launch Cost	\$150M
Total Mission Cost	\$500M

It is important to note that the total cost of the spacecraft does not include the cost of developing the propulsion module and that the estimate was not detailed. Given that there has never been previous robotic servicing of a spacecraft, and given the rough nature of the estimate, the true cost of the mission would likely be significantly higher.

1.2.3 Constellation EVA architecture for zero-g and lunar surface missions

According to NASA's exploration architecture study [7], NASA plans a robust EVA presence on the lunar surface. The planned airlock design will be based in the Lunar Surface Access Module (LSAM) and may have accommodations for up to 3 or 4 astronauts simultaneously. This will enable many lunar surface EVAs.

However, NASA plans a much more limited EVA capability for zero-g beyond the ISS orbit. Current plans for the Crew Exploration Vehicle (CEV) do not include an airlock. Any excursions from the crew capsule would require all crewmembers donning their suits, which have umbilicals for life support, and depressurizing the cabin. These suits are being designed primarily for launch and entry requirements, so it is unlikely that EVA operations would be as easy as with purpose-designed spacesuits.

In the event that the lunar airlock were used in zero-g along with lunar suits, this would require at minimum an Ares V launch to get the LSAM to the desired orbit, as well as some level of redesign to make the airlock functional in zero-g.

Potential EVA operations that could benefit a lunar telescope might be connecting electrical infrastructure between parts of an interferometer to enable beam combining, removing launch restraints from mechanical telescope assemblies, and installing new scientific instruments. The possibility of EVA operations in zero-g from the CEV is negligible. Therefore, staging EVAs beyond the ISS will only be cost-feasible from the lunar surface, unless consideration is given to the adaptation of the existing Constellation architecture.

2. Existing and Proposed Telescopes

A further result of the literature search was a large amount of information on existing telescopes and proposed concepts, both in free space and on the lunar surface, which provide a context for development of the proposed lunar telescope facility. This section presents some of the details of these existing and proposed concepts.

2.1 Existing Major Space Telescope Designs

2.1.1 Hubble Space Telescope

The Hubble Space Telescope, deployed into Low Earth Orbit in 1990, has arguably been the most successful of the space telescopes launched as part of NASA's Great Observatories program. Its 2.4-m diameter primary mirror observes over near-infrared, visual, and UV wavelengths. It was designed to be human-serviceable and has been serviced in orbit 4 times, with a 5th and final servicing mission planned for early 2008. The final servicing mission will extend its life until at least 2013. The HST has been a fantastic success, expanding our understanding of star birth, star death, and galaxy evolution, and helping move black holes from scientific theory to fact. In addition, the HST has garnered a great deal of public support with the release of many captivating images that are immensely popular the world over. The HST required \$2 billion in development costs and has an operations cost of \$452 million per year [8].



Figure 3. The Hubble Space Telescope [8].

2.1.2 James Webb Space Telescope

The James Webb Space Telescope (JWST), planned to start operating around the time when the HST reaches the end of its life, is NASA's next major space telescope. The JWST, operating at near- and mid-infrared wavelengths, will be deployed at the second Earth-Sun Lagrange point, 1.5 million km from Earth.

With a primary mirror 6.5 m in diameter, JWST will have a collecting area seven times that of Hubble, and will achieve four primary astronomical objectives: identification of the first bright objects that formed in the early universe, determination of how galaxies and dark matter evolved to the present day, study of the birth and early development of stars and solar systems, and understanding the physical and chemical properties of solar systems where building blocks of life may be present. Current cost estimates for the James Webb put it around \$3.5 billion [9].

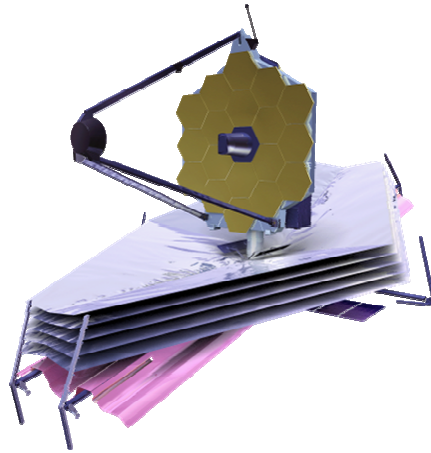


Figure 4. The James Webb Space Telescope [9].

2.1.3 Spitzer Space Telescope

The Spitzer Space Telescope, formerly known as the Space Infrared Telescope Facility (SIRTF), is the element in NASA's suite of Great Observatories that operates in the mid- to far-IR wavelengths, where it serves to study astronomical targets including the brown dwarfs, the early universe, protoplanetary and planetary debris disks, and active galactic nuclei. Located in a heliocentric, Earth-trailing orbit, the Spitzer Space Telescope can conduct both imaging and spectroscopy, and its 85-cm aperture produces 5 x 5 arcminute exposures. This is the state of the art facility for IR astronomy, and cost around \$700 million to develop [10].



Figure 5. The Spitzer Space Telescope [10].

2.1.4 Herschel Space Telescope

Slated for a July 2008 launch aboard an Ariane-5, the three-year mission for the Herschel Space Telescope at the Earth-Sun L2 point will conduct astronomical science into the far-IR spectrum. Jointly launched with the Planck science mission at an estimated cost of \$2 billion, the 3.5-m primary mirror will enable the study of the formation of galaxies in the early universe, the creation of stars, the chemical composition of the atmospheres and surfaces of comets, planets, and satellites, and the molecular chemistry of the universe [11].



Figure 6. The Herschel Space Telescope [11].

2.1.5 Single Aperture Far-IR Observatory

The Single Aperture Far-IR (SAFIR) observatory is planned as the next extension of JWST. With a primary mirror diameter of 10 m, the telescope would be cooled to temperatures around 5 K, allowing currently unparalleled ability to observe the epoch of reionization, trace the formation and evolution of star formation and active galaxies, explore black holes, study planetary system formation, and search for prebiotic molecules in the interstellar medium. The proposed 5-year mission is scheduled for development by around 2020 [12].

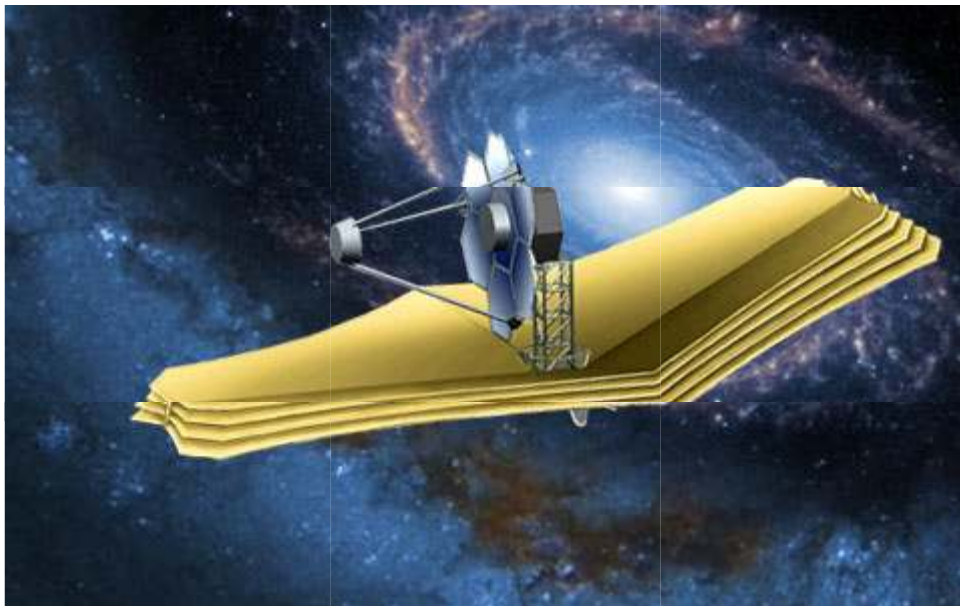


Figure 7. The SAFIR observatory [12].

2.1.6 Terrestrial Planet Finder

NASA's Terrestrial Planet Finder (TPF) is a suite of two space observatories whose purpose is to study various aspects of planets outside our solar system. The coronagraph and nulling

interferometer observatories (TPF-C and TPF-I, respectively) would work in tandem to probe the disks of dust and gas around newly forming stars. Plans exist to launch TPF-C by 2016 and TPF-I by 2020, but the missions are currently in a state of indefinite hiatus [13].



Figure 8. The Terrestrial Planet Finder telescope [13].

2.1.7 Highly Advanced Laboratory for Communications and Astronomy

The Highly Advanced Laboratory for Communications and Astronomy (HALCA) is an orbital radio telescope, and is the first astronomical satellite dedicated to the Very Long Baseline Interferometry Space Observatory Program, which enables imaging of astronomical radio sources with a significantly improved resolution over ground-only observations. Targets observed by the system include active galactic nuclei and extragalactic radio sources such as quasars, radio galaxies and pulsars. Observations can be made in the wavelength ranges of 18 cm, 6 cm, and 1.3 cm. The maximum angular resolution achieved by this telescope is 0.4 milliarcseconds. Along with the ground radio telescopes, the effective aperture of this device is more than 30,000 km, which, at microwave frequencies, produces angular resolution more than a hundred times higher than the Hubble Space Telescope [14].

2.1.8 Low Frequency Array

Located in the Netherlands, the Low Frequency Array (LOFAR) is a radio-frequency array of antennas currently being implemented with funding primarily from the Dutch government. It is expected to achieve breakthrough sensitivity for astronomical observations at radio frequencies below 250 MHz. The large computational power required to run the array is expected to improve as processing ability continues to advance rapidly [15].

2.2 Proposed Lunar Surface Telescope Concepts

There have been numerous concepts published for telescopes based on the Moon. This section details some of the most recent and most interesting ideas for lunar telescopes.

2.2.1 Large Lunar Telescope

The Large Lunar Telescope (LLT) study conducted by the NASA Marshall Space Flight Center in 1991 describes a 16-m segmented mirror telescope to be located at an equatorial latitude, on the lunar limb (about 0° latitude, 85° west longitude), where the Earth would always be low on the horizon. Expected to achieve nominal resolution performance of 10

milliarcseconds in the visible spectrum, it would scan wavelengths between 0.1 and 100 μm . With the lunar day-night cycle lasting approximately 28 Earth days, the LLT could passively reach temperatures as low as 70K, but would require shielding during the day to avoid the temperatures of up to 380K.

The optical design consists of a four-reflection system, with a Coudé focus and imaging equipment buried beneath lunar regolith to protect sensitive photodetectors from cosmic rays and particles. The primary reflector is made up of 1,098 hexagonal mirrors 0.5 m in diameter, which are clustered in 18 groups, each with a diameter of 4 m [16]. Figure 9 shows a concept for the LLT.



Figure 9. Conceptual design for the Large Lunar Telescope [16].

2.2.2 Liquid Mirror Telescope

Another concept that has been proposed is a Liquid Mirror Telescope (LMT). A LMT consists of a spinning reflective liquid, usually mercury, which forms a perfect parabola. At least two LMT's are in use today: a 3-m version used by NASA in New Mexico, and a 6-m version in Vancouver, Canada. A LMT on Earth is limited in size because wind on the surface of the liquid distorts its ideal shape.

The presence of the Moon's gravity (required for the parabola to form) in combination with no atmospheric disturbances provides the rationale behind a liquid mirror telescope. A 20-m LMT on the moon would have 3 times the resolution of the JWST, and with a year of continuous viewing, could potentially observe an object 100 times fainter than the faintest object the JWST could observe.

Two challenges to the concept are finding a reflective liquid that flows properly at extremely cold temperatures, yet still retains adequate reflective properties, and developing bearings to smoothly spin the liquid platform [17, 18].

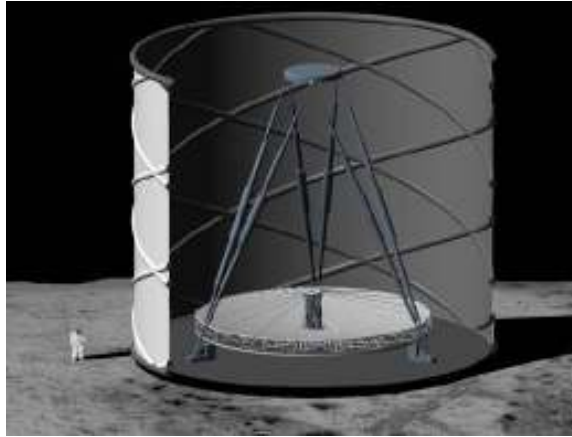


Figure 10. Artist's rendition of a liquid mirror telescope on the Moon [17].

2.2.3 Monolithic Primary Aperture

A study done for NASA in 2002 led by the Colorado School of Mines discusses a mid-infrared telescope located in a permanently dark crater at the Moon's south pole. This telescope would have a 25-m diameter primary mirror made up of hexagonal segments, each about 2.3 m in diameter. It would rotate on 2 axes and take advantage of the permanently dark and cold crater to keep the telescope at around 35K. In 2002, its cost was estimated at \$32 billion [19].

2.2.4 Interferometric Array (Lunar Surface)

A study done between NASA and JPL on a Lunar Interferometer Technology Experiment (LITE) in 1996 addresses the feasibility of an array of 1-m class ultraviolet telescopes deployed with a 100-m baseline. The system could deliver observation capabilities not possible on Earth [20].



Figure 11. A lunar interferometer concept [20].

2.2.5 Radio telescopes on the far side

The far side of the Moon provides a radio-quiet environment for a telescope in the form of a giant dish situated in a crater, similar to the Arecibo Observatory in Puerto Rico, or a distributed series of collectors spread across the surface, either of which would be of great value in detecting

astronomical signals at low frequencies [21].



Figure 12. A radio telescope on the Moon uses a crater to support its large primary dish [21].
Artwork done for NASA by Pat Rawlings.

2.3 Proposed Free-Space Telescope Concepts

2.3.1 Cislunar space observatories

Along with observatories on the lunar surface, there also exist possibilities for putting a telescope in cislunar space. The most relevant locations are the Earth-Sun L2 Lagrange point, the Earth-Moon L1 Lagrange point, and in low lunar orbit. Both Lagrange points have the advantage of semi-stable orbits relatively close to Earth. The JWST is an existing concept for an observatory at the Earth-Sun L2 point. Low lunar orbit may pose problems related to station-keeping, as the Moon's gravitational field is non-uniform, but any observatory in space rather than on the Moon has the advantage of not requiring powered descent to the lunar surface.

2.3.2 Interferometric Array (space-based)

A study done by JPL on the Lunar Configurable Array Telescope (LCAT) [22] details a lunar surface deployment with characteristics similar to those mentioned above, but also addresses deploying this same system in lunar orbit. Due to the difficulty and time involved in configuring a large array of telescopes, particularly in orbit, the study concludes that the expense to put a system in orbit for ten years would not adequately serve the greater astronomy community. The array would be less expensive than the Hubble Space Telescope, but the same array deployed on the surface would provide greater benefit.

2.3.3 Prototype microsatellite

A space-based telescope architecture is being developed in conjunction with the European Space Agency (ESA). This concept is modeled after Dobsonian telescopes used by amateur astronomers. The prototype unfolds from a suitcase-sized box to a space telescope with a 0.5-m primary mirror capable of 30 cm resolution from orbit. The prototype would be considered a microsatellite, with dimensions smaller than 60 cm x 60 cm x 80 cm, and a mass less than 100 kg. This concept could potentially be scaled up to provide significant cost savings [23].

3. Stakeholder Analysis

This section presents the stakeholder analysis, one of the first steps taken in the design process for the lunar telescope facility. The stakeholder analysis is developed as a springboard for further analysis of the best means to deliver scientific value, leverage the planned crewed lunar transportation architecture, and ensure both technical and budgetary feasibility for the proposed lunar telescope facility.

3.1 Stakeholder Identification

For the proposed lunar telescope facility, all the relevant stakeholders in the program were identified using resource flow input/output diagrams. The major stakeholders are shown in Figure 13.

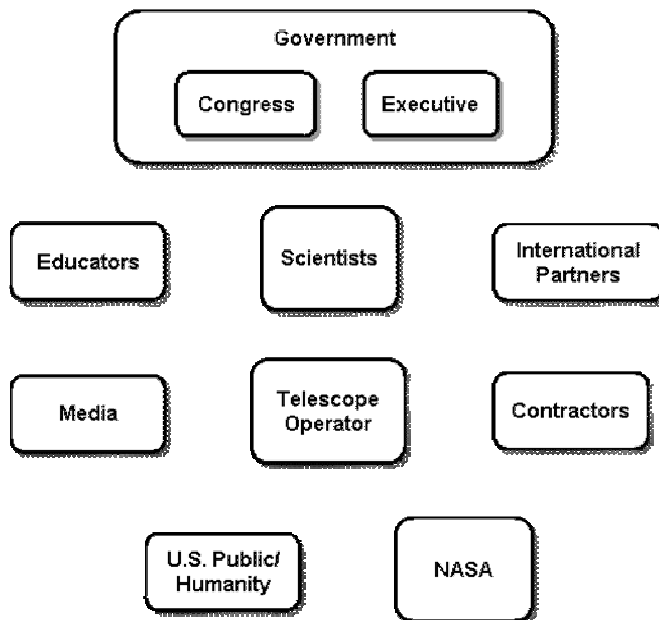


Figure 13. Major stakeholders in the design and development of a lunar telescope.

In this analysis, it quickly becomes evident that certain stakeholders are more important than others, and that satisfying needs of the more important stakeholders is critical to the overall success of the program. For this reason, each stakeholder was assigned a ranking from 1 (Helpful, but not particularly important) to 5 (Essential). These rankings were then combined in a consensus-building discussion in which the overall rankings of the stakeholders were established. The resulting rankings are shown in Table 2.

Table 2. Importance of each stakeholder.
 (5 = Essential, 1 = Helpful, but not particularly important)

Importance	Stakeholders
5	Scientists, NASA, Congress
4	Executive Branch, Telescope Operator
3	Contractors, U.S. Public/Humanity
2	Media, Educators, International Partners
1	

The important stakeholders (scoring 4 or 5) were identified as scientists, NASA, Congress, the Executive branch, and the telescope operators. Note that no stakeholder scored 1; this is reflective of a natural bias to exclude stakeholders of lesser importance from the overall analysis.

3.2 N² Representation of Stakeholder Flows

The process of identifying stakeholder flows involved building a consensus on the type and importance of resource flows that occur between each pair of stakeholders. The results are displayed here in an N² diagram describing these flows. In Figure 14, cell *m-n* contains the type of resource required by the stakeholder in row *m* from the stakeholder in column *n*. For example, cell *j-f* indicates that NASA requires a policy directive from the president, and cell *g-j* indicates that the contractors require money and human resources (in this case, jobs) from NASA.

Type of Flow		a	b	c	d	e	f	g	h	i	j
Educators	a	a	K	H	K						
Media	b		b		K						
U.S. Public/Humanity	c	H	K	c	K			H			H
Scientists	d				d	S	S		S	D,O	\$,D
Congress	e			\$,S		e	\$		S		
Executive	f			S			f		S		S
Contractors	g							g		H	\$,H
International Partners	h				D,H	S	S		h		S
Telescope Operator	i									i	\$
NASA	j			H	D,H	\$,S	P	H,I	S,I		j

Figure 14. N² diagram indicating the types of flows between stakeholders. The meanings of the symbols are: \$ = Money; P = Policy directive; S = Political support; I = Instruments, hardware; O = Observing time; D = Data; H = Human resources (e.g., jobs or students); and K = Knowledge, images, pictures. The meanings of the colors are ■ = Essential; ■ = Very important; ■ = Important; ■ = Somewhat important; ■ = Helpful; and ■ = Irrelevant.

Similarly, a corresponding N^2 diagram, shown in Figure 15, presents the importance of these same resource flows (note that the importance scores are also indicated in Figure 14 by color). The numbers (and colors) indicate the importance of the given flow to the stakeholder *receiving* the resource, i.e. to the one in row m . This is not necessarily the same as the importance of that flow to the provider of the resource or to the program as a whole. In addition, the level of importance refers only to value delivery in the lunar telescope program. Therefore, the contributions of international partners to other scientific missions or to the International Space Station (ISS) are not reflected in the scores presented in these tables.

Importance of Flow		a	b	c	d	e	f	g	h	i	j
Educators	a	a	3	5	4						
Media	b		b		3						
U.S. Public/Humanity	c	4	2	c	2			2			3
Scientists	d				d	5	5		3	5	5
Congress	e			5		e	5		1		
Executive	f			3			f		1		4
Contractors	g							g		4	5
International Partners	h				5	4	5		h		4
Telescope Operator	i									i	5
NASA	j			3	4	5	5	5	2		j

Figure 15. N^2 diagram indicating the importance of each flow between stakeholders. The meanings for numbers and colors are 5 = ■ = Essential; 4 = ■ = Very important; 3 = ■ = Important; 2 = ■ = Somewhat important; 1 = ■ = Helpful; and 0 = ■ = Irrelevant.

3.3 Estimates of Resource Flows

Although the importance of each flow has been identified, it is instructive to present actual metrics to which those scores of importance correspond. Because the lunar telescope is a long-term endeavor, it is not possible to predict the exact values of these flows in advance. Nevertheless, rough estimates for many of the flows based on historical data and current budgetary figures can be provided. Estimates for the paths of several flows of money and knowledge are:

- Knowledge, Images, and Pictures
 - Scientists → Educators
 - Scientists → Media
 - Media → Public
 - Media → Educators
 - Scientists → Public
- Money
 - Public → Congress
 - Congress → NASA
 - NASA → Scientists
 - NASA → Contractors.

3.3.1 Metrics for the flow of knowledge, images, and pictures

The flow values for knowledge, images, and pictures are taken from current and historical data about the Hubble Space Telescope (HST). The rationale for using the HST for this purpose is that it is the current flagship large-scale space telescope facility and, therefore, the closest analogue to the lunar telescope program. Since launch, images and information from Hubble have been used in approximately 2800 news references [24]. This number is used as the estimated value for three flows: Scientists \rightarrow Media, Media \rightarrow Public, and Media \rightarrow Educators.

Since Hubble began sending data back to Earth, it has resulted in an unprecedented number of scientific papers. For the first several years, the number of papers published each year increased steadily. This trend is shown in Figure 16. After seven to eight years, the annual number of papers began to reach a steady state of about 450 papers per year. This publication rate is used as the value for the flow Scientists \rightarrow Educators.

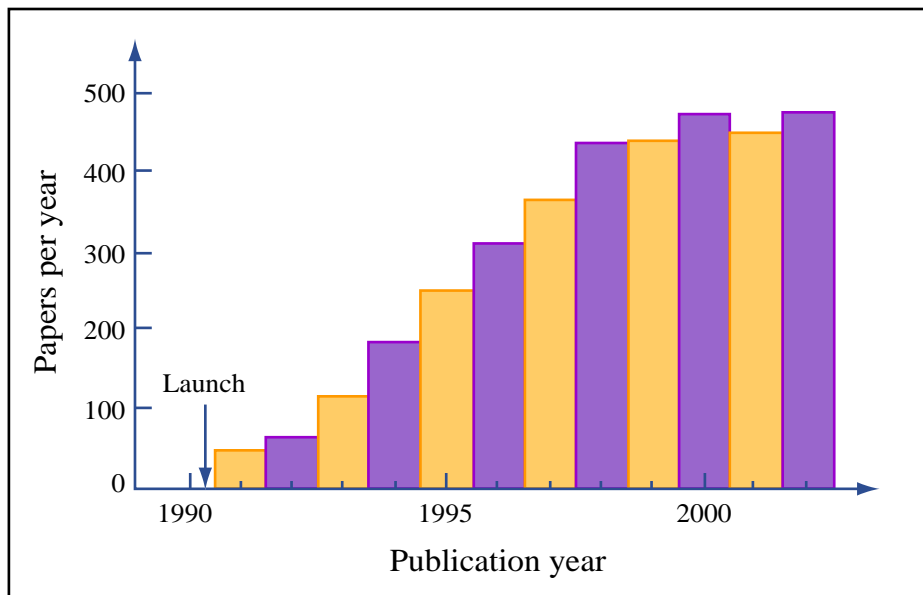


Figure by MIT OpenCourseWare.

Figure 16. Rate of publication of papers using Hubble data [24].

Finally, the flow of knowledge directly from scientists to the public without the media as an intermediary also plays a part in the stakeholder value delivery network. The proxy used for this metric is the number of kiosks in science museums provided by the scientists of the Space Telescope Science Institute. More than 150 kiosks have been provided for this purpose [24].

3.3.2 Metrics for the Flow of Money

To estimate the flow of money from the public to Congress, the total amount of federal taxes paid could, in principle, be used. Since not all of these funds are available for discretionary projects like a lunar telescope, however, the total federal non-defense discretionary budget is used as a rough estimate of an upper bound for the flow Public \rightarrow Congress. For 2007, this value is \$492 billion in current year dollars [25], or \$538 billion in 2010 dollars. In turn, NASA's total discretionary budget is used as the value of the flow Congress \rightarrow NASA. The 2007 estimate for this budget is \$16.354 billion in current year dollars [26], or \$17.870 billion in 2010 dollars. Finally, the flow NASA \rightarrow Scientists is determined from NASA's total science budget, which is \$5.330 billion according to the 2007 estimate [26], or \$5.824 billion in 2010 dollars. This value, of course, is only an upper bound for the conceivable budget of the lunar

telescope, since NASA will have competing scientific programs as well.

In addition, an estimate for the flow of money from NASA to contractors is also informative. Because the monetary values of contracts (including Hubble’s contract) are not often publicly available, we use the average cost of instruments on Hubble as a rough estimate for the flow NASA → Contractors. This average, which can be seen in Figure 17, is roughly \$110 million in 2000 U.S. dollars, or \$144 million in 2010 dollars.

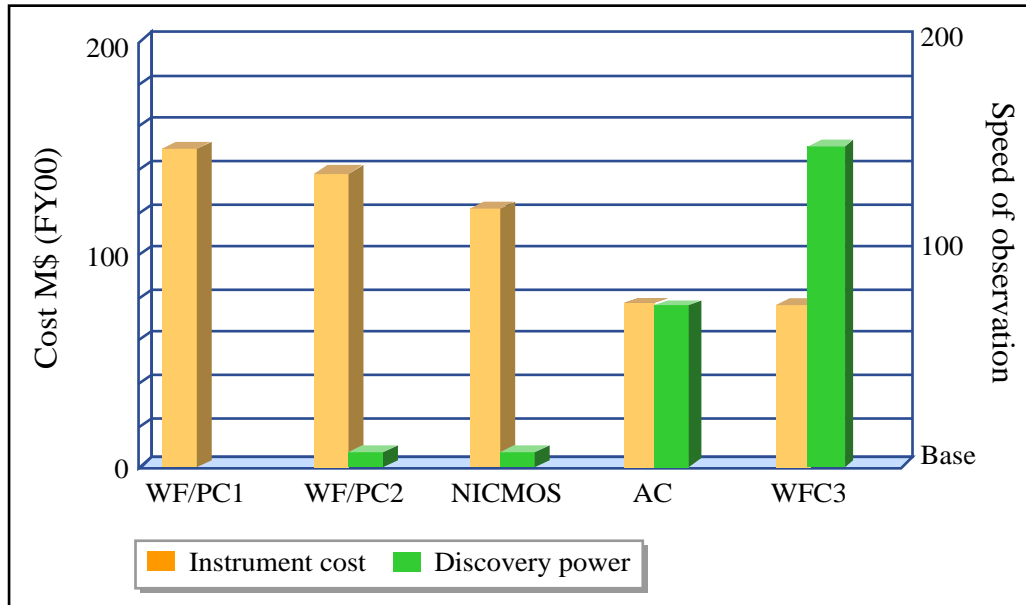


Figure by MIT OpenCourseWare.

Figure 17. Cost and speed of observation for instruments on the Hubble Space Telescope [24].

3.4 Stakeholder Value Delivery Network Model

With the N^2 diagram constructed and the actual values of many of the flows determined, the matrix was then used to construct a network model linking the stakeholders and showing the value delivery flows between them. The resulting model, shown in Figure 18, includes the representation of the identified stakeholders presented in Figure 13, but this time connected by arrows, which represent the flow of resources from one stakeholder to another. This model is similar to a prior one developed by Cameron, Catanzaro, and Crawley to investigate the stakeholders and value delivery flows for space exploration more generally [27].

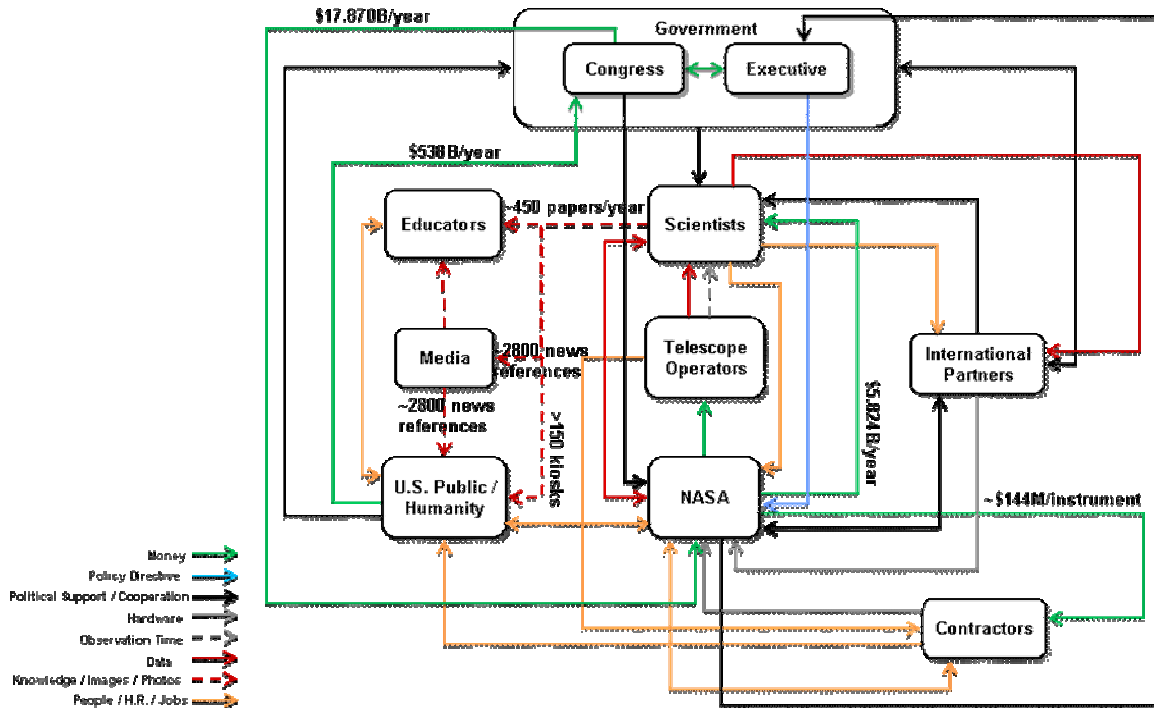


Figure 18. Stakeholder value delivery network model.

3.5 Important Loops in the Stakeholder Value Delivery Network

From the entire value delivery network model developed in the previous section, it is then possible to identify and evaluate the most important loops in the network. These loops are:

- Public → Congress → NASA → Scientists → Public
- Public → Congress → NASA → Scientists → Media → Public
- NASA → Contractors → Public → NASA
- NASA → International Partners → Scientists → NASA
- NASA → Scientists → Public → NASA
- NASA → Telescope Operator → Scientists → Public → Congress/Executive → NASA

The first of the above loops is the most important in the network because it represents the flows between the most important stakeholders (scientists, NASA, and Congress). All flows in this loop except the Scientists → Public flow primarily represent the transfer of money. The Scientists → Public flow, on the other hand, takes the form of knowledge, images, and pictures.

In addition, the flow that does not involve money is the only one in the loop in which the receiving party is not one of the three most important stakeholders. Furthermore, only a portion of that flow is direct. The second loop in the list above actually shows the same loop but recognizes that much of the Scientists → Public flow also occurs via the media. As this is essentially an alternate route for the most important flow, it is depicted in the representation of that flow, shown in Figure 19.

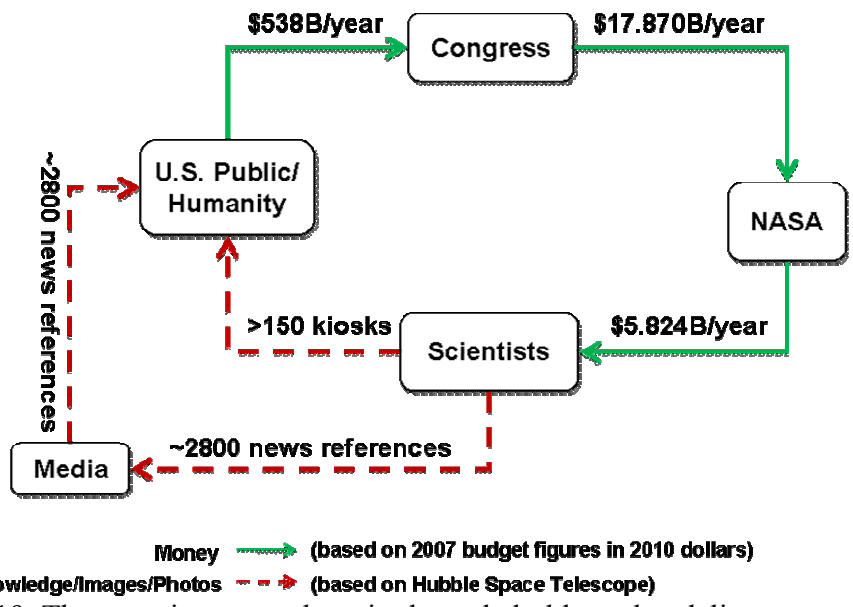


Figure 19. The most important loop in the stakeholder value delivery network.

Given the media’s unique intermediary role, the flows of knowledge, images, and pictures between scientists, the media, educators, and the public can also be highlighted in a set of interactions described collectively as “public outreach” flows. This set of flows is shown in Figure 20.

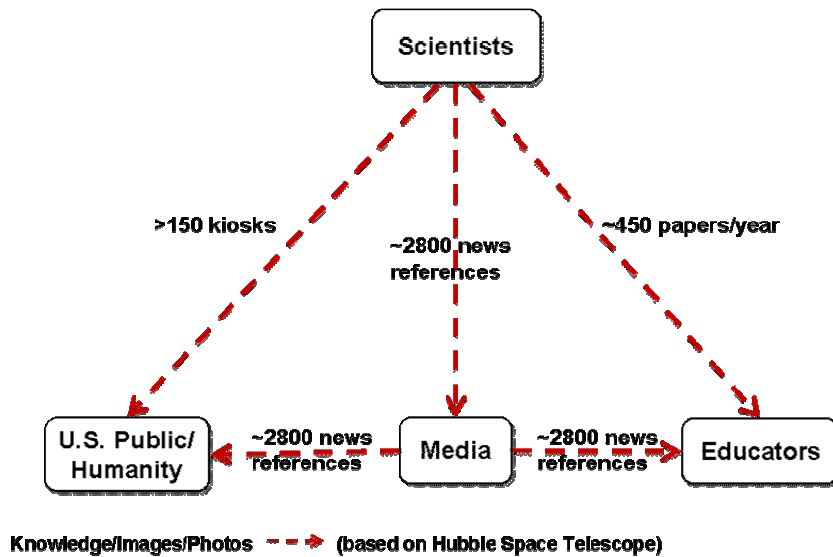


Figure 20. Public outreach flows. Knowledge, images, and pictures flows highlight the unique role of the media in the stakeholder value delivery network.

4. Science Goals

The primary driving motivation for building any telescope is to perform observations of the universe which will deliver significant value to the scientific community. Accordingly, an analysis of the most appropriate and valuable scientific goals for the proposed lunar telescope facility was conducted.

4.1 Needs and Goals

This section details the goals of the lunar telescope facility, as derived from stakeholder needs. Primary and secondary program goals are established based on major stakeholders, identified via stakeholder analysis as the scientific community, NASA, and Congress. Also presented are candidate scientific programs that address the goals and visions of the aforementioned communities. Further details on stakeholder needs are drawn from the NRC Decadal Survey, *Astronomy and Astrophysics in the New Millennium*[28], as well as the *Connecting Quarks with the Cosmos* report [29], and these needs are then ranked based on their importance to each stakeholder.

4.1.1 Primary needs and goals

- To study the large-scale structure of the universe, such as its matter and energy contents, its age and its expansion history, by collecting and communicating data from photons, using a lunar telescope facility.
- To investigate extrasolar planets, and to study the problems of planetary and stellar formation by collecting and communicating data from photons, using a lunar telescope facility.
- To create a symbiotic relationship between this system and the human spaceflight program, by leveraging overlapping technologies, using booster and other relevant subsystems, and potentially providing other spaceflight opportunities.

4.1.2 Secondary needs and goals

- To investigate phenomena such as galaxy formation, by collecting and communicating data from photons, using a lunar telescope facility.
- To investigate the relationship of the Earth to its astronomical environment, by collecting and communicating data from photons, using a lunar telescope facility.
- To perform other astronomy as opportunities arise, by collecting and communicating data from photons, using a lunar telescope facility.

4.2 Candidate Scientific Programs

Particular astrophysical science objectives could be particularly enabled -- or at least significantly facilitated -- by the return to the Moon. In addition to bypassing atmospheric absorption and turbulence, an observatory in the lunar environment offers many advantages, as are described in Section 1.1. The options presented below are not meant to be mutually exclusive. In fact, it is common to integrate near-infrared with optical in existing observatories, which would permit meeting multiple candidate science programs.

A - Epoch of reionization: The transition of the universe from its early state of close-to-perfect uniformity to one of galaxies and inhomogeneous structures is currently an area where data is

much needed. This period is best studied in the radio waveband, especially at low frequencies, which are inaccessible to ground observatories. In addition, these low frequency waves offer a window on the universe that is unexplored at present. This increases the potential for new and unexpected discoveries.

B - Active galactic nuclei: These gigantic cosmic engines are the most energetic sources in the universe. Radiation coming from the accretion of matter by supermassive black holes at the center of galaxies provides the ability to look back to the earliest periods of the.

C - Extrasolar planets: Long-standing questions about the existence and the formation of extrasolar planets have just started to be answered in the last two decades. The infrared is the most suitable band for a planet search and for the investigation of planetary formation.

D - Galaxy and star formation: Studying the formation of the first galaxies both tackles questions about our origins and increases our understanding of the cosmological universe. Because of the immense separation between us and the first galaxies, their radiation reaches us as infrared waves. In addition, infrared radiation is able to penetrate the gas and dust clouds which have kept us from understanding mechanisms behind the formation of stars.

E - Supernovae and the study of dark energy: The expansion of the universe is one of the most important discoveries in cosmology. This discovery, the direct result of a supernova search, implied the existence of an unknown source of repulsive energy, dubbed dark energy. Extending the supernova search deeper will shed light on the mysterious nature of dark energy.

F - Weak gravitational lensing: Another mysterious component of the universe is dark matter. Weak gravitational lensing studies allow the mapping of the distribution of dark matter, which is the largest component of the large-scale structures of the universe.

4.3 Ranking of Science Objectives

The stakeholder value delivery network was used to perform a utility analysis of the six candidate broad science objectives. The goal of the analysis was to eliminate any science objectives that provided significantly less value than the others, and to identify science objectives that looked the most promising. The six scientific objectives under consideration are denoted as:

- A. Epoch of Reionization (EOR)
- B. Active Galactic Nuclei (AGN)
- C. Extrasolar Planets (XSP)
- D. Galaxy and Star Formation (GSF)
- E. Dark Energy (DE)
- F. Weak Gravitational Lensing (WGL)

Each stakeholder has one or more needs that must be met by the lunar telescope facility. These needs are essentially met by inputs from other stakeholders, which are indicated as value flows between them. By tracing the flows through the system, it is possible to identify “value loops” that begin and end with a particular stakeholder. The success of the overall project

depends on satisfying the needs of each stakeholder and ultimately managing the value flows inside the loops.

To enable a utility analysis of each candidate science objective, a series of metrics was developed based on the individual stakeholder needs. Each objective received a score between 1 – 5 for each metric; 1 indicating that the science objective would perform poorly, and 5 indicating that it would perform exceptionally. Scores were determined based on group consensus or averaging different scores from individual design team members.

Table 3 shows the metric scores for each science objective. Note that for the last three stakeholders, the degree to which their needs are fulfilled was assumed to be independent of the chosen science objective and thus no metric scores were given.

Table 3. Example of stakeholder value metrics for NASA and the media.

Stakeholder Metrics (1 = strong no; 5 = strong yes)	Science Objective					
	EOR	AGN	XSP	GSF	DE	WGL
Congress & Executive						
Will Congress & Executive gain public support for this objective?	3	3	4	3.5	3.5	2.7
Are concepts within this objective likely to stay within NASA's budgetary limits?	4.7	4.5	2.3	2.7	2.3	2.3
Are concepts within this objective likely to be completed within a timely schedule?	4	4	3	3	3	3
NASA						
Does this objective enhance support for the lunar exploration program?	3	3	4.5	4	3.5	1.5
Is this objective uniquely enabled by the lunar exploration program?	4	4	1.5	1.5	3	3
Scientists						
Does this objective provide high-priority scientific value?	4.5	1	4.5	3	4	2
Would this objective provide a unique scientific capability?	3	2	2	2	1	1
Are scientists likely to receive funding and support for this objective?	2.5	3	3	2.7	2.5	2
Media						
Will this objective provide exciting pictures and information for the media?	2.3	3	4	4	5	3
Educators						
Will this objective inspire students?	2.5	3.5	5	5	4	2
Will educators be able to get knowledge from this objective and pass it along to students?	2.5	3.5	5	5	3.5	2
General Public						
Will the general public get excited about this objective?	2	2.7	4.7	4	3.3	1.7

Stakeholder Metrics	Science Objective					
(1 = strong no; 5 = strong yes)	EOR	AGN	XSP	GSF	DE	WGL
International Partners						
[Metrics independent of objective]	-	-	-	-	-	-
Contractors						
[Metrics independent of objective]	-	-	-	-	-	-
Telescope Operator						
[Metrics independent of objective]	-	-	-	-	-	-

For each science objective, each stakeholder’s metric scores were averaged and normalized from 0-1 to produce a single blended utility score. This score approximates the utility a stakeholder would derive from each candidate science objective. These scores are shown in Table 4 below. The last three stakeholders were assigned utility scores of 1.0 for each objective to reflect that their preferences were believed to be unaffected by the choice of science objective.

Table 4. Derived stakeholder utility scores for each science objective.

Stakeholders	Science Objective					
(0 = no utility; 5 = maximum utility)	EOR	AGN	XSP	GSF	DE	WGL
Congress & Executive	0.78	0.77	0.62	0.61	0.59	0.53
NASA	0.70	0.70	0.60	0.55	0.65	0.45
Scientists	0.67	0.40	0.63	0.51	0.50	0.33
Media	0.47	0.60	0.80	0.80	1.0	0.60
Educators	0.50	0.70	1.0	1.0	0.75	0.40
General Public	0.40	0.53	0.93	0.80	0.67	0.33
International Partners	1.0	1.0	1.0	1.0	1.0	1.0
Contractors	1.0	1.0	1.0	1.0	1.0	1.0
Telescope Operator	1.0	1.0	1.0	1.0	1.0	1.0

To approximate the strengths of the value loops identified in Section 3.5, each link in a loop was assigned the utility value derived above. The product of the utility values of all links in a loop then roughly correlates with the strength of that loop during the lifetime of the project. For example, a perfect loop would be one whose stakeholders derive maximum value (loop score $1.0 \times 1.0 \times 1.0 = 1.0$) from the selected science objective. A moderately successful loop might equal $0.8 \times 1.0 \times 0.5 = 0.4$. A multiplicative rule was used so that any individual link with a score close to zero would result in a loop score also close to zero. Finally, each loop score was multiplied by 100 to indicate a “percent strength” score. Some of the more important value loops and their strength scores are shown in Table 5 below. At the bottom of the table, the sum and average of all scores for each science objective are shown. The average scores were then normalized by the highest-scoring science objective to indicate relative strengths of each objective. The loops with the strongest scores (score > 35) are highlighted in green bold font. The loops with the weakest scores (score < 15%) are highlighted in red italic font.

Table 5. Expected level of strength for each stakeholder value loop.

Value Loops (Expected strength of each loop – “% strength”)	Science Objective					
	EOR	AGN	XSP	GSF	DE	WGL
Public → Congress → NASA → Scientists → Public	15	11	22	14	13	3
Public → Congress → NASA → Scientists → Media → Public	7	7	18	11	13	2
NASA → Contractors → Public → NASA	28	37	56	44	43	15
NASA → International Partners → Scientists → NASA	47	28	38	28	33	15
NASA → Scientists → Public → NASA	19	15	35	22	22	5
NASA → Telescope Operator → Scientists → Public → Congress/Executive → NASA	15	11	22	14	13	3
SUM	131	109	191	133	137	43
AVERAGE	22	18	32	22	23	7
NORMALIZED AVERAGE	0.68	0.58	1.00	0.70	0.71	0.22

These scores can be expressed numerically as:

Stakeholders: S_n , $n = 1, 2, 3, \dots, 10$
 Objectives: C_x , $x = A, B, C, \dots, F$
 Stakeholder utility: $K_{n,x}$, (Utility score for S_n , C_x)
 Value loop: $L_{abcd,x}$, $a,b,c,d = \text{values for } n$
 # of value loops: m
 Value loop score: $L_{abcd,x} = K_{a,x} * K_{b,x} * K_{c,x} * K_{d,x}$

$$\text{Average loops score: } L_{avg,x} = \frac{\sum_1^m L_{abcd,x}}{m} \quad (\text{Eq. 1})$$

$$\text{Normalized loop score: } L_{norm,x} = \frac{L_{avg,x}}{\max(L_{avg})} \quad (\text{Eq. 2})$$

The relative strengths of the science objectives are shown graphically in Figure 21 below. The results from this analysis show that Objective XSP (Extrasolar Planets) clearly shows the greatest promise, while Objective WGL (Weak Gravitational Lensing) is significantly weaker. Objectives EOR (Epoch of Reionization), AGN (Active Galactic Nuclei), GSF (Galaxy and Star Formation), and DE (Dark Energy) show little differentiation, other than being somewhat less

promising than Objective XSP (Extrasolar Planets).

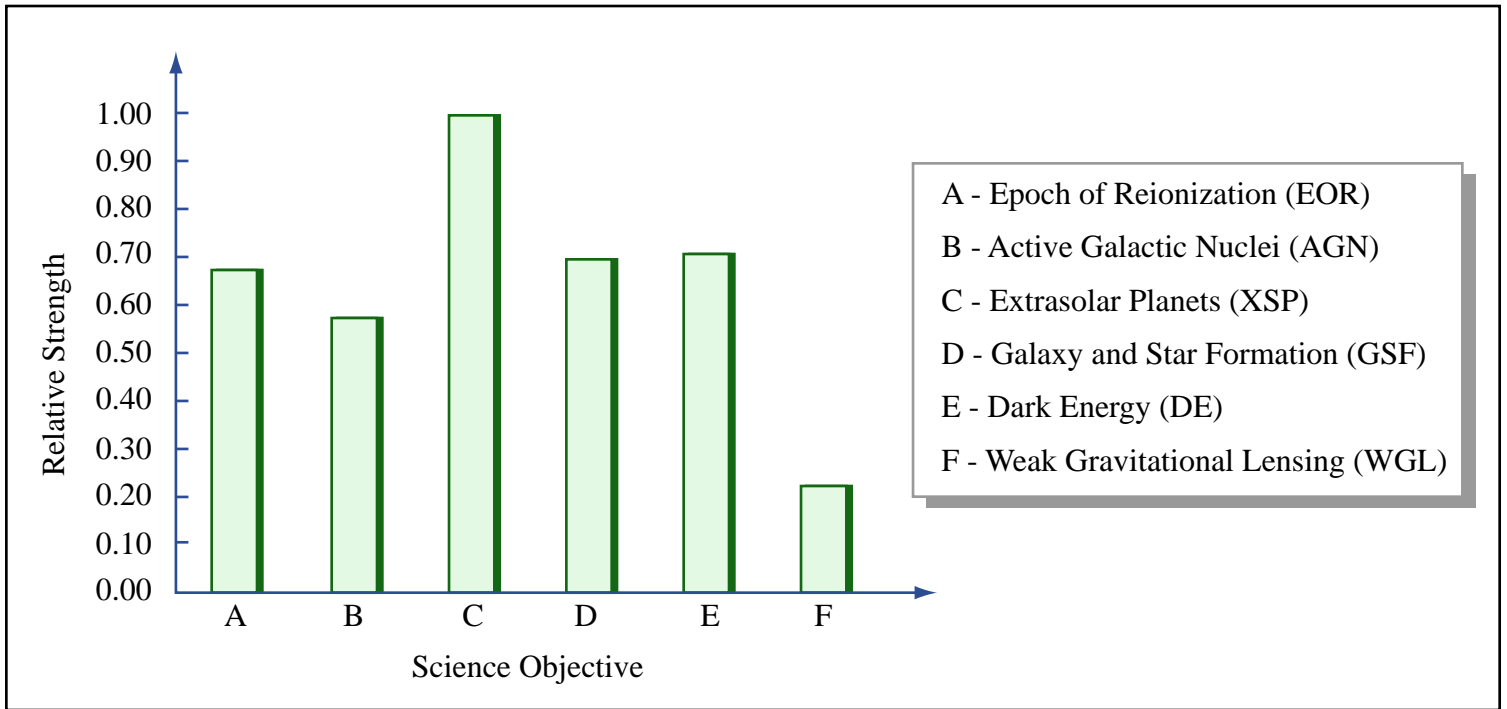


Figure 21. Relative strength of six candidate science objectives based on stakeholder utility analysis.

Figure by MIT OpenCourseWare.

Finally, once an objective is chosen, this analysis can be used to predict the weakest value loops during the life of the telescope program. For example, if Objective AGN were chosen (see Table 6), the analysis would show that the loop involving Public → Congress/Executive → NASA → Scientists → Media would be the weakest of all the stakeholder value loops. This information is helpful, as greater resources nurturing that loop throughout the lifetime of the program could help increase the chances of success for the project.

Table 6. Expected strength of each stakeholder value loop for science objective AGN.

Value Loops	Science Objective
(Expected strength of each loop – “% strength”)	AGN
Public → Congress → NASA → Scientists → Public	11
Public → Congress → NASA → Scientists → Media → Public	7
NASA → Contractors → Public → NASA	37
NASA → International Partners → Scientists → NASA	28
NASA → Scientists → Public → NASA	15
NASA → Telescope Operator → Scientists → Public → Congress/Executive → NASA	11
SUM	109

Value Loops	Science Objective
(Expected strength of each loop – “% strength”)	AGN
AVERAGE	0.58

The results from this analysis allowed the team to eliminate one of the six candidate science objectives altogether. Of the remaining five objectives, four are roughly equal in strength, and one shows significant promise for delivering value to all the identified stakeholders. During the development of specific concepts for each science objective, this stakeholder utility analysis complemented and helped inform the downselection process and some of the other analyses that are presented later in this report.

5. Broad System Requirements

General telescope system requirements were developed early in the design phase, informed by the stakeholder analysis described in Section 3 and based on the scientific goals delineated in Section 4. These general requirements are presented in Table 7. Tentative numbers were chosen for some metrics, in order to provide a framework for defining more specific requirements for the two reference designs. These more specific requirements are presented in Sections 7 and 8.

The nomenclature in Table 7 is described as follows. Science goals which drive particular requirements are described using a brief acronym, as listed in Section 4.2.

- Requirement Number: X. = Level 0 requirements, X.Y = Level 1 requirements.
- Requirement Statement: Quantified description of scientific and engineering requirements.
- Priority: Rigidity of requirement statement on A-C scale, A being highest.
- Rationale: Source and reasoning for requirement.

Table 7. Level 0 and Level 1 requirements.

Req #	Requirement	Priority	Rationale
1	The system shall be capable of collecting radiation in the EOR,AGN) radio band, XSP,GSF) IR band, or DE,WGL) Optical band.	A	From stakeholder: Scientific Community, NASA
1.1	The system shall collect radiation in the following wavelength ranges: EOR) 1.5-3m AGN) 1cm-1m XSP) 1-20microns GSF) 10-300 microns DE,WGL) 0.3-1 microns	A-C	TBD
1.2	The system shall provide a minimum angular resolution of EOR,AGN,GSF,DE) TBD and XSP) 1 milli-arcseconds for each wavelength.	A-C	TBD
1.3	The system shall be able to point at a particular target with an accuracy of TBD arcseconds.	A-C	TBD
1.4	The system shall provide an effective collecting area of EOR) $3 \times 10^4 \text{ m}^2$ DE) 50 m^2 AGN,XSP,GSF) TBD	A-C	TBD
2	The system shall be able to view TBD degrees of the sky in one year of operation.	A-C	Scientific Community, NASA
2.1	The field of view of the system shall be EOR,AGN,XSP) TBD sq. deg. DE) 30 sq. deg. WGL) 0.5 sq. deg.	A-C	TBD
2.2	The system shall be able to maneuver to face a target within TBD degrees of its nominal position.	A-C	TBD
3	The system shall be located in cislunar space.	A	To leverage NASA's lunar exploration architecture and assist in fulfilling the Vision for Space Exploration.

Req #	Requirement	Priority	Rationale
3.1-n	The system shall be capable of surviving in the environment of cislunar space.	A-C	
4	The system shall be able to communicate data back to Earth.	B	The data need to be communicated to Earth either directly or via relays (e.g., satellites) to be analyzed by ground-based personnel.
4.1	The system shall have a data rate of TBD bps.	A-C	TBD
4.2	The system shall transmit data in the TBD band.	A-C	TBD
5	The entire system payload shall fit into less than TBD number of Ares V booster vehicles and have a throw weight no greater than the maximum throw weight of less than TBD number of Ares V boosters.	B	The use of Ares V as the launch vehicle was a constraint for this project in order to leverage planned NASA capabilities for lunar exploration.
5.1	The mass of system components launched on a single Ares V shall be less than 18 metric tons.	A	NASA Lunar Surface Access Module (LSAM) payload delivery capability [7].
5.2	The system components launched on a single Ares V shall fit within the LSAM cargo container.	A	Volume constraints for the LSAM are as yet undetermined by NASA.
5.3	The system shall be able to survive launch loads as defined in the Ares V user's guide.	A	
6	The system shall have an operational lifetime of at least TBD years.	B	From stakeholders: Scientific Community, NASA
6.1	The system shall have a reliability of at least TBD.	A-C	TBD
6.2	The system shall have interfaces for servicing by robotic/human missions.	A-C	TBD
6.3	The system shall employ redundancy for critical subsystems.	A-C	TBD
7	The system shall employ a modular design for flexibility and upgradability.	B	A modular design that is upgradable was believed to be a better choice due to its resiliency to budget cuts.

Req #	Requirement	Priority	Rationale
8	The system shall have a cost of the same order of magnitude as telescopes with similar scientific objectives.	A	The system needs to deliver higher value to the major stakeholders for a cost either lower than or equal to other proposed programs.

6. Concept Development Methodology

This section explains the process used to move from the generalized design goal to a detailed analysis and two specific reference designs. Figure 22 shows the development of the concepts and reference designs.

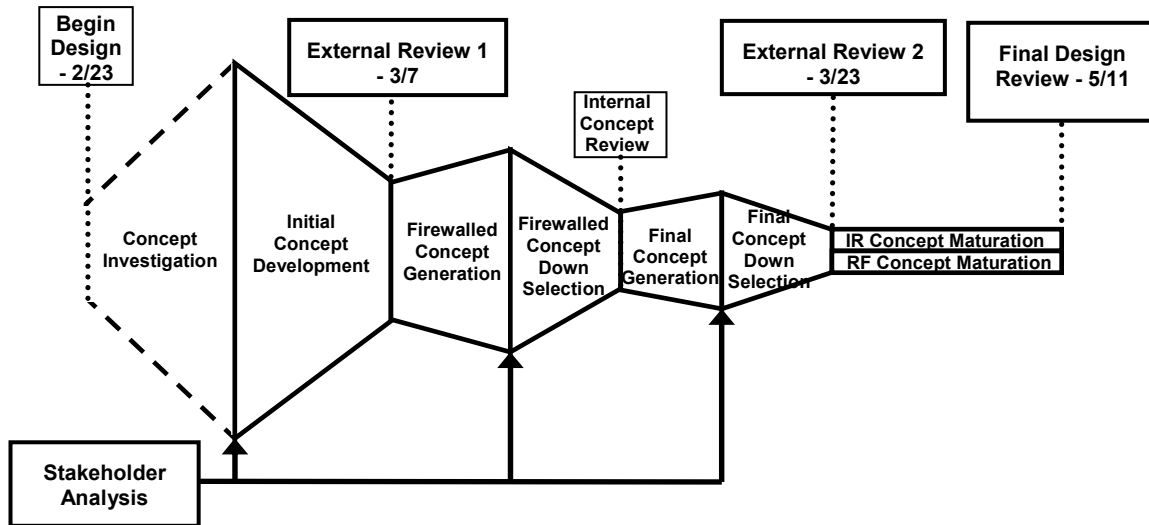


Figure 22. Concept development process.

6.1 Initial Formulation of Concept Space

In identifying the concepts to be considered for a lunar telescope, the concept space must be firmly described in terms of architectural objectives. A lunar telescope architecture embodies the overarching concept while allocating functions to elements of form. Furthermore, the surrounding context defines the interfaces and constraints on the system [30].

It is thus necessary to define a concept space that will be explored creatively, completely and rationally in the search for specific realizations of operation that fulfill the defined needs and goals in the best possible way. Some key definitions which will help in the process of establishing the concept space can be drawn from the primary and secondary needs and goals, listed in Section 4. These definitions include the primary need of the system and a solution-neutral statement of function. From these the value-related operand, the value-related attribute, and the function can be inferred. The specific definitions for the system being developed are:

6.1.1 Primary Need:

To study the large-scale structure of the universe, the formation of planets and stars.

6.1.2 Solution-Neutral Statement of Telescope Function:

Collecting and transmitting information gathered from photons emitted by distant astronomical objects.

This statement constrains the method to be used to achieve the broader goal to a telescope by

differentiating the light gathering concept from others, like human or robotic exploration, or collection of information from sources like subatomic particles.

6.1.3 Value-related operand

Photons, or equivalently, their wave signature in the electromagnetic field, are the objects on which the function is being performed. The photons can be generated or transformed by different extraterrestrial phenomena and they carry within their state intrinsic information about these events.

6.1.4 Value-related attribute

Information has been identified as the characteristic of the photons which is to be operated onto to give value to the designed system. The information carried by the photons can be obtained by measuring different characteristics of their present state and from it, details about the phenomena that generated or acted on them. Some of these characteristics are energy, location, direction, time of arrival and polarization.

6.1.5 Function

Gathering is the main function of the system, acting over the *information* attribute of the photons. It is performed in the sense of obtaining, through measurements, specific characteristics that will reveal scientific details about the source or phenomenon that generated or transformed the radiation.

This main function can be subdivided in a set of specific sub-functions that are intrinsically required to achieve the main goal. These characteristics are listed here, but the order in which they are mentioned is not necessarily a chronological or hierarchical categorization.

- First, in order to reach the photons the instrument has to be placed at some location that will affect the availability of sources and amount of photons that can be discriminated.
- Second, the instrument has to be pointed at some explicit direction to receive the specific light from the source to be studied.
- Third, the photons have to be collected at a given surface, generally referred as the aperture stop.
- Fourth, these photons are selected through some filtering process that generally takes place simultaneously to the collection process, so that only a very specific band or window of the spectrum is processed.
- Fifth, the photons have to be localized, that is, their relative states have to be correlated in a timely manner to allow the acquisition of information. In the case of direct combination, there is a focusing process that permits the mapping of the signal at different locations into the detector. In other concepts, like interferometers, the signal is correlated and the localization is done through its frequency content.

6.2 Object-Process Methodology Diagram and Concept Space Matrix

The following diagram, Figure 23, shows the elements of form and their association with process-specific functions. It aids in visualization of the relationships between different aspects of the architecture, and provides a convenient method for construction of a morphological matrix.

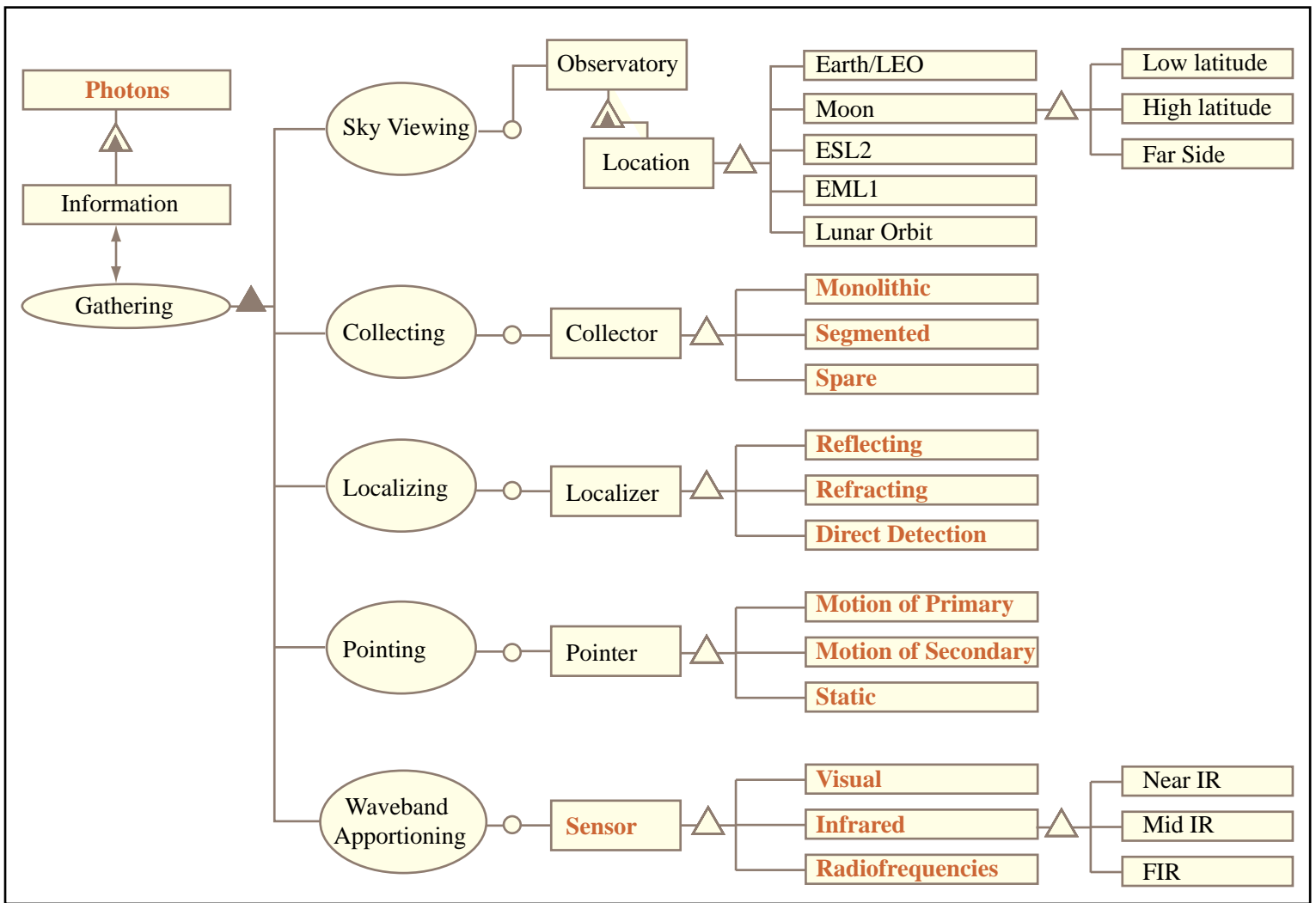


Figure by MIT OpenCourseWare.

Figure 23. Object-Process Methodology description of telescope design.

The elements in the matrix shown in Table 8 represent particular concepts of operation that can be applied to satisfy the required functions of the telescope system. By selecting a possibility from each row in the matrix, thereby making a trace from the top to the bottom, a concept for the overall telescope system can be formed (note, however, that some rows contain possibilities that are a subset of only one of the previous rows' choices). All possible permutations of concepts of operation then define the total concept space for our system, which includes all basic telescope architectures possible. The completely-detailed matrix defines a space containing 6048 individual concepts. While some of these concepts will not work, will have severely limited capabilities, or will fall outside the parameters of this study, this initial concept space allows consideration of all varieties of telescopes that can satisfy the listed needs.

Table 8. Detailed concept space matrix.

Collecting	Monolithic				Segmented				Sparse							
Localizing	Reflecting				Refracting				Direct							
Pointing	Move Primary				Move Secondary				Static							
Waveband	Radio		Radio/Far IR		Far IR		Mid IR		Near IR		Near IR/Vis		Visual			
Location	Earth				Moon				Deep Space							
	Surface		Orbit		Surface		Orbit		Orbit		EM		ES			
	Place	LEO	HEO	GEO	Lo	Hi	Eq	Pole	Lo	Hi	Ecc	1	2	3	4	5
					Near	Far	Limb									

A trace through the expanded concept space matrix provides a description of a telescope concept. The specific concepts of operation defined in the matrix are as follows:

6.2.1 Collecting

Monolithic

A monolithic aperture is a solid, completely filled collecting surface. This type of aperture maximizes the total amount of collecting area for a particular diameter of the aperture. Monolithic aperture design is widely used in telescopes in all wavebands (examples include the Arecibo radio telescope, and the Hubble space telescope). Monolithic apertures are by definition single units, and consequently must be constructed and deployed as such. In addition to providing the largest collecting area per size, monolithic apertures have the additional advantage that, once constructed, they generally need minimal adjustment to ensure that they correctly correlate the incoming photons compared to the other aperture options. However, monolithic apertures generally increase the cost for a particular diameter (and hence make high resolutions more difficult to achieve) and large monolithic apertures may present transportation challenges.

Segmented

Segmented apertures use multiple elements smaller than the aperture size to construct the full aperture. These types of apertures do not necessarily need to reconstruct the entire equivalent monolithic aperture, and in many cases may have a filling-factor (percentage of the equivalent full circular aperture that is sampled) of less than unity. Examples of segmented aperture telescopes include the Keck telescopes and the original Multiple Mirror Telescope (MMT). Segmented apertures allow large apertures to be constructed in pieces, potentially sequentially, which simplifies manufacturing of a large aperture.

Sparse

A sparse aperture refers to a low (much less than unity) filling-factor aperture. These types of designs typically will use interferometric techniques to correlate incoming photons. Sparse apertures can attain extremely large effective diameters and consequently high angular resolution. However, this technique will result in much less collecting area compared to a monolithic aperture of equivalent diameter. Examples of sparse apertures include the Very Large Array radio telescope and the Cambridge Optical Aperture Synthesis Telescope (COAST). Sparse apertures are generally easier to construct at lower frequencies because the techniques used to correlate the photons (typically interferometry) require much lower precision and are much more mature at the lower frequencies. Sparse apertures also tend to act as a spatial filter.

6.2.2 Localizing

Reflecting

Reflecting telescopes use the principle of reflection to collect and localize light. These designs consist of curved reflecting surface, which causes collimated incoming light to be focused above the reflector. Reflectors have the advantage that the mirror can be supported fully on the back side. However, the fact that the focus is in front of the mirror means that either the instrumentation package or a secondary mirror needs to be placed in the light path, which will reduce the aperture efficiency. Some examples of reflecting telescopes are the Keck telescopes or the individual elements of the Very Large Array.

Refracting

Refracting telescopes use lenses to refract incoming light into a focal point. This type of system allows the instrumentation to be placed behind the optical system. Refracting telescopes present challenges for large diameter lenses because the lenses become quite massive and consequently expensive, and can only be supported on the perimeter, giving them the propensity to deform or break under their own weight.

Direct

Direct detection of photons is also used to collect light. In these systems, the individual detector is the size of the aperture, so the light is not gathered and focused, but is merely detected. In the wavebands considered in this report, this method of detection is most commonly found in low frequency radio telescopes, where the detection elements consist of dipole antennae which simply detect the electromagnetic radiation.

6.2.3 Pointing

Moving Primary

Telescopes with moving primaries physically slew the primary collecting structure to point at the intended target. Over the course of the observation, the telescope continues to slew to track the target. This type of system consequently requires that the entire collecting structure be precisely steerable. Examples of this include the Magellan Telescopes or the Parkes radio telescope. Space telescopes also generally fall into this category, as the entire system slews to point at the observed target.

Moving Secondary

Telescopes with moving secondaries keep the primary collecting structure essentially fixed and instead steer by changing the location of a secondary reflector. This type of telescope allows large primaries to be built without designing a complex system to give them all the necessary degrees of freedom to effectively track an astronomical target. However, this type of arrangement means that usually the effective aperture is significantly less than the actual primary aperture size, and that only a limited area on the sky is visible.

Static

Telescopes can also be designed without active steering mechanisms. This type of design mainly includes interferometric arrays which have elements with wide fields of view. In this case, variation of the light phase delay can be used to effectively steer the telescope.

6.2.4 Waveband Apportioning

Radio

The radio range covers wavelengths more than roughly 1mm. Observations at wavelengths longer than ~10 meters cannot be performed within the Earth's ionosphere, and the ionosphere presents calibration difficulties on meter-scale wavelengths.

Far IR

The far-infrared range spans wavelengths of roughly 30–1000 μm . Far-IR measurements must be done outside of the Earth's atmosphere, with cryogenic detectors. The techniques for these observations become more similar to radio observations.

Mid IR

The mid-infrared range spans wavelengths of roughly 5–30 μm . These observations must be conducted outside of the Earth's atmosphere and require cryogenic detectors.

Near IR

The near infrared range spans wavelengths of roughly 0.75–5 μm . Many of the shorter wavelength near-IR observations can be conducted similar to traditional optical astronomy, although past 1 μm requires special detectors, and atmospheric opacity starts becoming problematic.

Visual

Visual light spans the range roughly between 350 and 750 nm. This is the traditional optical astronomy band, and can be done within the Earth's atmosphere with limited resolution.

Note that wavebands which lie adjacent can be combined into the same telescope.

6.2.5 Location

Location has a number of levels, reflected in the four rows allotted to describing the location of the telescope. Each row is not necessarily available after every choice in the previous row; for instance, a telescope placed on Earth makes the selection of Farside, Nearside, or Limb location irrelevant.

Earth

Refers to telescopes on the surface or in orbit around Earth.

Moon

Refers to telescopes on the surface or in orbit around the Moon.

Deep Space

Refers to telescopes which orbit at a significant distance from the Earth and the Moon, i.e. at one of the Lagrange points of the Earth-Moon or Earth-Sun systems.

Orbit

In the case of an orbit near the Earth or the Moon, an orbiting telescope can be placed in low, high, stationary, or eccentric orbit. In the case of the Earth, an eccentric orbit is not a useful feature, and a high stationary orbit is also known as geosynchronous orbit, which may be useful. In the case of the Moon, stationary orbit confers no advantages, but an eccentric orbit might, as it could potentially allow extended periods in shadow from Earth's radio emissions, but also permit direct transmission to Earth ground controllers during the brief passes over the Moon's Nearside.

Lunar Orbit

A lunar orbit would place the telescope in orbit around the Moon. This has the possible advantage of allowing the telescope to use the Moon's shadow to shield it either from the Earth or the Sun to make observations, but then to transmit information back to the Earth when on the Earthward side of the Moon.

Low Earth Orbit

A telescope in Low Earth Orbit (LEO) would get the telescope outside the Earth's atmosphere, but would be close enough to the Earth for easy access by current and future launch systems, allowing comparatively easy human serviceability. LEO orbits also allow easy downlinks to Earth and the characteristics of telescopes in LEO are well known (the Hubble Space Telescope occupies LEO, for example). Putting a telescope in Low Earth Orbit, however, is not a concept enabled by the return to the Moon. Concepts including this space in the concept matrix will be used as baselines for comparison, rather than as actual design candidates.

Lagrange Points

Lagrange points are any of the five locations in a two-body system where a third body remains at relative rest to the other two. Here, the interest is confined to the Earth-Moon and Earth-Sun systems.

Earth-Moon L1

This Lagrange point, located between the Earth and Moon, has been proposed as a waypoint between the Earth and Moon.

Earth-Sun L2

The second Earth-Sun Lagrange point is located on the opposite side of the Earth from the Sun. A telescope located at this point would require small amounts of station-keeping, benefit from the observing advantages afforded in space, and still be relatively close to Earth. This is a space location, and consequently would offer nearly full sky coverage.

Other Lagrange Points

Both the Earth-Moon and Earth-Sun systems contain five Lagrange points, three of which are collinear to the major pair of bodies in the system and two of which lie on the orbit of the smaller body around the larger at 60-degree offsets in front of or behind the smaller body. In general, not all these points are of immediate interest, and the characteristics of one of the non-collinear points are not distinguishable from those of the other non-collinear point; however, all five are included in the broad concept space matrix to allow for the maximum number of concepts from which to downselect.

Earth Surface

Telescopes have been built on the Earth's surface for centuries. Although Earthbound sites have the distinct disadvantage of being below the atmosphere and the ionosphere, which can affect many wavelengths, the costs of transporting and constructing a telescope on the Earth's surface are dramatically lower than any other potential site, and the telescopes are inherently human serviceable. Earth-based telescopes, however, are not enabled by the return to the Moon, and will serve only as baselines.

Lunar Low Latitude

Lunar low latitude refers to placing the telescope near the lunar equator. This type of site provides the largest viewable portion of sky to the telescope.

Lunar High Latitude

This type of site, also including the lunar poles, would place the telescope near the north or south pole of the Moon. This type of site would limit the percentage of the sky that is viewable, but would allow more observing time on particular portions of the sky.

Lunar Poles

A site exactly at one of the poles, especially at the Shackleton Crater near the lunar south pole, may allow for leveraging the permanent shadows that exist there.

Lunar Nearside

A site on the side of the Moon which faces the Earth would allow for easy communications, but might suffer from interference generated by the radio output of the Earth.

Lunar Farside

This type of site (which can be combined with either a low or high latitude selection) would place the telescope on the far side of the Moon relative to Earth. While this would make telemetry with Earth more difficult, it would shield the telescope from Earth's auroral radio emission.

Lunar Limb

The limb region of the Moon's surface is that where the Earth always hangs low on the horizon. This region is on the boundary between Nearside and Farside, and represents a possible compromise between competing advantages.

6.3 Existing Concept Investigations

Existing designs for telescopes can be traced through the concept space matrix. Examples can be seen in the existing concepts discussed in Section 2 of this report. The advantages of doing astronomical observations, or Earth observations, from the Moon have led to a number of lunar telescope concepts worth discussing here. While some are conceived because of their similarities to free-flying space telescopes in their relative performance over Earth-bound ones, other concepts are unique to the lunar environment. As can be verified in the concept space matrix of Table 8, each of the previously investigated concepts falls within the space under current study.

For example, the Hubble Space Telescope is a monolithic reflecting telescope with a movable primary reflector, operating in the visual wavelengths from Low Earth Orbit. The proposed Large Lunar Telescope would be a segmented reflecting telescope with a movable primary reflector, operating in the visual wavelengths from lunar low latitudes.

6.4 Concept Downselection Cycles

An important part of the design development was the selection of valid concepts within the broad architecture space, and the subsequent ranking and more detailed analysis of the selected concepts.

6.4.1 First downselection cycle

A list of preliminary metrics was distributed to the concept-generation subteams from the requirements team. These included the binary criteria that the selected telescope 1) must be able to meet one of the selected candidate science program goals, 2) must have no components which do not fit on an Ares V booster, and 3) must be in deep space or near the Moon.

One method of downselection is the method of trees, an example of which is seen in Figure 24. A tree is a subset of possible traces through the concept space matrix. Starting with segmented telescopes only, the next step must be a reflector, as segmented direct detectors or segmented refractors are not sensible concepts. The table in the middle indicates that any frequency band may be chosen. Note that some of the Lagrange points have been removed or combined, and no Earth or Earth-orbit telescopes appear, per the requirement that the telescope be in lunar space.

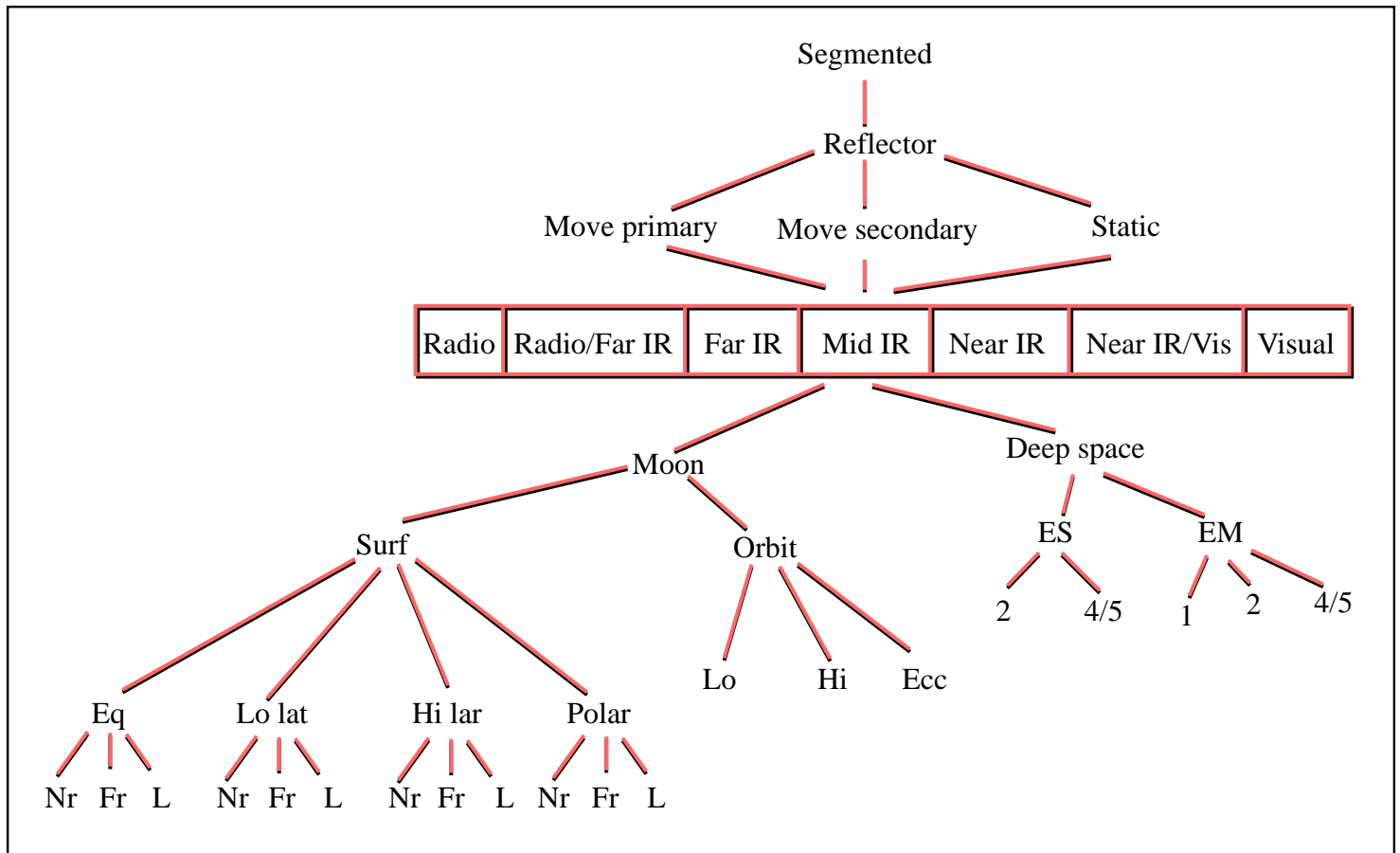


Figure 24. Concept tree for segmented reflecting telescopes. Figure by MIT OpenCourseWare.

By trimming the infeasible concepts immediately via the tree method, the total number of concepts available was cut from 6048 to approximately 2400. (Note that the tree in Figure 24 has only 420 possible concepts.) Further cuts in trees were conducted after better metrics were established, and trees were subsequently trimmed in greater detail.

The first development cycle culminated in a meeting during which the various concepts developed were discussed in detail. Duplications of concepts were removed, and approximately

twenty concepts were selected for ranking and further downselection. These concepts were split into three main sub-areas, based on common technology, after discussion. The three areas include near-IR/Visual, Far- or Mid-IR, and radio wavelength regimes.

6.4.2 Second downselection cycle

The second method for downselecting from the remaining possibilities involved the use of the Pugh method of concept ranking. Fifteen of the top concepts were quantitatively ranked against a baseline using 20 metrics based on performance requirements and implementation constraints. The resulting seven concepts were designated for further investigation. Figure 25, below, shows an example of Pugh rankings.

<u>Metrics for FIR Telescopes</u>	Baseline: JWST	Sparse Reflector Moving Primary Lunar Equatorial	Sparse Reflector Moving Primary Lunar Polar Crater	JWST Monolithic Reflector Lunar crater	JWST Monolithic Reflector Lunar surface equator
Can meet one science program	0	0	0	0	0
All components fit on Ares V	0	0	0	0	0
In cislunar space	0	0	0	0	0
Angular resolution	0	1	1	0	0
Wavelength range	0	0	0	0	0
Sky viewed over 1 year	0	0	-1	-1	0
Field of view	0	0	0	0	0
Mass	0	1	1	0	0
Delta-V required	0	-1	-1	-1	-1
Cost	0	0	-1	-1	-1
Single-fault tolerance	0	1	1	0	0
Capability can be increased	0	1	1	0	0
Capability can be restored	0	1	1	0	0
Leverages manned program	0	1	1	1	1
Complexity (# of parts)	0	-1	-1	0	0
Technology Readiness Level	0	-1	-1	0	0
Ability to spread cost over time	0	0	0	-1	-1
Ability to start and stop funding	0	0	0	-1	-1
Ability to be spread over districts	0	0	0	0	0
Incremental deliverables	0	1	1	0	0
Public wow factor	0	1	1	1	1
Extra science programs met	0	1	1	0	0
Total Score:	0	6	4	-3	-2

Figure 25. Exemplar Pugh matrix for Far-IR telescopes.

6.4.3 Concept review and final development

The final seven concepts were compared using utility analysis based on the ability of each concept to meet the candidate science programs, and three concepts were presented at the second external review, during which the concepts were carefully evaluated. Of these concepts, two were retained for final maturation, as both concepts showed promise. These two concepts appear as the reference designs in Sections 7 and 8.

7. Lunar Interferometric Radio Array (LIRA)

This section discusses one of the top two selected concepts, developed into a reference design. The concept is an array of simple dipoles operating in the radio band, situated on the far side of the Moon. Details of the science objectives and the subsystems design are described in this section.

7.1 Approach and Assumptions

7.1.1 Design approach

The design of the LIRA telescope was done using a Microsoft Excel-based model similar to a modified and tailored version of ICEMaker [see 31]. Each of the subsystem designs is implemented in one to two worksheets. The parameters that are passed between the subsystems are managed on a central repository worksheet functioning as a simplified version of the ICEMaker central server.

This approach makes feasible a straightforward calculation of the system's science output per unit cost, which is detailed further in Section 7.9.3. Because of the structure of the model and the central repository worksheet, it was possible to maintain all of the key technical parameters and their relationships in a single location. Figure 26 summarizes the relationships between these parameters, and Figure 27 serves both as a key for Figure 26 and as the central repository of all parameter values in the LIRA telescope design.



Figure 26. N² diagram of the major relationships between parameters in the LIRA telescope design. The outputs of each subsystem or function are listed down the columns, and the corresponding inputs are shown across the rows.

MODULE OUTPUTS

Architecture Constants Vector		Electronics	
1 - Dipole Separation	0.15 wavelengths	31 - Computer Mass	68.2 kg
2 - Minimum Frequency	10 MHz	32 - Computer Cost	\$28.20 M
3 - Maximum Frequency	130 MHz	33 - Computing Power Required	226 W
4 - Instrument Bandwidth	32 MHz	34 - Central Computer Output Data Rate	0.839 Gbps
5 - Lunar Day Length	29.53 Earth days		
Design Vector		Communication System	
6 - Design Frequency	100 MHz	35 - Central Communication System Mass	9.95 kg
7 - Field of View (FOV) at Design Frequency	35 deg	36 - Central Communication System Power	3.86 W
8 - Signal-to-Noise Ratio (SNR) at Design Frequency	4	37 - Cluster Transmitter Mass (per Cluster)	0.785 kg
9 - Angular Resolution at Design Frequency	10 arcsec	38 - Cluster Transmitter Power (per Cluster)	0.2944 W
10 - Integration Time to Achieve Desired SNR	3000 hrs	39 - Total Communication System Cost	\$6.53 M
11 - Latitude of Array	65 deg	40 - Relay Mass (including Power Needs)	27 kg
12 - Longitude of Array	50 deg	41 - Number of Subrelays	24
13 - Type of Central Power System	Solar		
14 - Type of Cluster Power System	Solar	Power	
15 - Leverage Human Base	N	42 - Central Power Mass	396 kg
16 - Telescope Duty Cycle at Night	1.00	43 - Total Power Cost	\$1.67 M
17 - EOR Resolution	15 arcmin	44 - Cluster Power Mass (per Cluster)	19 kg
18 - Number of Cassini RTG Material Equivalents	1		
Environment		Structures and Mechanisms	
19 - Maximum Eclipse Duration	495.104 hrs	45 - Cluster Structure Mass	33.25 kg
20 - Percent Illumination	0.70	46 - Total Structures Cost	\$71.49 M
21 - Attenuation	-32.44 dB		
22 - Angle Past Limb	5 deg	Deployment	
23 - Minimum Deployment Distance to Limb	151 km	47 - Deployment Hardware Mass	1007.25 kg
		48 - Deployment System Cost	\$256.62 M
		49 - Number of Launches Required	1
Array Design		Figures of Merit	
24 - Total Number of Antennas	3440	50 - Scientific Figure of Merit	7.32
25 - Number of Clusters	215	51 - Total System Mass	16,985 kg
26 - Dipole Length	0.7495 m	52 - Launch and Space Segment Cost	\$1,715.64 M
27 - Array Diameter	51.8 km	53 - Ground Segment Cost	\$271.46 M
28 - Cluster Area	24.1 m ²	54 - Total Development Cost	\$1,987.10 M
29 - Operating Power per Cluster	11 W	55 - Annual Operating Cost	\$31.03 M/yr
30 - Cluster Data Rate	0.054 Gbps		

Figure 27. All important technical parameters in the LIRA telescope design. The numbers and color codes correspond to those used in Figure 26.

The following sections describe the detailed design of the system. The details of the overall cost estimation will be discussed in Section 9.

7.1.2 Concept-specific requirements

Table 9. Requirements for LIRA.

Req #	Requirement	Priority	Rationale
1	The system shall be capable of collecting radiation in the radio band.	A	
1.1	The system shall collect radiation in the following wavelength ranges: 2 m to 30 m.	A	These wavelengths represent the relevant ranges of the radio band.
1.2	The system shall provide a minimum angular resolution of at least 10 arcseconds, depending on exact wavelength.	A	The exact resolution and optimum wavelengths required to observe the EOR in detail are not yet confirmed.

Req #	Requirement	Priority	Rationale
1.3	The system shall provide enough collecting area to observe the EOR signal.	A	Observation of the EOR is the primary science goal for this system.
2	The system shall be able to view TBD degrees of the sky in one year of operation.	B	TBD
2.1	The field of view of the system shall be 900 sq. deg.	B	TBD
3	The system shall be located on the lunar surface.	A	To leverage NASA's current Constellation program architecture and benefit from the radio-quiet environment.
3.1-n	The system shall be capable of surviving in the environment of the lunar surface.	A	
4	The system shall be able to communicate data back to Earth.	A	Data must be analyzed by Earth-based systems.
4.1	The system shall have a data rate of 10's of Mbps.	B	Exact transmission data rate is sized based on the number of dipoles in the system.
4.2	The system shall transmit data in the Ka band.	C	The Ka band allows the use of the Deep Space Network.
4.3	The system shall transmit data to a downlink station.	B	A downlink station provides access to ground stations via radio link without compromising the radio-quiet environment of the Moon's far side.
5	The entire system payload shall fit into less than 1 Ares V booster vehicle and have a throw weight no greater than the maximum throw weight of 1 Ares V booster.	B	Ares V booster will leverage NASA capabilities.
5.1	The mass of system components launched on a single Ares V shall be less than 18 metric tons.	A	LSAM surface payload capability [7]

Req #	Requirement	Priority	Rationale
5.2	The system shall be able to survive launch loads as defined in the Ares V users guide.	A	
6	The system shall have an operational lifetime of at least 10 years.	B	A lifetime of a number of years allows for detailed observation of large areas of the sky, as well as investigation of potential targets for serendipitous science.
6.1	The system shall have a reliability of at least TBD.	B	TBD
7	The system shall have provisions for incorporating new elements (antennas, instruments, etc.).	B	Incorporation of new elements may permit increased resolution of the EOR and improved performance in the primary scientific goal for this system.
8	The system shall have a cost of the same order of magnitude as telescopes with similar scientific objectives.	A	The system needs to deliver higher value to the major stakeholders for a cost either lower than or equal to other proposed programs.

7.1.3 Science goals

The key science drivers addressed by this telescope concept include: the Epoch of Reionization (EOR), extrasolar planets (XSP), solar science, and serendipitous science. These science drivers provide the motivation for the construction of this telescope.

The EOR measurement consists of measuring the redshifted 21-cm hydrogen line in the early universe. Before the universe created the first stars and galaxies, it consisted of neutral hydrogen that emits radiation at 21 cm (1.4 GHz). The frequency of this line is decreased with time due to the redshift caused by the expanding universe. As the first stars and galaxies formed, the energy produced by these objects ionized the hydrogen, which stops this line from being emitted. Determining the time and quality of this transition gives information on the way the first stars and galaxies formed. The signal is predicted to be redshifted into the low frequency radio regime, below 200 MHz.

Extrasolar planets with magnetic fields may also emit low frequency radio emission that can be detected with a lunar dipole array. Emission typically arises from the interaction of stellar-wind powered electron currents when they interact with the planetary magnetosphere. As Lazio et al [32] note, there is a correlation between planetary mass and emission wavelength such that observations above the Earth's ionosphere are needed to detect emission from sub-Jovian mass planets.

In addition to these major scientific objectives, another science goal is the study of particle acceleration and magnetic fields in the Sun. A radio observatory located above the Earth's ionosphere would provide a unique imaging capability at low frequencies, giving a previously unseen look at these processes.

Serendipitous science is another important key goal that this telescope system will provide.

Extremely low frequency radio astronomy is not possible due to the Earth's ionosphere, and high sensitivity observations at these frequencies in the vicinity of the Earth are precluded due to the strength of the Earth's own aural radio emission. Consequently the lunar far side provides a unique location that will allow high sensitivity observations a frequencies never before explored. As such, the conduction of serendipitous science, including the potential discovery of new astrophysical processes or objects, is a very real possibility with this telescope concept.

7.1.4 Location

The location of the telescope is driven in part by the need to take advantage of the Moon's uniqueness as a radio-quiet location near the Earth. This need dictates that the telescope be located somewhere on the Moon's far side. This section analyzes further the relationship between the telescope's proposed location and the utility of the location. Results of the utility analysis of location are used to inform further design efforts and are incorporated into the design model described in Section 7.1.1.

Noise attenuation

The attenuation of Earth-originating noise at any location is a function of the angle from the near side of the Moon. While little experimental data exists to confirm noise attenuation estimates, analytic studies have predicted the amount of noise attenuation on the Moon's far side. The results in Figure 28 are for a 50 kHz wave, which was used to estimate noise attenuation for all frequencies.

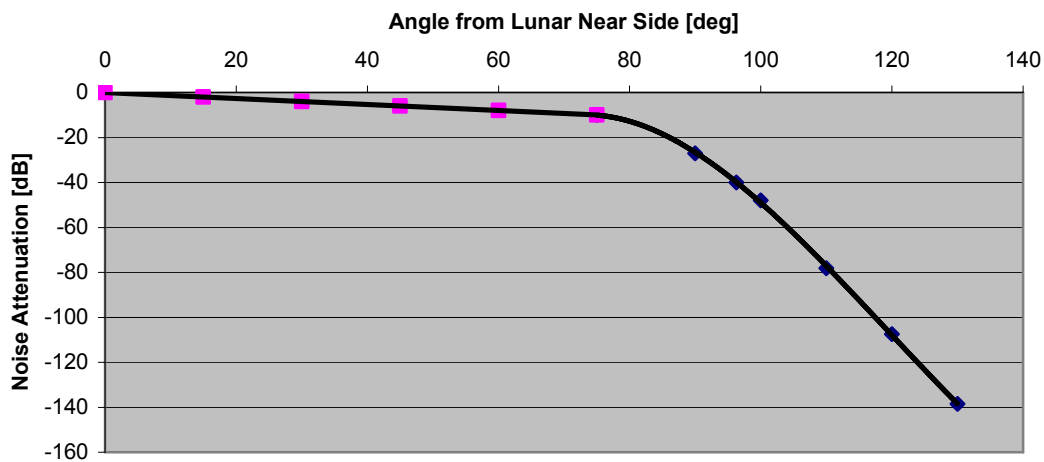


Figure 28. Lunar noise attenuation from the lunar far side.

Sunlight illumination fraction

For most latitudes, the lunar surface is illuminated 50 percent of the time. However, in the polar regions, the higher elevations receive up to 80% illumination, as shown in Figure 29. The relationship in Figure 31 between angle from lunar nearside and maximum illumination fraction was estimated from Figure 29.

Image removed
due to copyright
restrictions

Figure 29. Lunar polar sunlight illumination fraction [33].

Utility analysis

To compare potential telescope locations, a utility analysis was developed, in which total utility is assumed to be made up of three components: noise attenuation, sunlight availability, and angular resolution. Each component utility is normalized between zero and one and the total utility is simply the product of the three component utilities.

Noise attenuation utility is a function of the local noise attenuation at the location of the dipole array. Zero utility corresponds to the zero noise attenuation from the lunar noise environment. A utility of 1 corresponds to a noise attenuation of -40 dB. This roughly corresponds to the level of cosmic background noise. A plot of the attenuation utility is shown in Figure 30.

Light availability utility corresponds to the illumination fraction and is a function of the angle from the nearside of the Moon.

Angular resolution utility gives value to how finely the epoch of reionization can be resolved. Zero utility corresponds to an angular resolution of one degree while a utility of one corresponds to an angular resolution of 0.5 arc minutes. The utility decreases linearly with the log of angular resolution, as shown in Figure 32.

In addition to these utility measures, a mass model of the system was also developed. The mass model presumed a relationship between system mass and afforded angular resolution, using the number of dipoles as a parameter for both mass and angular resolution, with an estimate of the angular resolution necessary to perceive the EOR as a guideline. The mass model allowed a constant mass for deployment, a mass per dipole, and a mass for computing and processing equipment. The mass of the power system in this preliminary analysis was written as a function of the power source (RTGs or solar arrays) and the proximity to a lunar base which provides free power.

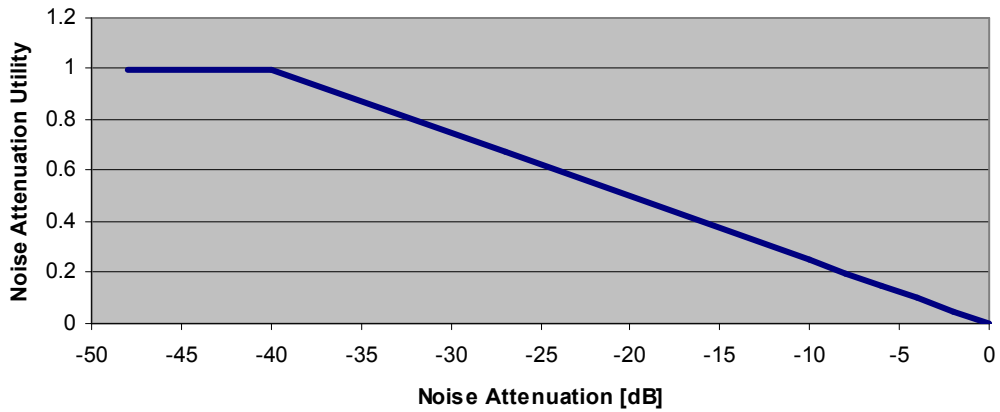


Figure 30. Noise attenuation utility.

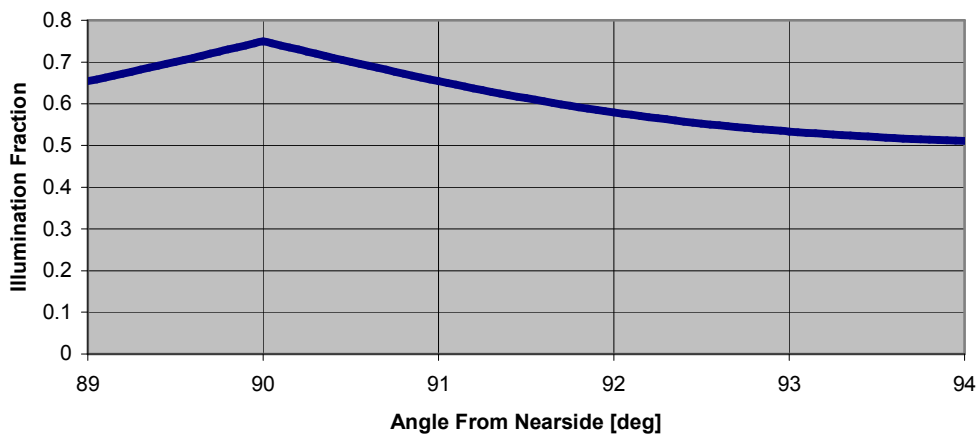


Figure 31. Illumination and utility versus angle.

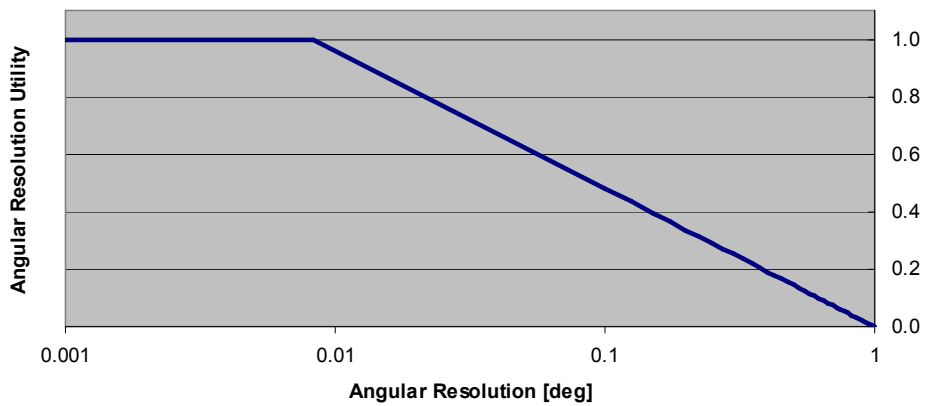


Figure 32. Angular resolution utility.

Results

The mass model delivers a component mass output based on the desired angular resolution and the choices for power source and deployment method, as shown in Figure 33.

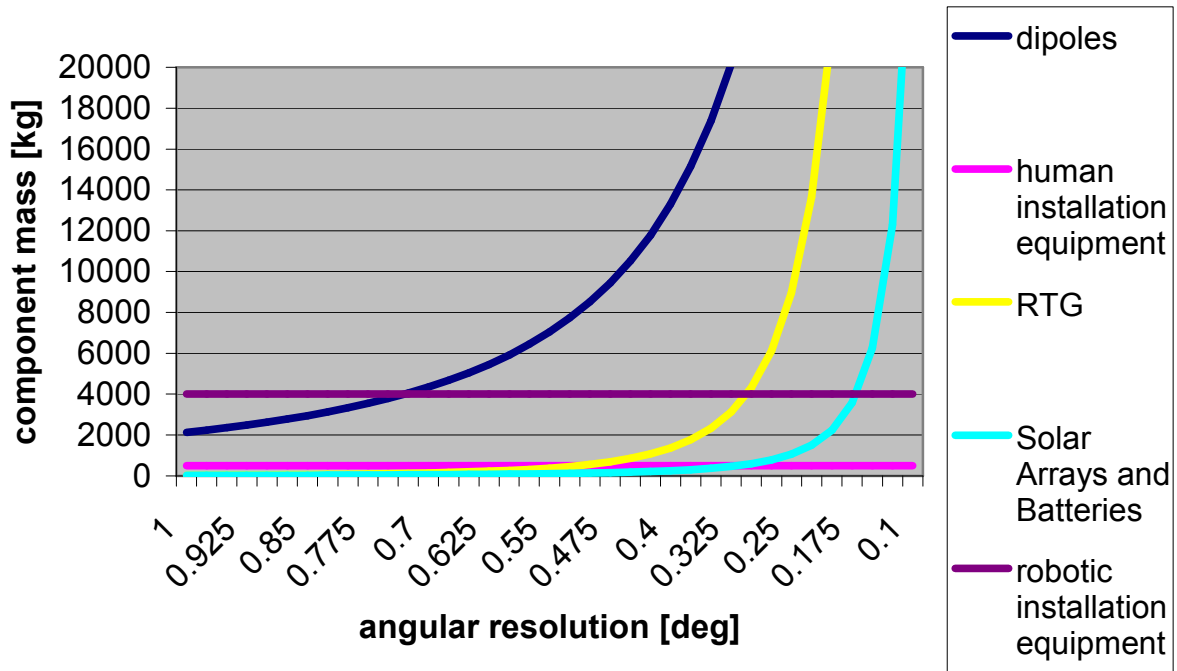


Figure 33. Component masses.

In order to arrive at the optimal preliminary design based on the utility analysis, the total utility per unit mass was plotted against angular resolution for three different concepts. In the lunar base concept, it is assumed that the array is located 20 km away from a polar lunar outpost and leverages the human presence to construct the array. In the lunar base free power concept, the array is located 10 km from the polar lunar base and receives power from the base's power generation capability. The only mass associated with the power requirement is the mass needed to transmit the data from the array to the lunar base. In the far side concept, the array is installed on the far side of the moon robotically at a location where the noise dissipation utility is maximized. Results of the utility analysis are shown in Figure 34.

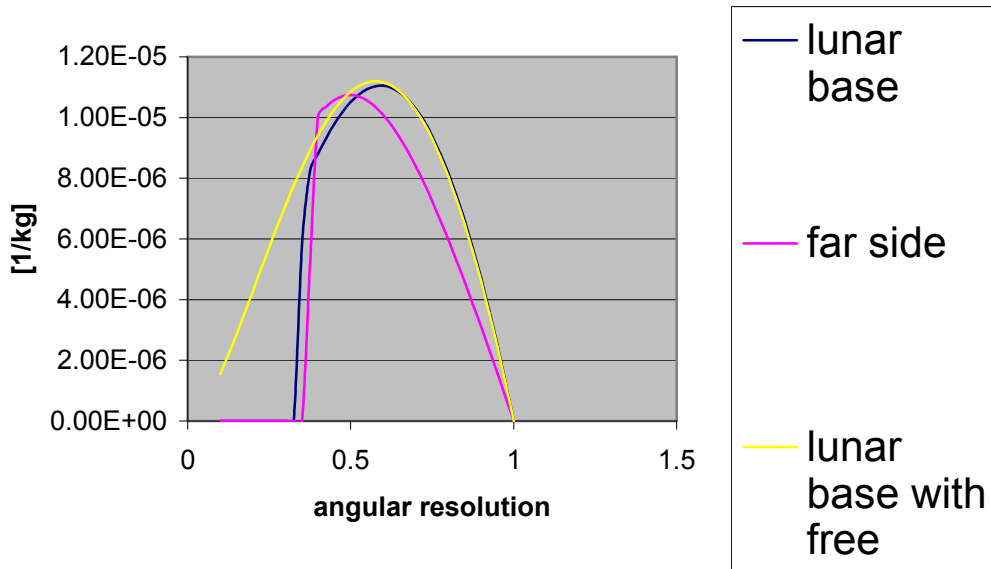


Figure 34. Utility versus angular resolution.

Each of the three concepts achieves maximums in the same region, at an angular resolution between 0.5 and 0.6 degrees. Characteristics of the optimal designs for these three cases are summarized in Table 10.

Table 10. Optimal value ranges.

Characteristic	Unit	Range of values
Angular Resolution	Deg	0.5-0.6
Total Mass	kg	6080-13700
Power System Mass	kg	270-560
Installation Mass	kg	500-4000
Antenna Mass	kg	5000-8500
Communication Mass	kg	150 – 400
Number of Dipoles	#	5300-7600
Number of Dipole Clusters	#	164-237
Power Requirement	kW	2.7-5.6

The ranges of design parameters developed from this preliminary analysis and listed in Table 10 inform further development of the LIRA telescope.

7.2 Instrumentation and Radio Array

7.2.1 Introduction

The overall design of the LIRA telescope was conducted using a top-down approach, starting with a set of desired preliminary reference capabilities which were then used to determine the more detailed characteristics of the array. This process allows the input reference capabilities, which are directly related to the resultant scientific value of the instrument, to flow into the more physical requirements of each subsystem. The epoch of reionization (EOR) is a principal driving scientific objective of the telescope, and is one of the more difficult scientific objectives to meet.

Consequently, the array design was conducted by requiring that the final design have the capabilities to observe the EOR. Based off of this requirement, and the specified observational attributes used to satisfy this condition, an overall set of array requirements are generated.

The basic form is an interconnected array of low frequency (10 to 130 MHz) dual-polarization dipole antennae. By combining these antennae into an interferometer, the antennae can be used to collect and determine the direction and other properties of incoming photons. The dipoles will be grouped into clusters, which will then each be connected to a central digital correlator to interfere these signals and produce radio measurements of the sky. The array will be located on the far side of the Moon, shielded from Earth's auroral radio emission, which will allow unimpeded observations of very low frequency radio bands that are normally hindered or totally obscured by the Earth's ionosphere, allowing access to previously inaccessible scientific investigation.

7.2.2 System definition and interfaces

The array design takes a set of capabilities-driven parameters as inputs. The selection of these inputs was designed to strike a balance between completely specifying the nature of the array and maintaining a suitable degree of simplicity such that the inputs can be effectively quantified and modeled. The inputs to the array design are:

- *Design Frequency* – Several of the system attributes are frequency-dependent (such as angular resolution, field of view and sensitivity). The design frequency is the frequency at which these frequency-dependent attributes are evaluated.
- *Instrument Bandwidth* – This parameter describes the amount of instantaneous frequency coverage that the instrument can accommodate.
- *Field of View (FOV) at design frequency* – This parameter describes the angular width of the square field of the sky that the array will obtain useful data from in a single observation.
- *Signal to Noise Ratio (SNR) of the EOR at design frequency* – This parameter describes how strong a detection the instrument will be able to make of the EOR signal after a specified integration time.
- *Angular Resolution at design frequency* – This parameter describes the maximum angular resolution of the array.
- *EOR Resolution* – This parameter describes the spatial resolution at which the EOR will be observable at the specified SNR in the specified integration time. This parameter is introduced to allow the optimization of the system for observing the EOR, while allowing a higher angular resolution for the total array, which would be useful for other scientific goals. By having a lower spatial resolution of the EOR, the instrument does not need the same sensitivity as it would if it were to be able to observe the spatial variations of the EOR over each of its pixels.

Using these inputs, and a number of relevant constants (both physical and architectural) a telescope configuration is calculated. The parameters of this configuration are then passed as inputs to other subsystem designs. The resulting output parameters from this process are:

- *Total number of antennae* – The total number of dipole antennae in the array.
- *Number of clusters* – The total number of clusters in which the dipoles are grouped. Each cluster is individually beamformed in order to give a decent field of view while minimizing the eventual data rate.
- *Dipole length* – The horizontal length (tip-to tip) of each antenna.

- *Array diameter* – The separation between the two most separated clusters in the array.
- *Cluster area* – The area of each cluster, assuming the clusters are of square geometry.
- *Operating power per cluster* – The amount of power used by each cluster for the amplifiers and beamformer.
- *Cluster data rate* – The resultant data rate from each cluster’s beamformer.

7.2.3 Assumptions and ground rules

In order to simplify the array design process a number of assumptions were made. These assumptions are as follows:

- *The performance of the array is independent of its UV distribution.* This analysis was conducted without considering the effect that the arrangement of the clusters will have on the overall performance of the array and what useful science it can do. The distribution of clusters, and the resulting way in which the UV plane is filled will have a strong impact on the response point spread function (PSF) and will affect the spatial scales on which the array is sensitive. Furthermore, the cluster distribution will affect the deployment of the array and communications requirements of the antenna tiles. Although a more thorough analysis of the distribution of the clusters is important before any eventual deployment of the array, it will not have major effects on a first-order estimate of the system properties.
- *Antenna Geometry* – The size/geometry of the antenna was assumed to be equal to 0.75 meters (1/4 wavelength at 100 MHz) and the antennae were spaced with 0.45 meters between their tips (0.15 times the wavelength at 100 MHz).
- *Antenna Properties* – During the analysis, the properties of the precise electrical/RF properties of the antennae were given assumed values and capabilities. The antenna system was given an “efficiency” of 80%, which corresponds to the percentage of incident radiation that is coupled into the telescope system (for comparison, a value of 60% was used for radio array estimates by Carilli, Hewitt & Loeb [34]). Furthermore, it was assumed that this efficiency remains constant across the entire band. The overall possible bandwidth range of the antenna design was assumed to be 10-130 MHz. The antenna effective collecting area was assumed to be equal to λ^2 , which assumes the dipole has a degree of directivity. It was also assumed that the electronics draw 0.5 W for the amplifiers in each antenna, and that each cluster beamformer draws 3 W.
- *Cluster Geometry* – For ease of deployment and structure design, it was assumed that each individual cluster will have a square geometry. Under this assumption, each cluster can have only perfectly square numbers of antennae, and will have equal width and height.
- *Bandwidth/Channels* – The total instantaneous bandwidth of the instrument was assumed to be 32 kHz, divided into 8 channels of 4 MHz each. This assumption is based on the capabilities of Earth-based radio arrays of similar form.
- *System Temperature* – The assumed receiver noise temperature was taken as 100 K, similar to estimates used for other radio dipole arrays.
- *Sky Temperature* – The background sky temperature varies with frequency and following Carilli, Hewitt & Loeb [34] was taken to have a value in degrees Kelvin of:

$$T_{sky} \sim 100 \left(\frac{\nu}{200 \text{ Mhz}} \right)^{-2.8} \quad (\text{Eq. 3})$$

7.2.4 Calculations

Number of Dipoles

In order to determine the number of dipole antennae required for the array, the chief science driver – being able to observe the Epoch of Reionization (EOR) – was first considered. Given the basic assumption that the array is required to get adequate signal to noise to observe this signal in a reasonable amount of time, it was then possible to determine rough estimates of the eventual form of this array.

Calculation of the array sensitivity is based off of the fundamental radiometry calculations of Carilli, Hewitt & Loeb [34], Wrobel and Walker [35], and Woan [36]. The basic equation to calculate the sensitivity of a radio interferometer is:

$$\text{Sensitivity} = \frac{2k_B T_{\text{sys}}}{A \eta N} \cdot \frac{1}{\sqrt{\nu \cdot \tau}}, \quad (\text{Eq. 4})$$

where k_B corresponds to Boltzmann's constant, T_{sys} is the effective system temperature, A corresponds to the effective area of each dipole, η represents the efficiency of the telescope, N represents the number of dipoles, ν represents the instrumental bandwidth, and τ represents the integration time. Calculating the necessary sensitivity needed to observe the EOR and using it with this equation allows a calculation of the number of dipoles necessary for the instrument.

In order to fully use this equation several other quantities must be determined. Following Carilli, Hewitt and Loeb [34], a radio dipole has a wavelength dependent approximate effective collecting area of:

$$A \sim \lambda^2, \quad (\text{Eq. 5})$$

with λ being the observational wavelength. Additionally, the system temperature is determined by combining the contributions from the effective instrument temperature (assumed to be 100 K) and the sky temperature:

$$T_{\text{sys}} = T_{\text{Sky}} + T_{\text{Inst}}, \quad (\text{Eq. 6})$$

with

$$T_{\text{sky}} \sim 100 \left(\frac{\nu}{200 \text{ Mhz}} \right)^{-2.8}, \quad (\text{Eq. 7})$$

in degrees K, with ν being the observational frequency.

In order to calculate the necessary sensitivity for the EOR measurement, a temperature of 10 mK was assumed for the EOR. The flux from this signal was calculated according to the relation:

$$S_{\text{EOR}} = \frac{\theta^2 T_{\text{EOR}}}{1360 \lambda^2}, \quad (\text{Eq. 8})$$

where S_{EOR} is the flux of the EOR signal (in Janskys), θ is the angular resolution of the EOR signal, T_{EOR} is the assumed value of 10 mK, and λ is the observational wavelength in centimeters.

Using the above relations and the assumption that the EOR flux must reach 4 times the sensitivity of the instrument (4σ) after 2000 hours of integration, with a bandwidth of 4 MHz (see assumptions in Section 7.2.3), the number of required dipoles in the entire array was calculated.

Array Size

The diameter, D , of the array is determined by the required maximum angular resolution, θ , that the array will achieve according to the standard formula:

$$\theta = \frac{\lambda}{D}. \quad (\text{Eq. 9})$$

It is important to note that this resolution is the maximal resolution of the telescope, which is different than the resolution at which the instrument will make the EOR measurement. The EOR signal will only be detectable on larger spatial scales than the instrument is capable of making.

Cluster Size / Number of Clusters

The size of clusters used in the array is determined by the field of view desired. The antennae in each cluster are phased in realtime with delay lines to act as a single effective antenna from the point of view of the correlator. The field of view of a cluster is determined by a similar equation to the array size:

$$\theta_{FOV} = \frac{\lambda}{D_{Cluster}}, \quad (\text{Eq. 10})$$

where $D_{Cluster}$ is the maximum width of a cluster. Using the assumptions for the size of dipoles (0.75 m) and the minimum spacing between them (0.45 m) and the constraint that the cluster must be square, the maximal number of antennae per cluster is calculated.

Power Requirements

The power design requirements for each cluster are calculated by adding the power required for each antenna in a cluster with the power required by the electronics to synthesize each tile beam.

Data Rate

The data rate for each cluster is calculated using Nyquist sampling across the entire band. The data is then integrated for a particular integration time before being outputted from the cluster. This gives a data rate equation of:

$$\text{Data Rate} = \frac{2\nu P}{T} \times 2, \quad (\text{Eq. 11})$$

where ν is the bandwidth of 32 kHz, P is the sampling precision of 8 bits, and T is the integration time, assumed to be 16 seconds. The extra multiplicative factor of 2 comes in because 2 polarizations are being observed with the array.

7.3 Electronics Subsystem

7.3.1 Introduction

The electronics subsystem performs all command and data handling (C&DH) functions that are required by the telescope. The data handling functions will include receiving the data signal from each cluster, performing interferometry calculations, storing the data if required, and sending the data stream to the communications subsystem. Other functions include controlling the solar panels at the central hub and interpreting any command data uplinked from ground controllers.

7.3.2 System definition and interfaces

The electronics subsystem comprises all of the C&DH functions of the central processing unit. Each 16-antenna cluster will have an associated command and data handling unit which has been designed into the structure of the cluster and is not a part of this analysis.

The electronics subsystem will receive raw observation data from each cluster via a laser communication network. The output of the system will be the processed data passed to the downlink communications network and sent to the radio downlink station via a series of laser relays. Refer to Section 7.6 for the details of the communications subsystem.

7.3.3 Assumptions and ground rules

The starting analysis of this subsystem design utilized equations and assumptions from Chapter 11 in Space Mission Analysis and Design (SMAD) [37], which are valid for currently-existing electronic systems. However, the rate of improvement in electronics and computer design is very rapid, and a viable means of improving the best estimates and calculations for the electronics and computer systems, to ensure the estimates reflect the probable state of the art at the time when the telescope will be constructed, was sought. Broad Reach Engineering, a company which specializes in space electronics, was selected to provide industry input for this purpose. The information gathered during discussions with Mr. Pala Manhas [38], an engineer at Broad Reach Engineering, was incorporated into the design analysis and assumptions.

Specifically, the processors were assumed to be able to operate near their capacity of 1.575 Gbps. The amount of data to be handled provided by the cluster arrays is a couple of orders of magnitude above the reference values provided in SMAD and the “normal” values designed for industry use. Therefore, the assumption was made that the data inputs to the electronics modules could be directly connected to the data processing cards to provide the total 14 Gbps processing requirement. The last assumption was that the amount of data stored by the system was only that required to allow for brief periods of signal interruption with the Earth base station.

7.3.4 Development process and final design

Computing Power

For large arrays of dipoles, there is a non-trivial power level needed to process the data

before it is transmitted and stored. Interferometers such as LOFAR can require up to 150 kW of power to compress the data to a manageable rate. This power requirement is proportional to the number of distinct paths between dipole clusters of an interferometer, which is proportional to the number of array clusters squared. The following expression was used to estimate the data processing power requirement.

$$P = kn_c^2, \quad (\text{Eq. 12})$$

where P is the power required in Watts, k is a constant (set to 0.1), and n_c is the number of clusters, set to 215. This results in a power requirement of approximately 4.6 kW.

Industry Involvement

After discussions with Mr. Manhas [38], the C&DH component values from the SIRA presentation [39] were used as the basis for the design of electronics system. These values reflect the actual values used in the SIRA C&DH system and are a good estimate of the values which would be expected for the LIRA telescope. The component values are shown in Table 11.

Table 11. Command & data handling parameters for LIRA.

Parameter	Value
Weight	9.7 kg
Power	38 W
Length	25.5 cm
Width	20.5 cm
Height	18.5 cm
Cost per unit	\$4.7M

7.4 Power Subsystem

7.4.1 Introduction

Two separate power subsystems were designed for the LIRA telescope: a larger system for the central processing unit, which requires about 230 W, and a smaller system for each of the clusters, requiring about 12 W. A system with solar panels and batteries are chosen for the design in the end, but Radioisotope Thermoelectric Generators (RTGs) were also studied as an alternative.

7.4.2 System definition and interfaces

The central unit power system will provide power chiefly for the computer, which will process signals from all the antenna clusters in the array. The system will also power the

communications system in the central unit, which collects signals from the clusters and transmits processed data to the radio downlink station.

The cluster power system will provide power to the amplifiers of each antenna, the beam combiner electronics, and the communications systems on each cluster.

7.4.3 Cost, mass, and volume models and assumptions

A model for estimating power system cost, mass, and volume was created based on measured performance of existing technology. The same model, with the same assumptions, is used for both LIRA's and LIMIT's (see Section 8) power systems to ensure consistency between both proposed concepts. Solar power constants for this model are derived from [40]. RTG constants are calculated from historical Cassini metrics with the adaptation of a new Sterling engine for increased efficiency as represented in [41]. In light of the possible political ramifications of sending radioactive material to the Moon in the form of RTGs, a third hybrid power subsystem model was made, which incorporated RTGs, solar panels, and batteries, while allowing adjustment of the actual amount of radioactive material deployed on the Moon. In general, the constants used for power densities and unit costs are for current or near-future technology. It is expected that, by the year 2020 (when this project is expected to fly), these performance constants will have improved. Table 12 shows the constants used in building the power systems model.

Table 12. Power subsystem constants.

Battery Storage Density	130	W-hr/kg
Solar Panel Power Density	25	W/kg
Solar Panel Power per Unit Area	200	W/m ²
Solar Panel Unit Cost	\$300	\$/W
Lunar Day/Night Duration	709	hrs
RTG Power Density	14.9	W/kg
RTG Unit Cost	\$45,000	\$/W

The model pivots around the type of power system desired and the input for total system power required. Inputs relevant to the solar power system include the percentage of daylight available and adjustable duty cycle during the night. Total system power required is estimated for each system based on individually-relevant factors.

The total power required is calculated by summing the power required from each of the subsystems power demands, which are outputs of each of those respective models. Next, the required power to be provided by solar panels is figured using the following equation:

$$P_{solar} = \frac{\frac{(P_{day})(t_{day})}{0.85} + \frac{(P_{night})(t_{night})(D_{night})}{0.65}}{t_{day}}, \quad (\text{Eq. 13})$$

where P_{day} is the required daytime power, P_{night} is the required nighttime power, t_{day} is the duration of the day, t_{night} is the duration of the night, and D_{night} is the night duty cycle.

The amount of batteries required is a function of the power demand at night and the hours of

night. The total subsystem cost, mass, and volume is output for a solar panel and battery system. Both models also consider an RTG-based power system. The required RTG size and cost is calculated by dividing the total required power by the power density and unit cost. For this study, an RTG with a GPHS-Stirling power system is used. This thermal-electric power conversion system being developed by NASA will produce almost 5 times as much electrical power as the Cassini system will, using the same amount of radioisotope material [40].

Outputs include total system cost, mass, volume, and surface area for solar arrays. Cost of system complexity, deployment, and other related expenses are considered for system selection, even though they are not directly accounted for in this model.

7.4.4 Development process, trade studies, and sensitivity

The final design puts the RF telescope at 85 degrees latitude. This study assumes that sunlight availability is 70% at that latitude, which leads to a lunar night that is 210 hours long. The array was assumed to operate continuously and the power subsystem was sized accordingly, although provisions were made in the model to adjust the duty cycle of the telescope at night. It was found that the relationship between the duty cycle at night and the cost and mass of the system was linear with no optimal point. A high duty cycle is possible for more cost and mass, but more science can be returned with a higher duty cycle.

The central power subsystem model also contains a hybrid solar panel/battery and RTG power system. This model portion calculated the total mass and cost of a system that may be limited in the amount of radioactive material to be used. The trade study in this area rendered a linear relationship of mass and cost between a purely solar-powered system and a purely RTG-powered system with no optimal point.

With the deployment of 215 clusters the option of powering each with a small RTG was discarded. RTG use is not efficient for use on systems with less than 100 W of required power. In addition deploying 215 small RTGs is probably not politically possible.

For the power system of the central processing unit, the use of an RTG is reasonable, has the potential to be possible politically, and is much lighter (but slightly more expensive when transportation costs are added). Thus a solar-powered system was chosen. For larger telescope designs (possibly double the current design point in number of clusters), and possibly for a telescope located closer to the lunar equator, the cost savings of an RTG would significantly outweigh the political price.

7.4.5 Final subsystem design

The final design of the central processing unit power subsystem is a solar panel system with batteries that will deliver 230 W continuously under 70% sunlight availability. The mass of the batteries makes up 96% of the mass of the power system for the central unit, and the power system in turn makes up 85% of the mass of the central unit. The cost, including transportation of the power system, for the central unit makes up 46% of the total central unit cost, including transportation. Thus the power system, especially the amount of batteries, tends to dominate the cost of the central processing unit. Any improvement in battery technology will have significant positive effects on the total system.

The final design of the cluster power subsystem is a solar panel system with batteries, which will deliver 12 W continuously under 70% sunlight availability. Again the mass of the batteries makes up 96% of the mass of the power system for the clusters. The power system in turn makes up 36% of the mass of each cluster. The costs, including transportation of the power system for

each cluster, make up 33% of the total cost, including transportation. The power system, especially the batteries, is a significant portion of the cost of the clusters and the whole telescope array.

Table 13. Final power subsystems design values (solar-powered).

Central Processing Unit Power System		
Mass	396	kg
System Cost	\$145,301.00	\$
Total Cost w/ Transportation	\$27.87	\$M

Cluster Power System		
Single Cluster		
Mass	19	kg
System Cost	\$7,078	\$
Total Cost w/ Transportation	\$1,337,078	\$
215 Clusters		
Mass	4085	kg
System Cost	\$1.52	\$M
Total Cost w/ Transportation	\$287.5	\$M

7.5 Cluster Structure Subsystem

7.5.1 Introduction

The cluster structure provides packaging for the radio dipoles, cluster communications system, and cluster power system. In addition, it deploys the dipoles from its compact launch and lunar transportation envelope into the large envelope dimensions of a fully-activated dipole cluster.

7.5.2 System definition and interfaces

The structure subsystem is designed based on parameters from other subsystems. These parameters include the number of dipoles per cluster, cluster surface area, dipole length, array diameter, cluster transmitter mass, and cluster power mass. The structure subsystem outputs the total mass and cost of each cluster.

Specific inputs for the LIRA telescope design are 215 clusters, with 16 dipoles per cluster. The deployed area of a cluster is 24 square meters and each dipole has a length of 0.75 meters. The total array has a diameter of 62 km and contains 3440 individual dipoles.

7.5.3 Assumptions and ground rules

Each dipole was assumed to have a length density of 0.1 kg per meter of dipole length. The base mass of the structure was estimated to be 1 kg per square meter of deployed area. Cost for the structure system is estimated at \$10,000 per kg of cluster structure.

It is desired that the entire array of clusters be coplanar. As the array become larger, the curvature of the moon means that the outside clusters must be raised to remain coplanar with the center arrays. Therefore, an additional mass factor is used to penalize large arrays. This factor is given by $(1+R\cos(\theta/2))$ and doubles the mass of the cluster structure for one meter of needed offset.

7.5.4 Final subsystem design

Results of the cluster design are a 30.8 kg cluster mass, not including power and communication mass. The cost for each cluster comes to \$308,000 per cluster.

The mechanical design of each cluster packages the dipoles in a 1.6 by 1.6 meter thin square-shaped volume. This compact volume allows for easy packing for launch and lunar transportation. Illustrations of the folded and deployed clusters are shown in Figure 35 and Figure 36, respectively. Sixteen dipoles fold out from the four corners via a lightweight foldable structure. The final deployed area is a 4.8 by 4.8 meter square.

Batteries are stored at the base of the square footprint for stability. The cluster rests on the corners of the 1.6 by 1.6 meter footprint and includes a capability to level the dipole cluster on an uneven surface.

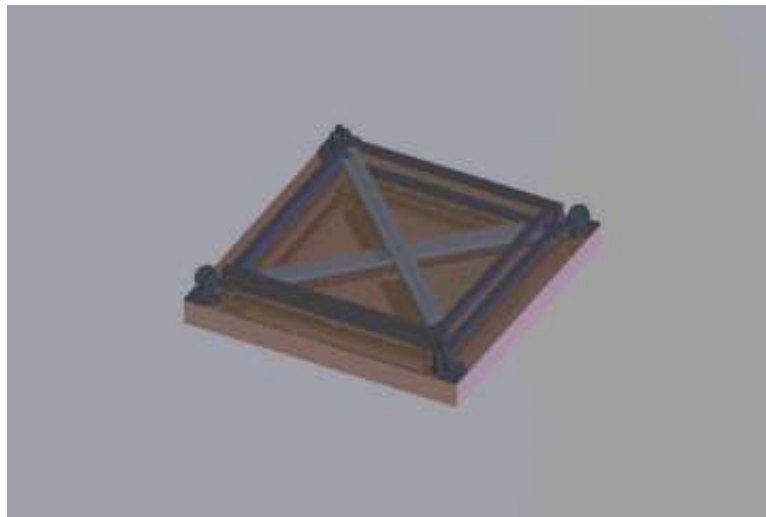


Figure 35. Folded LIRA cluster.

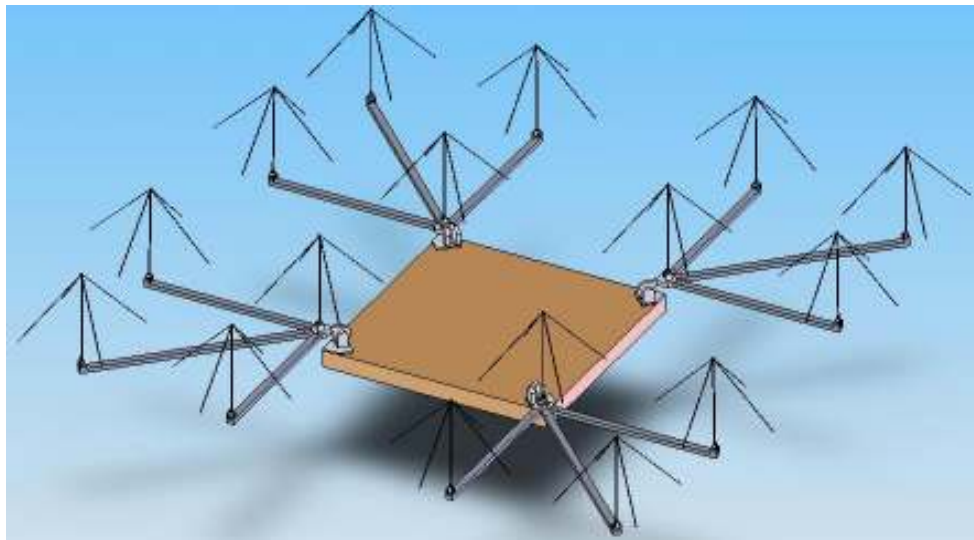


Figure 36. Deployed LIRA cluster.

7.6 Communications Subsystem

7.6.1 Introduction

The communications system is designed to carry data between the telescope location and the transmitter station, which will be situated at the end of a communications link to Earth.

7.6.2 System definition and interfaces

The communications system consists of three parts: the interior system, which carries data between clusters and the central processing station; the relay chain, which carries data to the Earth downlink station; and the downlink station itself, which communicates with Earth ground stations. The interior system interfaces with the electronics at the clusters and at the central station, where data preprocessing is carried out, and interfaces with the deployment systems for the purpose of laying the relay chain.

Analysis of mass, power, and cost of data processing is addressed by the design of the electronics subsystem, in Section 7.3.

7.6.3 Assumptions and ground rules

The communications system is sized according to the data rate to be carried, and because the data rate from the telescope to the ground stations will probably be much higher than the data rate from the ground to the telescope, the communications system is sized according to the downlink, not the uplink. It is assumed that tens of gigabits per second will flow down to the ground station, while only tens or hundreds of kilobits will be needed for periodic uplinked housekeeping and programming. These assumptions are based on the data rates for the JWST [42, 43] and the Spitzer space telescopes [44]. This data rate is the source of the initial consideration given to laser communications technology.

It is further assumed that laser communications systems, which are currently approaching the necessary Technology Readiness Levels for use in large-scale space systems, will be sufficiently developed that they can be included in the communications system. Scaling of laser communications systems was based on [45], and the figures used were for the largest system considered in [45]. Although laser communication at the predicted data rate has not yet been demonstrated, it is assumed to be feasible within the timespan allocated to design and implementation of this telescope, and has already been the subject of theoretical analysis [46].

Although the exact location of the telescope developed as the subsystems designs were evolved, it is also assumed that the telescope will be located somewhere on the far side of the Moon, to take advantage of the radio-quiet environment there.

Estimates of typical cost, diameter, and density for fiber optic cable and laser systems are taken from [47, 48], and the baseline costs of laser communications transmitters are estimated at \$5000 per kg, with radio systems baselined at \$1000 per kg, to reflect the relative differences in cost inherent in the difference in technological maturity.

7.6.4 Development process, trade studies, and sensitivity

For initial development of the system, a first-order model of the communications system was created. It was recognized that the first trades to be completed would involve internal communications system architecture, so the system modeled the cost of both a satellite constellation and a relay chain. The need for one or the other was driven by the assumption that the telescope would be located on the far side of the Moon. This assumption dictated that

the downlink signal be reflected to a point from which direct transmission to Earth would be possible. In order to preserve the radio silence and to prevent interference from the communications system, it was determined a priori that no radio transmissions would occur from the far side of the Moon. This necessitated either a physical cable link, a laser relay chain, or a laser-based satellite constellation. First calculations showed that a cable link might require up to an entire dedicated Ares V launch to bring up the required mass of fiber optic cable, and this was deemed untenable. A trade study comparing the estimated costs of a single satellite to a relay chain was conducted.

This preliminary trade study results are shown in Figure 37, where the horizontal axis displays different size estimates of the communications system. Smaller data rates and equipment masses are to the left, larger data rates and equipment masses are on the right. Note that the two systems scale similarly, but that an offset exists at all levels of cost.

It should be noted that the cost model includes only one satellite, where a constellation would probably be necessary to allow constant coverage, and that no allowance was made for orbit selection and stationkeeping or replacement costs, which would probably be higher than average for lunar orbits due to the orbital irregularities introduced by the mass concentrations (mascons) on the surface of the Moon. Noting this, and noting that cost may be an especially important factor to programmatic survival, especially in the early stages of development, it was decided that a relay would be a better architecture choice.

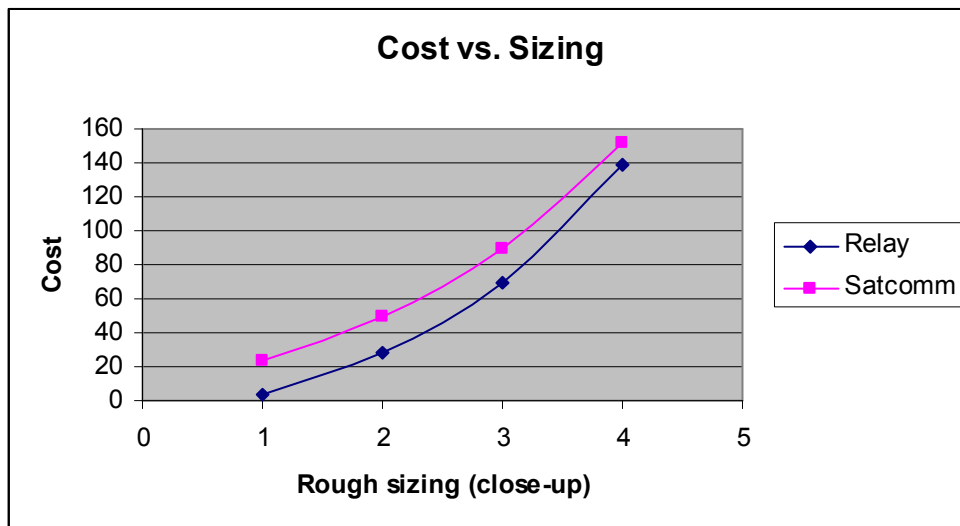


Figure 37. LIRA communications systems cost and size scaling.

A detailed parametric model was developed from the results of the first trade study, which allowed for fiber optic wiring inside clusters and small laser links webbing together all the clusters, with the central segment containing a main processor and the first leg of the relay chain. The small laser links were traded for fiber optic cables webbing together all the clusters after the mass of the cable required to connect a large-diameter array was found to be too large to include in one launch. The relay chain was also assumed to be laser-based, and analysis determined that the cost was dominated by the relay chain and the sublinks on each cluster, so that the location of the telescope could affect total cost significantly, as could telescope size and data rate.

It was noted that the relay could terminate at the human base, which would allow the

crew to download the data and then link it to Earth via their existing communications system, or the relay could terminate near the limb, which would allow direct communication with Earth ground stations. Although one choice entails the creation of a dedicated radio transmission station, this station is not overly large, and does not dominate cost concerns, so the choice of whether or not to leverage the human base is not as critical as the selection of the exact location of the telescope. In the end, the choice is left to future work on the LIRA telescope, as it does not represent an immediate impact on the current design.

A final trade study used the mini-ICEMaker (see Section 7.1) modeling tool to investigate whether it would be cheaper to process the data on site or to simply downlink it all to Earth. The relay costs would remain approximately the same, as would the interior system costs, but processing costs would change, as would end-station transmission costs and design, since a radio link would not be possible, given the anticipated data rates. This necessitated a laser link to Earth. Trade study analysis showed that the total cost decrease would be about 1% of initial estimated costs, if the system were redesigned to transmit all the data to Earth without on-site processing. However, a laser communications system large enough for the predicted data rate has a Technology Readiness Level of no more than 3, while the lower-data-volume system has a TRL of approximately 6. Development costs inherent to reducing this gap in TRL may be significant. Furthermore, the lower-volume system allows for the use of a radio link to Earth, which may or may not require the construction of a dedicated ground station. The high-volume laser link will, however, require a purpose-built ground station. Table 14 shows the comparison between the two systems.

Table 14. High-flow and low-flow data systems.

	Low data rate, radio downlink	High data rate, laser downlink
Mass	17,249 kg	16,680 kg
Power	2955 W	2492 W
Cost	1987.10 M\$	1951.65 M\$
TRL	6	3

It may be possible to re-optimize a trade in this design space at a later date, as technology progresses and development of laser communications systems continues. It should be noted that the savings in power for the higher data rate system translate to mass savings for the telescope, and that if pre-processing were to occur at the human base, a radio downlink might still be a viable option, as solar power is expected to be readily available at the human base.

7.6.5 Final subsystem design

Based on the selected architecture, more detailed design of the communications system was completed. The relays were sized and an overall architecture was laid out.

Interior subsystem

The telescope is arranged in a series of clusters of antennae, each of which is designed to feed into a small laser, which will then beam the cluster's data to a central collector and processor. Figure 38 shows this design.

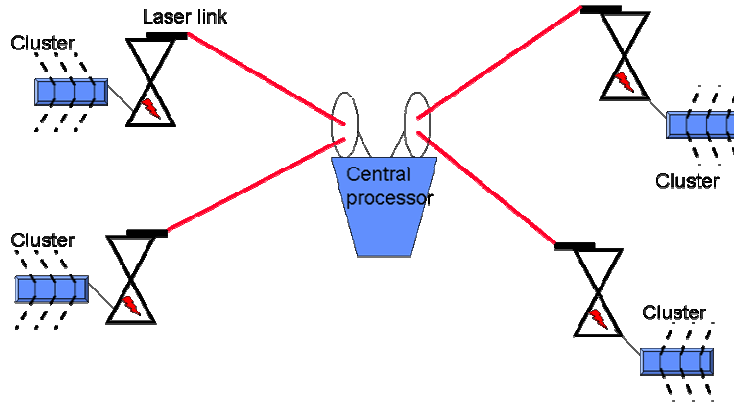


Figure 38. Interior communications system arrangement.

Relay subsystem

The details of the relay system can be seen in Figure 39. Link budgets from [49] showed that the radio link at the far end will be approximately the same size for downlinking to either the human base (for retransmission) or to the Deep Space Network (for direct reception by Earth ground crews). The antenna is set to the Ka-band, operating at 32 GHz. For the distance scales under consideration, the data rate expected ought to be attainable via Ka-band radio [50].

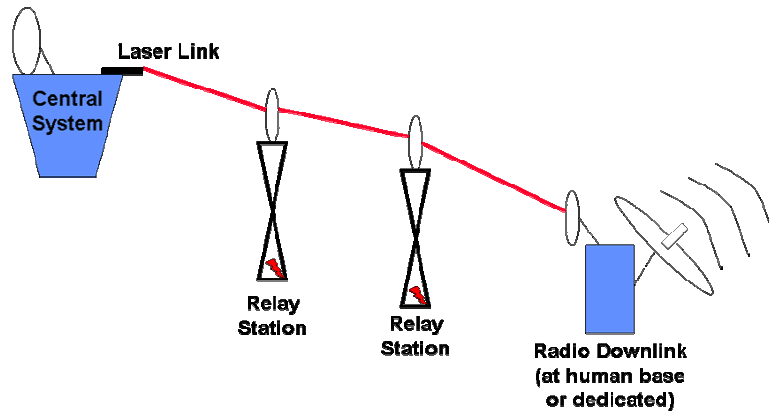


Figure 39. Relay subsystem.

Overall system

The system as a whole functions as conceptually illustrated in Figure 40, as a web of laser connections to a central point, from which a relay chain carries the signal to a downlink station.

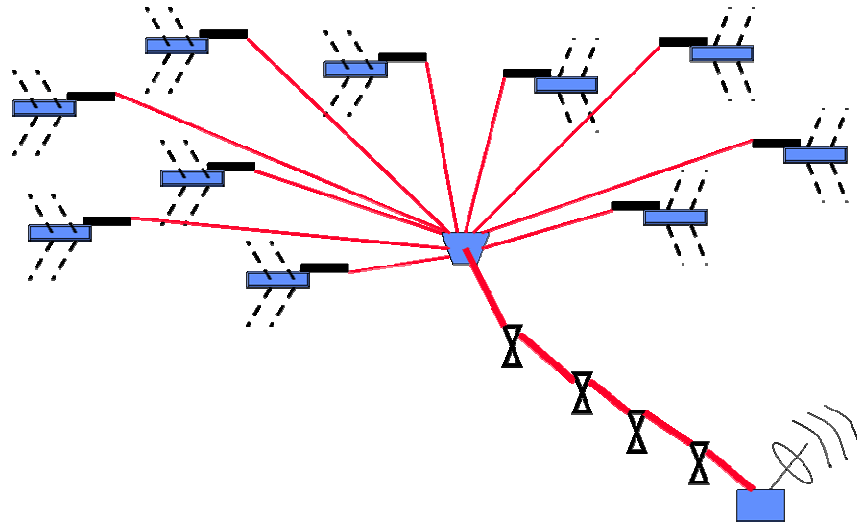


Figure 40. Total system view.

System characteristics and performance

The relay elements of the system were designed to be collapsible, self-sufficient, and reliable. Accordingly, each deploys from a 1-m high storage mode to a 3-m high transmission mode, as seen in Figure 41 to Figure 43 below. The outer shell and the structural elements are titanium alloy, chosen for strength, weight, and resistance to temperature changes; the interior sections are sealed and contain batteries and a suite of motors and acquisition-pointing-tracking (APT) mechanisms. The uppermost section, which telescopes out of the lower two, is covered with miniature solar arrays to provide power when needed, and crowned by an optical laser lens.

The optical package, seen in detail in Figure 44, requires no power. It simply accepts the laser beam from the previous relay, refocuses it, bends it slightly around the curvature of the Moon's surface, and sends it on to the next relay. Power is required for extension during deployment, initial acquisition, and aiming adjustments after disturbances (e.g., meteor impact nearby). Accordingly, the largest power drain is at the start of the lifetime of the solar arrays and batteries, and therefore degradation will not interfere with later performance. Furthermore, the power requirement is minimized by allowing for passive optical packages, although the internal mirrors are equipped with powered aiming systems, to allow for tight refocusing of the incoming beam and thus increase overall robustness of the relay chain. The fact that the laser relays will transmit through vacuum, and thus not be required to compensate for atmospheric attenuation, adds to the ability of the relay chain to successfully transmit data to the downlink station.

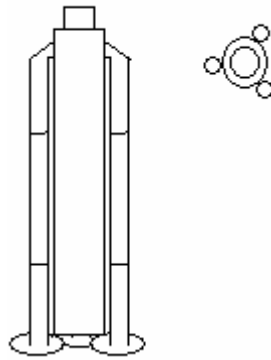


Figure 41. Storage mode, front and top views.

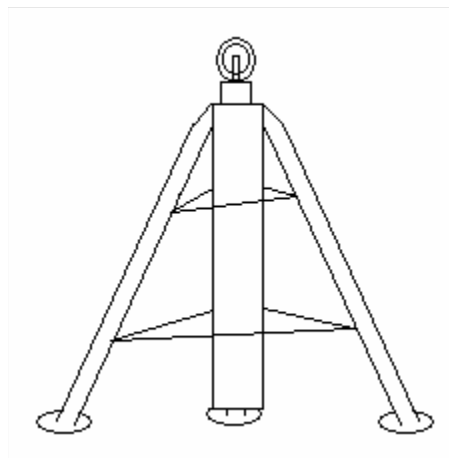


Figure 42. Partially-deployed standing mode.

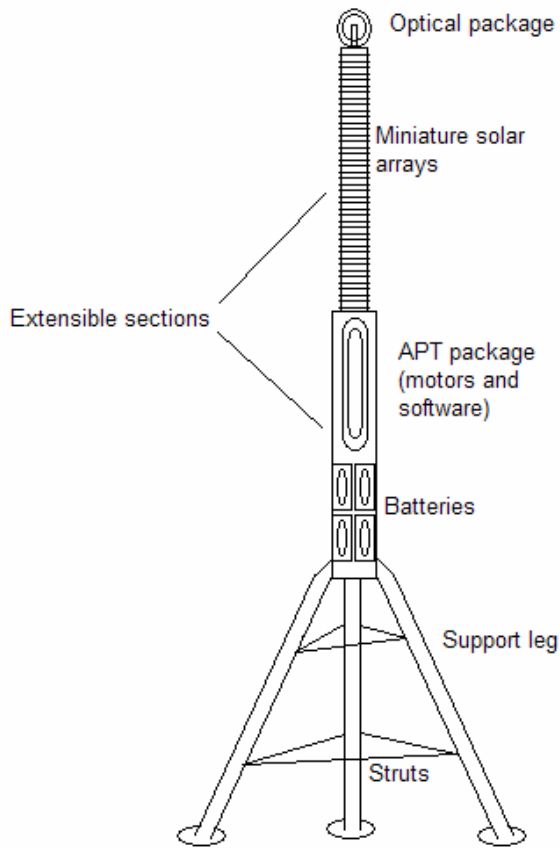


Figure 43. Fully-deployed relay.

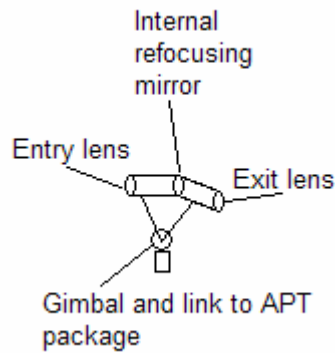


Figure 44. Relay optical package.

The estimated power, mass, dimensions, and cost of a relay appear in Table 15. The deployed height allows a spacing between relays of 6.45 km.

Table 15. Relay properties.

Mass	26 kg
Power	0.5 W or less each
Cost	\$27,750 each
Upper tube diameter	0.10 m
Middle tube diameter	0.15 m
Leg diameter	0.075 m
Stored height	1 m
Deployed height	3 m

7.7 Transportation Subsystem

7.7.1 Introduction

The transportation subsystem is responsible for transporting all telescope components from Earth to the desired location on the lunar surface.

7.7.2 System definition and interfaces

The transportation system is only concerned with the total mass of components to be transported. It is assumed that components are prepackaged with appropriate interfaces to the offloading system on the lunar landing vehicle.

7.7.3 Assumptions and ground rules

One of the objectives of this project is to leverage the lunar exploration architecture developed by NASA. Therefore, this system tries to use elements from the lunar exploration architecture wherever possible.

The main assumption is the availability of the Ares V launch vehicle, seen in Figure 45, with a Trans-Lunar Injection performance of 54.6 mT, as listed in the Exploration Systems Architecture Study report. Additionally, as an abort capability is not required on this mission, it was assumed that the transportation system may enter any orbit around the moon before descending to the desired location and that the same average delta-V was required to descend to the lunar surface from any of these orbits. This value was assumed to be 900 m/s, as a rough average of the delta-V required for human missions to different locations on the moon from [7].



Figure 45. Artist's conception of the Ares V launch vehicle [51].

Finally, it was assumed that a variant of NASA's Lunar Surface Access Module, as seen in Figure 46, capable of transporting prepackaged cargo in an unpressurized container, would also be available for use by this project.



Figure 46. Artist's conception of NASA's Lunar Surface Access Module.

7.7.4 Subsystem calculations and description

In order to calculate the total mass that the Ares V can deliver to the lunar surface, the landing vehicle was assumed to use a LOX/LH₂ propellant combination having an I_{sp} of 450 s. Assuming a structural mass fraction of 0.15, the rocket equation was used to find the maximum payload that could be delivered to the lunar surface, with the landing vehicle weighing 50 mT, given the 54.6 mT Trans-Lunar Injection capability of the Ares V. This payload mass was found to be around 20 mT. To provide a mass margin, the final value was taken to be 18 mT for this project.

Additional considerations for this subsystem included offloading of cargo from the LSAM. The current NASA documents outlining the lunar exploration architecture do not contain any details about offloading elements from the LSAM. For this project, a simple system composed of a ramp and a winch would suffice to unload telescope elements packaged together into a large container attached to the winch. For purposes of this project, it was assumed that the cargo version of the LSAM would have such a system, or one with similar characteristics, and this project would be able to utilize it with minimal modifications.

Finally, it is envisioned that the Trans-Lunar Injection stage left in lunar orbit before descent to the surface would be outfitted with a simple radio communications system, in order to provide contact between the telescope on the lunar surface and ground controllers on the Earth before the laser communications system has been set up.

7.7.5 Final subsystem design

Transportation of telescope components from the Earth to the lunar surface is provided by the Ares V launch vehicle and the Lunar Surface Access Module developed by NASA. The total mass of components that can be landed on the moon with one launch is 18 mT. Currently, the total mass of all telescope components, including the communications and deployment systems, is 17.2 mT. Therefore, a single launch is required for transportation of the entire telescope to the Moon.

7.8 Deployment Subsystem

7.8.1 Introduction

The deployment subsystem is responsible for moving the telescope components from near the LSAM to desired locations on the lunar surface.

7.8.2 System definition and interfaces

The deployment system is responsible for positioning the various clusters in the array, as well as the communications relays, at the proper distances from each other. It is not responsible for the unfolding of clusters or relays. Inputs to the subsystem are the following:

- Coordinates of array location
- Cluster mass
- Number of clusters
- Distance between clusters
- Relay mass
- Number of relays
- Distance between relays

7.8.3 Assumptions and ground rules

One of the objectives of this project is to leverage the lunar exploration architecture developed by NASA. Therefore, this system tries to use elements from the lunar exploration architecture wherever possible.

The main assumption for this subsystem is the availability of long-range unpressurized rovers capable of being modified with attachments. The Exploration Systems Architecture Study and the Lunar Architecture Team's study both mention plans for an unpressurized rover at the human lunar outpost [7][52]. However, no details are provided. In addition to a range of several hundred kilometers, the rovers are assumed to have a rechargeable power source as well as basic radio communication devices. The maximum payload capacity of each rover is assumed to be 480 kg based on the Apollo Lunar Roving Vehicle (LRV) [53]. Finally, for calculation of deployment times, the speed of the rovers is taken to be 2 km/h [54].

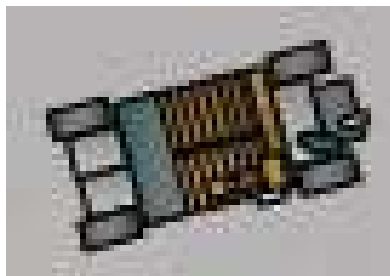


Figure 47. NASA's unpressurized rover concept [52].

7.8.4 Subsystem calculations and description

Subsystem Concept Description

Since the deployment system is responsible for locating several telescope array elements and communications relays over a distance of several hundred kilometers across the lunar surface, it was not considered feasible to land the components separately from each other. Rather, it is

envisioned that the transportation system will place a single module on the lunar surface containing all telescope components. Each of these components will then need to be positioned at the proper location on the lunar surface through a surface transportation system, in this case rovers. The number of rovers employed is dependent on the mass of the telescope as well as the payload capacity of each rover. These rovers will be modified from NASA's design in several important ways:

- Each rover will be equipped with a robotic manipulator to load and unload cargo. Thus, its function will be similar to automated vehicles moving inventory in a warehouse.
- A gimbaled laser receiver will be placed on each rover to enable tracking of the communications system laser during the deployment of communications relays.
- Each rover will navigate using lunar maps based on precursor satellite missions as well as a computer guidance algorithm using gyroscopic and possibly visual inputs. Currently, NASA has placed a contract for a prototype lunar GPS system [55]. If a functioning version of this system is available at the time of detailed telescope system design, it is recommended the rover be equipped to use the system instead due to its higher accuracy.
- Each rover will be capable of communicating via radio with the Trans-Lunar Injection stage left in lunar orbit. This will ensure contact with the Earth and supply an additional means of verifying navigation.
- Each rover will also be able to interface with the telescope power system to recharge itself if necessary.

The limiting factor in the deployment is the total mass of all the communications relays, which is approximately 650 kg for the current design point, while the maximum payload capacity of the rover is assumed as 480 kg. Thus, the current design entails the use of two rovers, which provides both payload margin for the deployment of relays and redundancy in the deployment system, but still results in a total mass below the payload limit of the LSAM.

Operations

The rovers are responsible for deploying the telescope array elements as well as the communications relays. The rovers are initially stowed on the LSAM close to the ground. An automated unloading system, likely consisting of an unfolding ramp, is used to deploy the rovers. Each rover then unfolds and drives to the package, unloaded from the LSAM, consisting of telescope components.

Array Deployment

The sequence of operations for array deployment is as follows:

1. The rovers will load the components of the central power/communications system and clusters from the LSAM onto the rover cargo platforms using a robotic manipulator. (Note: the number of clusters the rovers can carry at any one time is dependent on its payload capacity and the mass of a single cluster.)
2. When fully loaded, the rovers will drive to the desired locations and offload elements, starting with the central power/communications system.
3. This process will be repeated until all clusters are deployed, with the rovers periodically recharging from the central power system as necessary.

Figure 48 shows a notional view of array deployment.

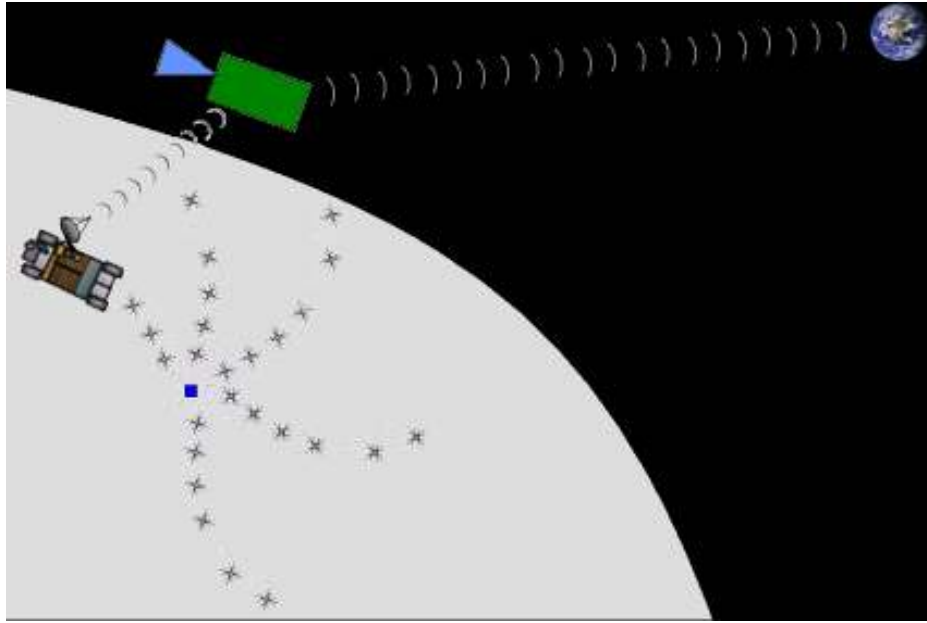


Figure 48. Notional view of array deployment.

Array Deployment Time

Given 215 clusters, each having a mass of about 54 kg, and an array diameter of 62 km, the approximate array deployment distance was calculated as follows:

$$L_{deploy} = \frac{N_{cluster} m_{cluster}}{m_{p,rover}} D_{array} \quad (\text{Eq. 14})$$

where L_{deploy} is the array deployment distance, $N_{cluster}$ is the number of clusters, $m_{cluster}$ is the cluster mass, $m_{p,rover}$ is the payload mass of the rover, and D_{array} is the array diameter. With the given parameters, the array deployment distance is calculated as about 1,670 km.

With a speed of 2 km/hr, the rovers would spend at least 18 days deploying the array elements, with added time due to terrain as well as the unloading of clusters and recharging of the rover power system.

Communications Relay Deployment

For better efficiency, the deployment system is designed such that all the relays can be carried aboard the rovers to avoid having to drive back and forth from the landing site to retrieve relays. The deployment scheme is as follows:

1. The two rovers at the telescope location retrieve communications relays from the landed stack.
2. The rovers drive from the telescope towards the limb offloading relays at the required distances from each other.
3. Once all relays have been deployed, the rovers then return to the telescope location where they remain on standby for deployment of upgrades or replacements.

Figure 49 shows a notional view of communications relay deployment.

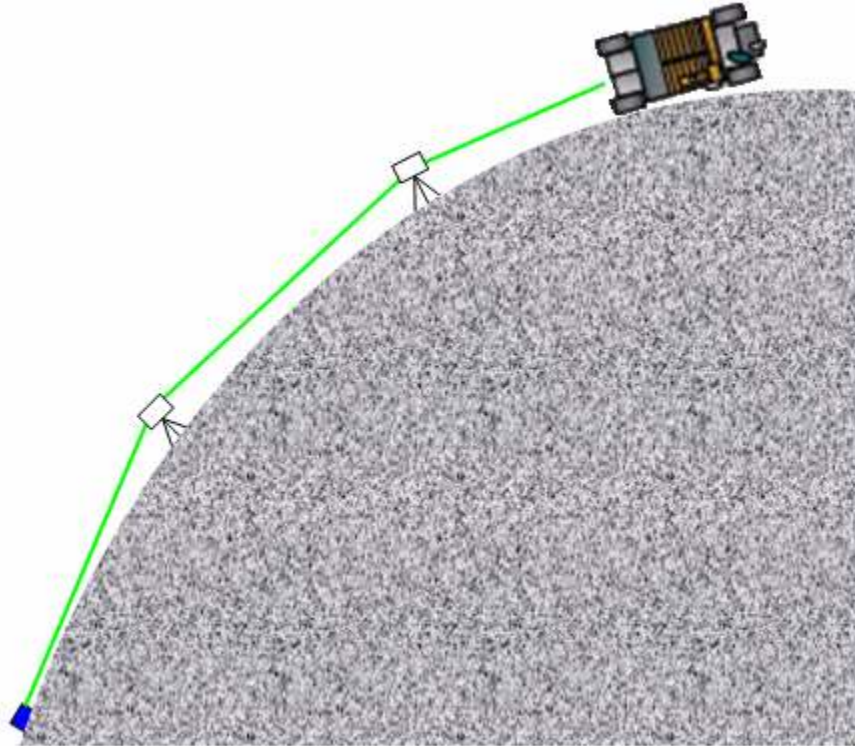


Figure 49. Notional view of communications relay deployment

Communications Relay Deployment Time

Given a distance of 151 km between the telescope location and the limb, including a meander distance contingency of 20% and a rover speed of 2 km/hr, at least 2 days would be required to deploy the communications relays, with added time required for stopping and unloading the relays.

Rover Communications

To carry out the above deployment scheme, the rovers must communicate with the various telescope elements and relays. This communication occurs in the radio frequency through small beacon transmitters placed on telescope elements and relays as well as antennas on the rovers themselves. The main data communicated is the condition of the clusters and relays, i.e., whether or not their unfolding occurred properly. The rovers also communicate with the orbiting Trans-Lunar Injection stage to establish contact with Earth during the deployment phase. This allows monitoring of the deployment by ground controllers and correction of any problems that may arise. It is recognized that following this approach allows for some blackout periods in communications with Earth. However, the rovers are assumed to have a low speed, resulting in a deployment time long enough to allow mission control to make changes or corrections to the deployment.

Rover Navigation

The rovers deploy the relays at the separation distances required through computer-aided navigation. Additionally, gimballed laser receivers on the rovers can be used ensure that line of sight is established between the different relays. For this purpose, the central communications system and a laser transmitter at the human lunar outpost must provide “dummy” laser beams

during the deployment phase, which do not necessarily contain array measurements, but are just used to align relays.

Alternative Deployment Schemes

Finally, it should be mentioned that a deployment scheme consisting of landing all relays at the human lunar outpost and deploying them towards the telescope was also considered, in order to ensure continuous communications with Earth during deployment. However, with this scheme the telescope would not be deployed till after all the relays were deployed. By using the deployment scheme chosen for this project, the telescope can be set up and tested before laser communications are established.

Rover Sizing

Due to the lack of details on NASA's plans for an unpressurized rover, it was decided to use the Apollo Lunar Roving Vehicle (LRV) data to obtain a rough mass estimate of the rover [53]. The new rover was assumed to have the same payload capacity. All LRV subsystems were included in this estimate except the power system and crew stations. The power subsystem was removed from the estimate because the Apollo LRV utilized primary batteries that are not rechargeable. To allow for contingencies as well as efficient usage of the rover, it was decided that the new rover should have a rechargeable power source.

For a conservative estimate, rechargeable batteries were selected as the power source, as these are heavier than other common power systems such as solar arrays. For these calculations, the battery storage density was assumed to be the same as that of the power system for this telescope, 130 W-hr/kg [56].

To find the mass of the rover power system, two other quantities were required. The first is the required range for the rover. Two different numbers were used for this, one being the deployment range, which is the distance the rover has to drive while carrying payload, and the other being the return range, which is the distance covered by the rover when it is empty. These were calculated as follows:

$$L_{deploy} = 1.2(D_l + D_{array}), \quad (\text{Eq. 15})$$

where L_{deploy} is the deployment range, D_l is the distance to the limb, and D_{array} is the array diameter. Note that the factor of 1.2 is meant to provide a margin for meandering and obstacle avoidance. Using

$$L_{return} = D_l + D_{array}, \quad (\text{Eq. 16})$$

where L_{return} is the return range, and setting the distance to limb as 151 km and the array diameter as 62 km, the deployment range is found to be 255 km, and the return range is found to be 213 km.

The second quantity required was the energy expenditure of the rover. This value, the Surface Mobility Energy Requirement, was found from Human Space Mission Analysis and Design (HSMAD) to be 0.15 W-hr/km-kg [57]. Note that HSMAD provided a range of values and the most conservative of these was selected for the calculations. With these quantities at hand, the energy required for each leg of the trip was found using:

$$E = L * 0.15 , \quad (\text{Eq. 17})$$

where E is the energy required, L is the distance of a trip leg, and the factor 0.15 is the Surface Mobility Energy Requirement, in W-hr/km-kg.

The battery mass for deployment and return was found using the relations:

$$m_{batt,deploy} = \frac{(m_{s,rover} + m_{p,rover}) * E_{deploy}}{130 - E_{deploy}} \quad (\text{Eq. 18})$$

and

$$m_{batt,return} = \frac{(m_{s,rover}) * E_{return}}{130 - E_{return}} . \quad (\text{Eq. 19})$$

Where m_{batt} is the mass of the battery, $m_{s,rover}$ is the rover structural mass and $m_{p,rover}$ is the rover payload capacity. The rover structural mass of 170 kg was obtained from the Apollo LRV with some mass budgeted for the inclusion of a robotic manipulator to load and unload cargo from the rover.

Table 16. Rover energy requirements and battery mass.

Surface mobility Energy requirement	0.15	W-hr/km-kg
Battery storage density	130	W-hr/kg
Deployment energy Requirement	38	W-hr/kg
Deployment battery mass	271	Kg
Return energy Requirement	32	W-hr/kg
Return battery mass	55	Kg
Total rover power system Mass	327	Kg

To find the total mass of one rover, the structural mass added to the power system mass. The total rover mass is then estimated as approximately 497 kg.

The final deployment system mass was found by adding a 20% mass margin to the mass of two rovers for a total of 1192 kg. Note that this is a highly conservative number due to the following reasons: incorporation of a mass margin, assumption of structural mass based on Apollo-era technology, and oversizing of batteries.

However, this is considered reasonable due to the current early stage of the design.

7.8.5 Final subsystem design

Positioning of array elements and communications relays on the lunar surface is carried out by automated unpressurized rovers, modified from those developed for the lunar exploration architecture with robotic attachments to load and unload cargo and specialized communications

equipment. Additionally, it is assumed that the rover power system is rechargeable.

The deployment limiting factor is the total mass of the communications relays, 650 kg. For better efficiency, all the relays need to be carried aboard the rovers to avoid having to drive back and forth from the landing site to retrieve relays. For this reason, two rovers each having a payload capacity of 480 kg, are landed with the telescope. The rovers are capable of deploying elements over a maximum range of 255 km in any direction on a single charge and returning to the telescope location for recharging. The total mass of these rovers is 1192 kg.

Assuming a rover speed of 2 km/hr, deployment of all telescope components takes at least 20 days, plus time required for offloading of the telescope elements and recharging of the rovers.

7.9 Trade Study and Optimization

7.9.1 Introduction

In order to determine the precise form of the LIRA concept, a trade space analysis was conducted to maximize the actually scientific value the array would provide for its cost. In order to perform this analysis it was necessary to first define a scientific figure of merit which would encapsulate the value of the science the array can produce and to scale it in a way that corresponds to value. Using this type of metric, an optimized design for the array can be calculated.

7.9.2 Scientific figure of merit

In order to quantify the scientific value of a particular design a metric was developed with an aim to be similar to the “discovery efficiency” metric used by the Hubble space telescope and other similar instruments. This type of figure of merit attempts to estimate the amount of science that can be performed with a telescope by analyzing its sensitivity and viewable area of the sky. For the figure of merit for LIRA, this concept is modified to incorporate the value of having greater EOR resolution. The figure of merit is as follows:

$$FOM = \text{Constant} \times \text{Log} \left(\frac{1/t_{\text{survey}}}{\sqrt{\theta_{\text{EOR}}}} \right), \quad (\text{Eq. 20})$$

where t_{survey} represents the time it takes for a survey of half of the sky to a target sensitivity over the entire frequency band and θ_{EOR} is the EOR resolution. The survey time is calculated by determining the field of view at enough frequencies to fully cover a 10-130 MHz bandwidth with 32 MHz observations, and calculating both the field of view and sensitivity at these frequencies. The survey time then becomes the sum of the number of observational hours required to get down to a target sensitivity of 10 mJy for half of the sky. The square root and logarithm are used to balance the components and reflect the fact that incremental increases in the capability become less important as the instrument becomes more capable. This figure of merit includes a constant multiplicative factor to make the scale of the values easier to work with.

7.9.3 Optimization trade study

An optimization trade study was conducted by dividing the figure of merit by the total system cost and calculating this quantity over a range of input parameters. For a discussion of

the total LIRA system cost, which was calculated as \$1.987 billion, see Section 9.2. The two parameters used were EOR resolution and field of view, with the other relevant parameters given assumed values. The tradeoff surface, seen in Figure 50, shows a pronounced maximum, which was then taken as the optimal value of the system.

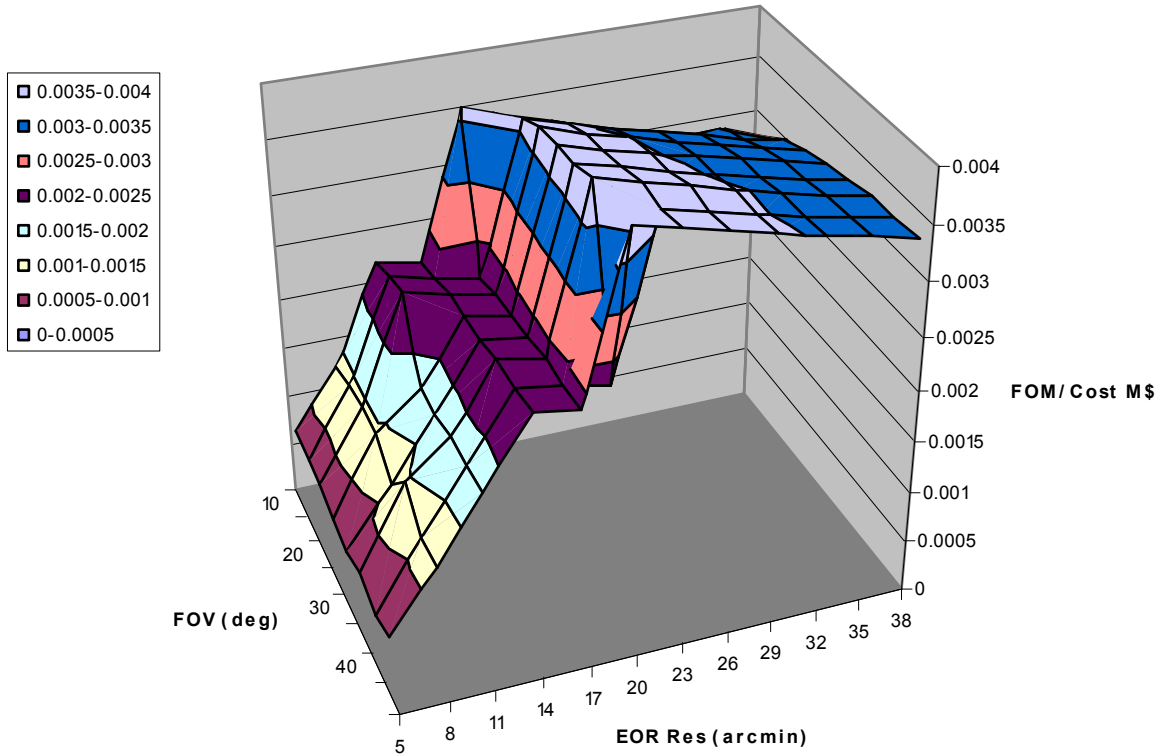


Figure 50: Scientific Figure Of Merit/Cost trade study surface.

This optimal point is calculated under the assumption that 3440 dipoles will be sufficient to resolve the EOR signal and thus achieve the desired scientific goal of the telescope. This point design provides a good baseline on which to evaluate the science goals which the point design can perform, a detailed assessment which is left for future work. If it becomes necessary to scale up LIRA by adding more dipoles, the total system cost and the scientific FOM will both be affected. The relationship between the number of dipoles and the total system cost is discussed in Section 9.2.7.

7.9.4 Results

The results of the trade study analysis yielded the optimal configuration for LIRA. This optimal configuration had properties as follows:

Characteristics

- Frequency Range: 10-130 MHz
- Instantaneous Bandwidth: 32kHz
- Number of Dipoles: 3440
- Number of Clusters: 215
- Array Diameter: 62 km

Capabilities

- EOR Resolution: 12 arcminutes
- Max Resolution: 9.2 arcseconds (at 130 MHz)
- Sensitivity: 3.6 mJy at 10 MHz, 0.6 mJy at 130 MHz
- Field of View Diameter: > 25 degrees

This resulting array configuration provides the strongest scientific value per dollar for the LIRA concept.

7.9.5 Comparison with Previous Concepts

Comparing the optimized LIRA concept to other instruments provides a useful gauge of how useful LIRA will be in the context of planned/existing telescopes and their capabilities. Figure 51 and Figure 52 compare the sensitivity and angular resolution of LIRA with the Mileura Widefield Array (MWA) and the LOFAR radio telescope, two radio instruments currently being developed to observe the EOR.

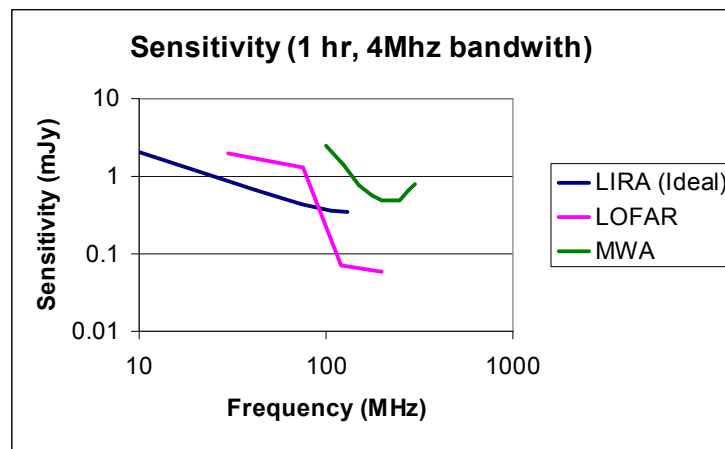


Figure 51. Sensitivity of LIRA.

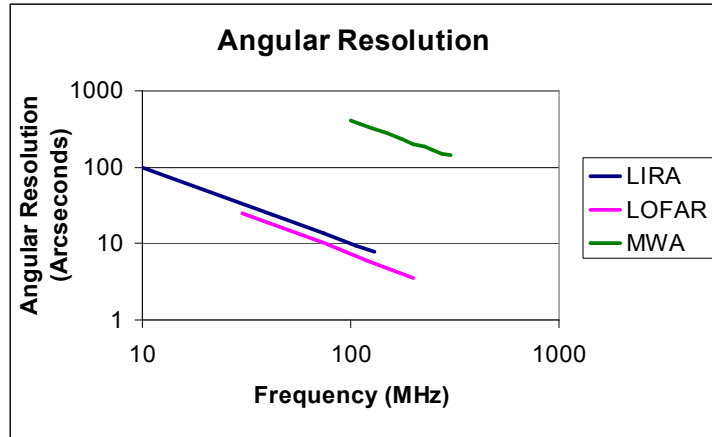


Figure 52. Angular resolution of LIRA.

The sensitivity for LIRA is actually an idealized sensitivity, assuming that the dipole antennae have equivalent efficiencies across the entire frequency band, which will likely not be the case for a production system; however it still provides a useful analysis of the range of capabilities for the instrument.

As can be seen in these figures, LIRA's performance is similar to these other cutting edge instruments where the edges of their bandpass overlap, and LIRA in fact extends these high performances to previously unexplored low frequencies. In this aspect, LIRA provides essentially a low frequency complement to the Earth-based systems currently in development.

8. Lunar Infrared Modular Interferometric Telescope (LIMIT)

8.1 Approach and Assumptions

8.1.1 Design Approach

The design of the Lunar Infrared Modular Interferometric Telescope (LIMIT) presented here evolved from numerous iterations of the two IR concepts retained after the concept downselection cycle. The first concept was a sparse interferometer with multiple 1-meter and 3-meter diameter elements located on the lunar surface. During the first phase of deployment, five to ten 1-meter telescopes would be deployed with separations of 10 to 500 meters between each element. Five to ten 3-meter telescopes would be deployed during the second deployment phase, at separations of 60 – 500 meters between each element. This concept would benefit from being located on the lunar surface by allowing for large fixed distances between each interferometer element. Additionally, the concept would be flexible and easily scalable.

The second IR concept was a single large 14-meter segmented telescope located in a lunar polar crater. The telescope would be deployed in three stages – during the first stage, a 6-meter segmented telescope would be deployed. Additional segments would be deployed during the second stage to increase the effective diameter to 10 meters, and the third stage would increase the diameter to 14 meters. This concept would take advantage of human-assisted deployment of a large telescope in a phased approach, rather than needing to launch the entire 14-meter telescope in an 8-meter diameter launch vehicle.

Building a “hybrid” telescope, which would consist of a large single telescope as the core and multiple smaller long-baseline outrigger telescopes, was also considered. An illustration of this concept is shown in Figure 53.

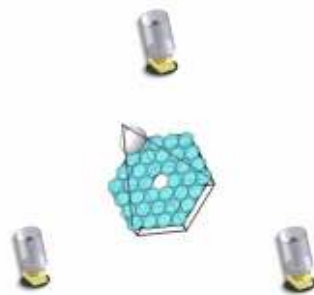


Figure 53: Hybrid IR telescope design.

The rationale for this design was that the telescope system could perform imaging using the large core element and interferometry using the long-baseline outriggers. This concept would be upgradable, as future improvements to the initial telescope could be made by either expanding the size of the central imaging element or adding additional elements to the interferometric array. These improvements would be made according to the priority of future science objectives and the availability of resources.

While this concept would benefit from its flexibility and scalability, it suffers from two major drawbacks. First, the central core telescope and the smaller outriggers would require drastically different optical and structural components. The central telescope would be constructed act as a Fizeau array while the outriggers would employ Michelson interferometry. These two subsystems would require separate beam combining optics, which comprise a major portion of

the development cost of any telescope. It was reasoned that this hybrid concept would essentially require the design and development of two independent telescope systems. This implies that the cost of the hybrid approach is likely to be significantly more than the cost of any singular telescope design.

A second major drawback of the hybrid approach is that the science programs that would be conducted by the central Fizeau array and the long-baseline outriggers would be significantly different. Because of the shared resources between the two systems, the telescope would likely be able to operate in only one mode at a time. This would mean that the telescope observing time would have to be split between the two major science programs, which would provide significantly less value than a telescope that could be dedicated full-time to a particular set of science objectives.

For these reasons, it was further reasoned that, assuming a fixed budget and schedule, a hybrid telescope design would produce two mediocre telescope systems with significantly reduced capabilities compared to an ordinary single telescope. Therefore, it was decided to focus on a single design, the central Fizeau array was chosen as the concept to develop further.

This decision was also motivated by the amount of achievable goals of the system. Whereas a Golay imaging interferometer would be well suited to achieve 4 of the 5 scientific goals established by the stakeholder analysis in Section 3, a very long baseline nulling interferometer would be limited to just planet detection. The configuration of the elements is an area for future study that will be informed by the development of future space telescopes, but the final design presented here is a concept for an imaging Golay interferometer with capabilities exceeding any existing or proposed IR telescope.

To capitalize on prior development and operational experience, each LIMIT outrigger will be identical to and based on the Spitzer Space Telescope design. Since Spitzer is an orbiting space telescope, much of the hardware can be simplified, as many of the design constraints would be relaxed for a human-serviceable lunar surface telescope. The telescope will be located in the darkness of the Shackleton crater at the lunar south pole, to take advantage of the thermally stable environment and access to the nearby lunar base. The design for LIMIT presented here represents a point design that is both technically and financially feasible.

8.1.2 Detailed requirements

Table 17. Requirements for IR interferometer.

Req #	Requirement	Priority	Rationale
1	The system shall be capable of collecting radiation in the NIR and FIR bands.	A	To meet selected science goals.
1.1	The system shall collect radiation in the wavelength range: 5 μ m to 90 μ m.	A	To meet selected science goals.
1.2	The system shall provide an angular resolution of at least 1.9 arcseconds.	A	From analysis.

Req #	Requirement	Priority	Rationale
1.3	The system shall be able to point at a particular target with an accuracy of 1% of field of view.	A	Pointing at particular targets enables accomplishment of scientific objectives in various regions of interest in the visible sky.
1.4	The system shall provide an effective collecting area of 5.1 square meters.	A	From Golay-9 configuration using Spitzer elements.
2	The system shall be able to view 3.5 strrad of the sky in one year of operation.	B	More coverage of the sky is desirable, but the siting of the telescope within a shadowed crater will limit the available sky that can be viewed.
2.1	The field of view of the system shall be 5 x 5 arcsec for the shortest wavelength of operation.	B	TBD
2.2	The system shall be able to maneuver to face a target within +/- 40 degrees of elevation from its nominal position.	B	Maneuvering allows focusing on science goals related to targets in various parts of the sky.
3	The system shall be located on the lunar surface.	A	To leverage NASA's current architecture and meet VSE.
3.1-n	The system shall be capable of surviving in the environment of the lunar surface.	A	
4	The system shall be able to communicate data back to Earth.	A	Data must be analyzed by Earth-based systems.
4.1	The system shall have a data rate of 1 Gbps or less.	B	This data rate allows for radio communications links, and is estimated from the data rates for similar telescopes.
4.2	The system shall transmit data in the Ka band.	C	The Ka band allows use of the Deep Space Network for data reception.
4.3	The system shall transmit data to a ground downlink station or to the Deep Space Network.	B	A dedicated ground receiving station may be built if sufficient access to the Deep Space Network is not anticipated.
5	The entire system payload shall fit into less than 1 Ares V booster vehicle and have a throw weight no greater than the maximum throw weight of 1 Ares V booster.	B	Ares V booster will leverage NASA capabilities.

Req #	Requirement	Priority	Rationale
5.1	The mass of system components launched on a single Ares V shall be less than 18 metric tons.	A	LSAM payload delivery capability [7].
5.2	The system shall be able to survive launch loads as defined in the Ares V users guide.	A	
6	The system shall have an operational lifetime of at least TBD years.	B	TBD
6.1	The system shall have a reliability of at least TBD.	B	TBD
6.2	The system shall have interfaces for servicing by robotic/human missions.	A	Servicing interfaces increase the ability to leverage the planned human base and pre-existing lunar exploration architecture.
7	The system shall have provisions for incorporating new elements (antennas, instruments, etc.).	B	Modularity and allowing for the incorporation of new elements permits easy upgrading of the system's capabilities.
8	The system shall have a cost of the same order of magnitude as telescopes with similar scientific objectives.	A	The system needs to deliver higher value to the major stakeholders for a cost either lower than or equal to other proposed programs.

8.1.3 Rationale

The near-infrared (NIR) to far-infrared (FIR) range, where this observatory will operate, offers many advantages. Dust, which permeates the plane of our galaxy, and which also obscures many processes of scientific interest in the optical band, is transparent in the infrared (IR) band. The IR window is optimal for the study of objects at cosmological distances, which have their bulk emission redshifted from the optical band to the IR. However, the observatory will not be only confined to the science mentioned above. Its relatively wide wavelength window, from NIR (with some elements possibly accommodating optical light) to FIR, combined with the advantage that the lunar surface presents in terms of the lifetime of the program (see Section 1) means that a wide range of targets will be studied with this instrument.

A main driver for this concept is the opacity of the atmosphere to the radiation from roughly 10 μ m to about 1mm. Whereas the planned Atacama Large Millimeter Array telescope will cover wavelengths upward of 300 μ m, there is a need for an instrument with sub-arcsecond resolution in the 50 μ m to 300 μ m band. This demand will be satisfied with the interferometric capability of this concept.

In addition to the scientific value outlined above, this concept offers scalability and flexibility by not entirely relying on one component to be operational. After the installation of the first phase, the success of the project is less dependent on budget uncertainties. The results of the first

phase will be useful to boost public support, and to emphasize scientific value, which would serve the deployment of the second phase that would make the concept fully operational.

Since this concept will utilize interferometric observation techniques, it will require and drive major technological research in a few areas with the potential to accomplish this task. These include using fiber optics for interferometry and terahertz correlators for FIR wavelengths, which would greatly simplify the design of the rest of system.

8.1.4 Science goals

The major science goals addressed by the LIMIT concept are:

- 1) Planet detection, including the study of planet formation and evolution
- 2) Galaxy formation at high redshift
- 3) Active galactic nuclei
- 4) Proto-stars and the study of stellar formation.

This observatory could optionally be designed with additional capability to carry out weak lensing surveys. These science goals are consistent with the important science objectives identified in the stakeholder analysis. A discussion of each science goal is presented below, followed by a comparison of some of the science goals of other current or planned IR telescopes.

Search for extrasolar planets:

The search for habitable planets and life has received strong support within the scientific community. The 2001 decadal review of astronomy and astrophysics, "Astronomy and Astrophysics in the New Millennium," prepared by the National Research Council, stated that: "The discovery of life on another planet is potentially one of the most important scientific advances of this century, let alone this decade, and it would have enormous philosophical implications [28]."

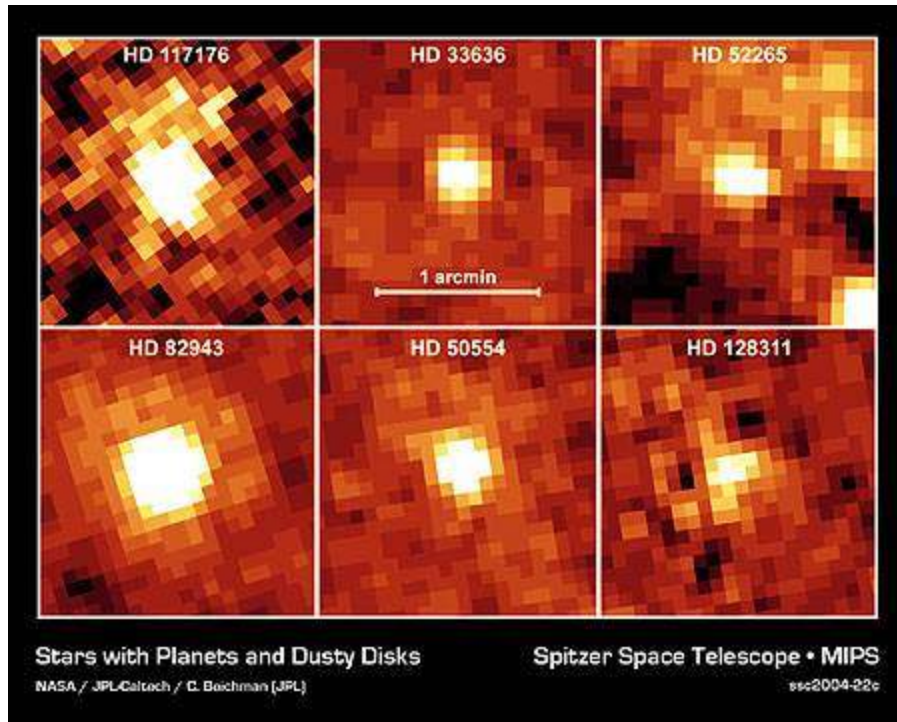


Figure 54. Stars with exoplanets seen by Spitzer.

Star with an exoplanet, removed due to copyright restrictions.

Figure 55. Star with an exoplanet.

Formation of protostars and planetary systems.

Sub-arcsecond angular resolution is essential to resolve protostellar disks and planetary systems during their formative stages. LIMIT will be used to image hundreds of these objects in the nearby regions of low-mass star formations like Taurus, ρ Ophiuchi, and Perseus. Such observations will permit calibration of the effects of variable viewing geometry and effectively allow for finely time-resolving the development stages of a protoplanetary disk. The Spitzer Space Telescope and the planned far-IR observatories Herschel and SOFIA lack the necessary resolution for this activity.

Active Galactic Nuclei:

A kilometer baseline is needed to image an average-sized torus in a nearby galaxy (like the M87 galaxy). Current information being produced by 8-m telescopes on Earth has established an upper limit to the size of this torus. However, higher resolution will be required in order to distinguish the torus in greater detail. With respect to angular resolution, there is no threshold above which valuable science cannot be accomplished in an improved fashion -- bigger is always better.

Debris disks

Dynamical models predict planet-induced resonant structures in debris disks. The resulting perturbed dust distribution will be most apparent in mid- and far-IR images. The Spitzer Space Telescope has found many tens of candidate debris disks within 30 pc, but Spitzer is able to resolve only four nearby debris disks. With angular resolution an order of magnitude better than that of Spitzer, LIMIT will image with comparable clarity debris disks located fifty parsecs from the Sun.

For comparison, below are the science goals of other space telescopes operating in the infrared wavelengths.

JWST science goals

- First light and reionization
- Galaxy formation
- Protostars and protoplanetary systems
- Planetary systems and the birth of life

Spitzer science goals

- Brown dwarfs
- Early universe
- Protostars and galaxy formation
- AGNs.

Herschel science goals

- Protostars and galaxy formation
- molecular composition and cooling rates of galactic and interstellar gas
- spectra of planets and nearby comets

Infrared wavelengths

The infrared spectrum can be segmented into Near, Mid-, and Far-IR wavelength ranges. Each wavelength range offers unique opportunities for discovery as well as unique engineering challenges for the telescope. A discussion of each wavelength range is presented below.

Near IR:

Targets: *Cool stars, large red giants, low mass red dwarfs.*

The near-infrared is the region where interstellar dust is the most transparent to infrared light.

Mid IR:

Targets: *Planets, asteroids.*

The planets in our solar system have temperatures ranging from about 53 to 573 degrees Kelvin. This is radiation that the planet or asteroid emits because it is being heated by a nearby star.

Far IR:

Targets: *Protostars, clouds of dust and gas, AGNs, starburst galaxies.*

In the far-infrared, stars are not especially bright, but emission is visible from very cold matter (140 Kelvin or less) which is not seen at shorter wavelengths. The Earth's atmosphere is opaque

over most of the far infrared, so that ground-based observations are limited to submillimeter wavelengths using high-altitude telescopes.

The general formula that links temperature T and wavelength of maximum emission λ is the following:

$$T \lambda = 3000 \mu\text{m.K} \quad (\text{Eq. 21})$$

The corresponding typical temperatures for each wavelength domain are thus:

Near IR: 4000 K

Mid IR: 400 K

Far IR: 60 K

8.2 Instrumentation and Interferometric Array

8.2.1 Introduction

The primary optical instrument for each LIMIT outrigger will be a replica of the Spitzer telescope. This is a Ritchey-Chretien optical telescope with a 0.85-m diameter. The optical parameters of this configuration are shown in Table 18.

Table 18. Optical parameters of Optical Units.

Operational Parameters	Value
Focal Length	10200 mm
f/#	12
Back Focal length (PM vertex to tows)	340 mm
Field of view (diameter)	320 arcmin
Spectral bandpass	3 μm – 200 μm
Aperture Stop Location	At primary mirror
Diameter of OD obscuration	850 mm
Diameter of ID obscuration	320 mm
Primary mirror hyperbolic radius (convex)	-2040 mm
Conic constant	-1.00284
f/#	1.2
Secondary mirror hyperbolic radius (concave)	-274.524
Conic constant	-1.526131
Clear aperture (OD)	135 mm
Clear aperture (ID)	38.846 mm

The baseline design includes a total of 9 Spitzer-derived collecting instruments in a Golay-9 configuration. The modularity of the design allows for easy upgradability to Golay-12 or Golay-15. Alternatively, the instruments could be deployed in a phased approach starting with a Golay-3 or Golay-6 configuration, depending on launch or budget constraints. The baseline configuration is shown in Figure 56. The Golay-9 configuration is chosen for the purpose of elaborating on a single point design in this study, but the number of elements can be scaled up if during further design iterations it is decided that 9 telescope elements will be insufficient to achieve the desired scientific objectives of angular resolution or sensitivity. The effects this will have on the total system cost as a function of the number of Spitzer elements is discussed in Section 9.3.11.

The collecting instruments are each attached to a power distribution box, which distributes power from the solar arrays located along the rim of the Shackleton Crater. The solar panels are expected to be a maximum of 10 km from the main telescope. The light from each collecting instrument will be collimated into a fiber optic cable, and all the fiber optic cables will terminate at the beam arranging unit. From there, the light from each telescope will be sent to the beam combining unit, which will be placed as far from the telescope instruments as possible to minimize the addition of heat to the local thermal environment. Inside the beam combining unit, the light from each telescope will be combined into a single beam, which will then be sent to the CCD. Attached to the beam combining unit is the cryocooler, which will actively cool the CCD sensors to the required temperatures. The signals from the sensors will be processed by a nearby computer. The computer will then send a signal to a nearby radio transmitter, which will transmit data back to Earth.

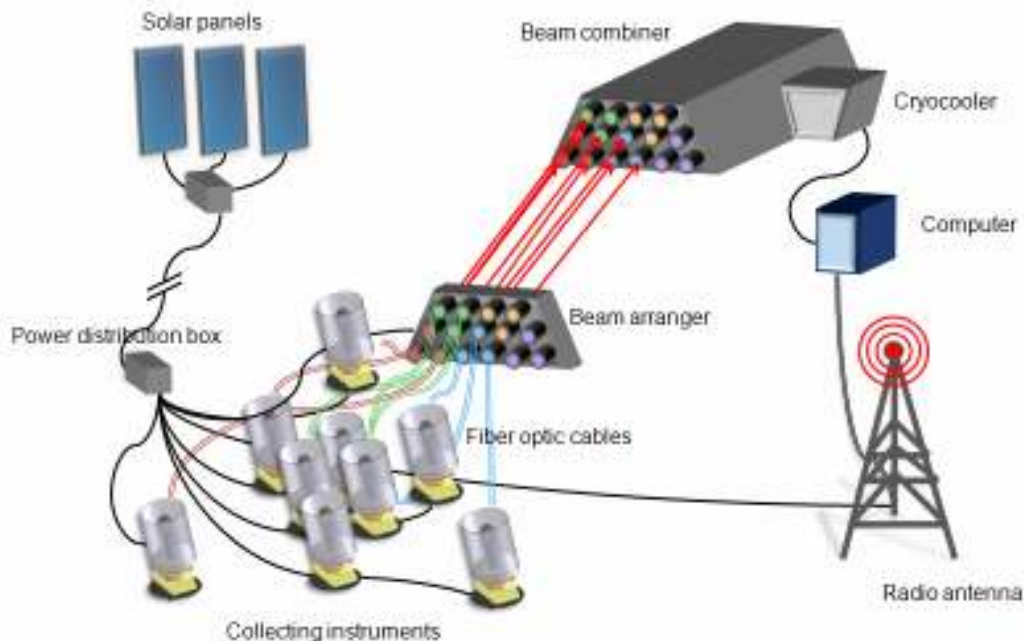


Figure 56. Baseline configuration for LIMIT concept (not to scale).

8.2.2 Optics

The array of telescopes will combine the beams in a central combiner acting as a Fizeau interferometer to capture images with the resolution of very large equivalent diameters. A Fizeau interferometer collects the light of the source in a distributed array, and combines the

light in central unit that focuses all the beams in a coherent manner in a CCD to form an image of the target. The resulting resolution can be equivalent to that of an aperture with a diameter of distance between the telescopes. For this design, the team adopted the beam combining technique of the ARGOS telescope, a sparse aperture imaging telescope with a Golay-3 configuration [58]. The LIMIT design employs up to five replicas of the ARGOS beam combining hardware to combine up to 15 sources of light into one single beam. Figure 57 below shows a schematic of the ARGOS beam combining hardware, and Figure 58 shows a schematic of duplicate systems for combining light in multiples of three in the LIMIT concept.

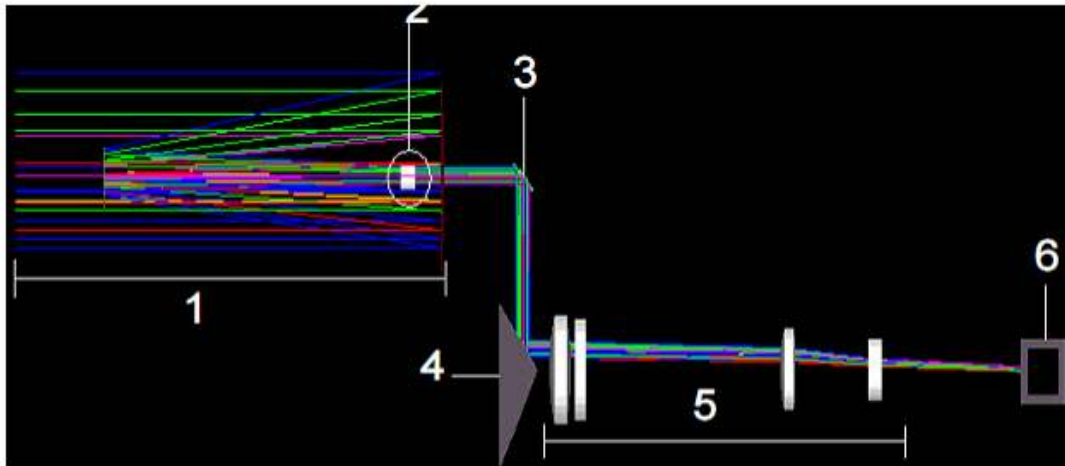


Figure 57: The final layout of the ARGOS optical train (only one aperture shown) 1-subaperture, 2-collimating lens, 3-FSMODL actuator, 4-pyramidal mirror, 5-beam combiner, 6-CCD [58].

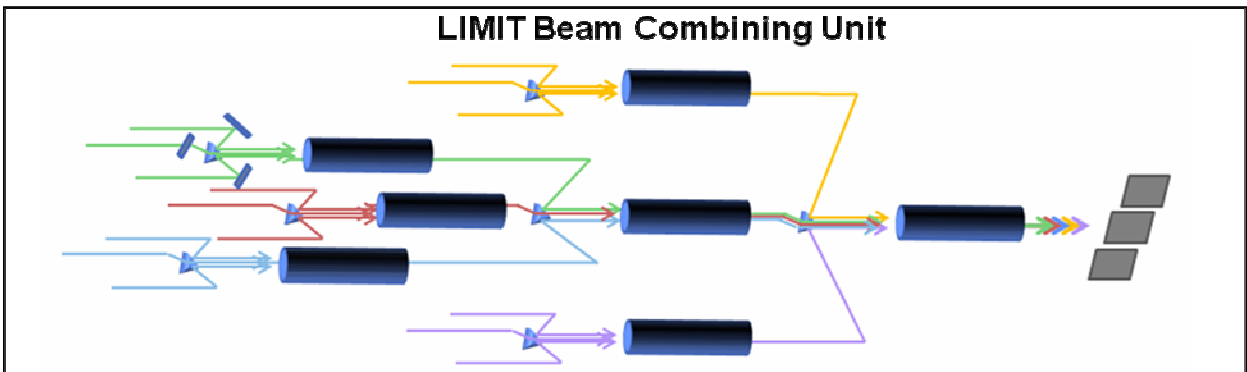


Figure 58: Beam combining layout for LIMIT beam combiner. The design incorporates multiple instances of the ARGOS beam combining optics to combine up to 15 light sources.

Instead of duplicating the ARGOS hardware for each group of three satellites in the LIMIT concept, a single multi-sided reflective mirror could be used to combine the light in a single step, as shown in Figure 59 below. This would require much less hardware and would be a worthwhile investment for the current design.

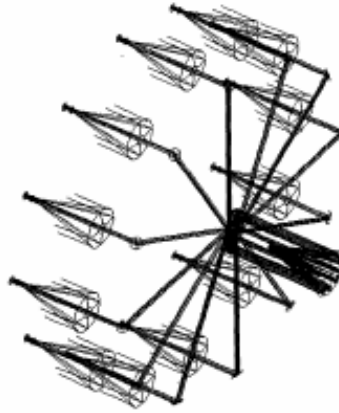


Figure 59: A sparse-aperture telescope implemented with twelve separate focal telescopes feeding a common beam combiner [59].

The expected angular resolution of the LIMIT concept is shown in *Figure 67* and compared to other existing telescopes. The middle line represents the nominal deployment of a Golay-9 telescope. The upper red line represents a Golay-3 telescope, and the lower red line represents a Golay-15 configuration.

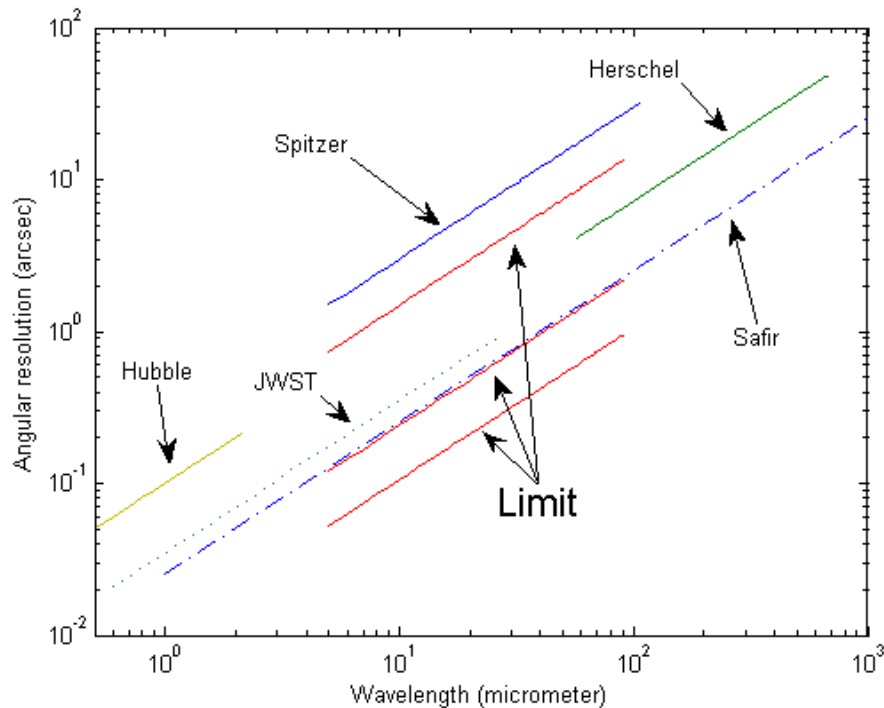


Figure 60. Existing telescope comparison of angular resolution.

Despite the improvements in image resolution that are afforded by sparse aperture imaging, the point spread function (PSF) of the telescope system is degraded because of the degraded coverage of the frequency plane.

However, there are configurations that allow for an optimal coverage of the frequency plane

for an equivalent radius. A Golay configuration is an effective way to cover the frequency plane, however, the collecting units are fixed on the Moon's surface and thus, the Golay coverage will be optimum only in a specified direction.

An optimization problem is then posed, which consists of finding the configuration that covers in an optimal way the largest region of the sky, taking into account that for a given elevation, the UV coverage pattern and the PSF will be defined by the projection of the aperture in the observation plane. It is also worthwhile to consider that, as the Moon rotates, the azimuth angle becomes a parameter that can be adjusted for optimal performance of a given configuration. An intensive study of the optimal configurations for UV plane coverage is described in Kong's work [60].

As a baseline for the design of a multiple-aperture system in a static configuration, Figure 61 and Figure 62 show the variation of the Point Spread Function for the proposed configurations: a deformed Golay-3 and a deformed Golay-9 configurations that are designed for optimal performance at an elevation of 45 degrees, obtaining an appropriate coverage of the band of the sky between 30 and 75 degrees.

Point Spread Function for a Golay-3 configuration,
removed due to copyright restrictions.

Figure 61. Point Spread Function for a Golay-3 configuration.

Point Spread Function for a Golay-9 configuration,
removed due to copyright restrictions.

Figure 62. Point Spread Function for a Golay-9 configuration.

8.2.3 Signal-to-noise ratio

Using the performance of an 0.85-m monolithic telescope as a baseline, Figure 63 compares the signal-to-noise ratio of the arrays.

The signal-to-noise ratio (SNR) is degraded as the filling factor is reduced. Even though the collecting area increases linearly with the number of telescopes, the encircled energy reduces at a non-linear rate. The plots were calculated assuming a constant background noise, however, the effects of sparse aperture for different observation objectives should be further analyzed. In order to obtain the same levels of signal-to-noise ratio as Spitzer, using the same sensors that were used in Spitzer, the time scale of light collection must be increased by a factor shown in Figure 64. However, due to the expected continuing improvement of IR sensing technology during the time before the LIMIT telescope is built, more efficient sensors than those used in Spitzer might become available, and then the collection time could be reduced.

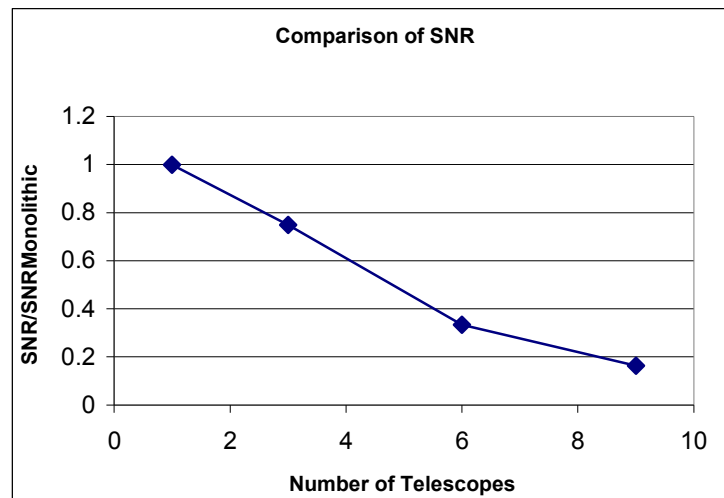


Figure 63. Comparison of SNR to a single telescope of equivalent diameter with a filled aperture.

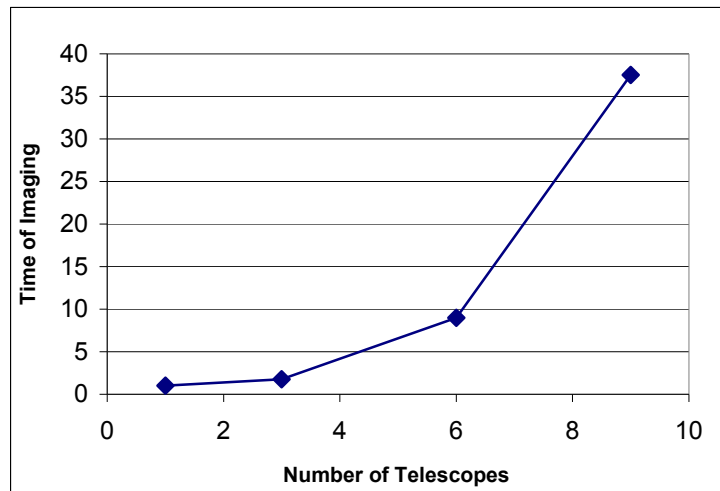


Figure 64. Required increase in imaging time for a sparse array.

8.2.4 Infrared Sensors

The sensors of the system are Charge Coupled Devices in three different regions of the IR spectrum. To continue the leveraging of Spitzer legacy designs, the instruments will be an upgraded version of the IRAC, IRS and MIPS devices. The sensors will provide waveband coverage from 5 to 90 μm .

Each instrument will consist of cryogenic sensor subassemblies and warm electronics subassemblies. The cryogenic subassemblies will share a cryocooled chamber. The cryogenic subassemblies perform the combining of light and the optical processing of the interferometer input beam and deliver a resulting signal to the infrared detector arrays, which produce a low-level analog output signal.

The instrument warm electronics subassemblies will provide the necessary electronic processing and state of health monitoring for detector operation and readout, including clock generation, analog-to-digital conversion, compression, formatting, and presentation to the communication system for storage and subsequent transmission to relay.

In each instrument the most critical performance-determining components are the infrared detectors and their associated cryogenic readout circuits. As the wavelength of operation increases, required operating temperature decreases.

The instruments access the focal plane of the Spitzer telescope through a flat mirror, whose position points the field of view to the specific instrument. The design of the interferometer uses three spectral sensors derived from IRAC, IRS and MIPS.

I-IRAC

The Interferometric Infrared Array Camera (I-IRAC) will be a multichannel imager, collecting light from 3 to 14 microns in a single unit.

I-IRS

The interferometric IRS will be comprised of four separate cold optical assemblies. Two of the modules produce low-resolution spectra with a one-dimensional image along a slit.

The interferometric array will have an important impact improving the capabilities of this instrument. This instrument could be operated with equal performance in most of the observed

sky, and the improvement in the resolution will present science data never before achieved with any previous telescope.

Each module will contain one infrared detector array, that may use Spitzer's legacy technology's arsenic doped silicon (Si:As) blocked impurity band detector (BIB) or an antimony-doped silicon (Si:Sb) BIB detectors.

I-MIPS

The Interferometric MIPS instrument will comprises a single cold optical assembly contains multiple optical trains that can be operated in one of three data gathering modes: 1) image in three bands simultaneously, 2) image with high magnification at 70 μm , and 3) low-resolution spectroscopy from 50 to 100 μm . A scan mechanism will modulate the signal to the Germanium detectors select among the three instrument operating modes.

The instrument may utilize two gallium-doped germanium (Ge:Ga) arrays as used in Spitzer. The improvements in long-wavelength sensing technology will be a key improvement in the sensitivity of this instrument, and will allow the generation of very high resolution Far-IR images that will largely increase the scientific value of the interferometric array.

8.3 Electronics Subsystem

8.3.1 Introduction

The electronics in the system would be distributed in two principal units: the collector command unit, and the central command unit.

Collector command unit

The computer on each of the collectors will acquire and monitor the state of health of the telescope and control the attitude state of the unit and any active optical elements in the process and will be in charge of receiving and communicating actuators command and state. These units require good performance for handling communications with the central unit, and command the control commands to the actuators in the telescope pointing system. A 100MHz processor is calculated to be able to appropriately handle communications, perform state-of-health monitoring, and control data communications.

Central command unit

The central command unit is the main processing unit of the system. This unit shall monitor the overall state of the system. It has the following functions:

- Distribute commands to the pointing system in each collector telescope.
- Receive information regarding the state of each collector.
- Calculate path delays for each telescope and sends control data at a very high frequency rate for the active optic units.
- Calculate data and commands for the thermal and power system.
- Monitor the overall state of the system.
- Command the back optics instrument selection.
- Provide precision clock and readout interfaces for data acquisition.

8.3.2 System sizing

The largest image size produced with the designed instruments is a 256 by 256 pixel image, using a minimum integration time of 500 seconds.

The data rate to be stored in buffer memory and sent back to the relay station is on the order of 200 kbps. The transmission rate should be greater than this value, therefore, assuming that communications are available for downlink on a 50% duty cycle, the communications electronics are sized for a transmission rate of 500 kbps.

8.4 Power Subsystem

8.4.1 Introduction

A scalable solar panel power subsystem was designed for the LIMIT telescope, with consideration given to a more expensive but possibly favorable RTG power system. The fully deployed Golay-9 array telescope requires a solar array designed to provide 2.7 kW to provide the requisite lifetime power. Solar panel deployment is designed for the rim of the Shackleton Crater, where light availability is expected to be high. The option of using an RTG power system is discussed in light of other mission constraints, including deployment, complexity, and location.

8.4.2 System definition and interfaces

The central unit power system will provide 250 W end-of-life power to each of the telescope units in the Golay-9 array, giving a total of 2.25 kW end-of-life power for the whole system. The system is highly modular, and much of the mass is due to batteries, making it feasible to construct the power subsystem for a partially deployed system, and upgrade it later with additional batteries. Due to the position on the rim of the Shackleton Crater, 10 km of wire will be necessary to power the array located inside the crater.

The RTG power system should be designed and locally deployed for the maximum power usage of the planned system. Although this system is modeled to cost \$80M more than a solar panel system, the benefits of lower mass, volume, simplicity, and local positioning may make it favorable. See Table 19 for comparisons of metrics between systems.

IR Power System Metrics								
		Solar Panels and Batteries				RTG		
Units	kW	Total Cost \$	Mass kg	Volume cm ³	Area m ²	Total Cost \$	Mass kg	Volume cm ³
1	0.3	\$ 128,860	229	3,109	1.35	\$ 13,050,000	18	38,486
4	1.20	\$ 515,442	915	12,438	5.39	\$ 52,200,000	71	43,843
6	1.80	\$ 773,162	1,373	18,656	8.08	\$ 78,300,000	107	47,414
9	2.70	\$ 1,159,744	2,059	27,985	12.13	\$ 117,450,000	161	52,771
12	3.60	\$ 1,546,325	2,745	37,313	16.17	\$ 156,600,000	214	58,129
16	4.80	\$ 2,061,766	3,661	49,751	21.56	\$ 208,800,000	286	65,271
Sunlight Availability		90%						
Night Duty Cycle		100%						

Table 19. Metrics for LIMIT power system.

Figure by MIT OpenCourseWare.

8.4.3 Cost, mass, and volume models and assumptions

To ensure consistency across designs, the same modeling and assumptions were used for

both the LIMIT power subsystem and the LIRA power subsystem. Please see Section 7.4.3 for details.

8.4.4 Development process, trade studies, and sensitivity

The power requirements were drawn primarily from comparison to Spitzer requirements. Comparisons to other space telescopes, including JWST, and SAFIR were made, and allowances for future technological development were estimated.

After power consumption was determined, the alternatives were compared in the model, and then external factors were taken into consideration. Consideration was given to phased development, as well deployment and operating risk factors not contained in the model. Sensitivities in the model were also considered, including sunlight availability, night time duty cycle, and power consumption.

The risks identified lie predominantly with the solar panels and batteries. Even though solar panels are relatively simple systems, the mass and volume of the batteries and power cables are concerning for deployment. Deploying a 10-km cable, weighing over 1 metric ton, across the lunar surface may be difficult and offers a long single point of failure. Even if deployed in segments, this is a significant amount of mass to drive on a lunar rover.

The risks associated with RTGs lie in the political ramifications. Given the present attitude toward such technology, it seems that it will not be a prohibitive system if treated properly.

Since the solar panel and battery system is very sensitive to the availability of sunlight, the positioning of this system is the most important factor in choosing a solar- or RTG-based system. The mass of batteries required to last during the lunar night increases rapidly as percent of sunlight availability decreases. In the worst case of only 50% sunlight illumination, the mass of batteries required is nearly 10,000 kg, more than one-half of the cargo capacity of an Ares V launch. Considering launch costs, the inflection point, where an RTG system becomes less expensive, is around 70% sunlight illumination. Most of the surface of the Moon around the Shackleton Crater receives about 70% sunlight illumination, making the precise location chosen very influential in the most cost-effective system.

The power requirements vary depending on the location on the lunar surface. If a polar site is chosen, where the sun angle is so low that most of the surface is in deep shadow, the solar arrays must be placed in a spot with almost constant sunlight. The regions around the southern pole have permanently shadowed places for the detector assemblies and spots that receive sunlight almost permanently for solar arrays. In placing the detector assemblies, a permanently-shadowed spot that is sufficiently close to an almost permanently-lighted place for acquiring solar power must be chosen. About 120 km from the crater is the 5-km-tall Malapert Mountain, a peak that is perpetually visible from the Earth. Therefore, it would be ideal to place a power station on the summit of Malapert and distribute power from there to the antenna units.

If a telescope with a certain aperture is chosen, its power requirement can be estimated by scaling from a model. Assuming the telescope will be made using ultra-lightweight optics as in the James Webb Space Telescope (JWST) by NASA, one of the potential JWST designs can be used as a standard model for the telescope. According to this design, a JWST-like observatory with an 8-m aperture is estimated to consume 760 W of power on average.

8.5 Structure Subsystem

8.5.1 Introduction

The optics for LIMIT are based on the Spitzer Space Telescope to take advantage of the existing knowledge and experience with that design. One of the main differences between using it in space versus on a solid surface is the structure required to support and control it. This section will examine the requirements for a support structure and mount for the optics.

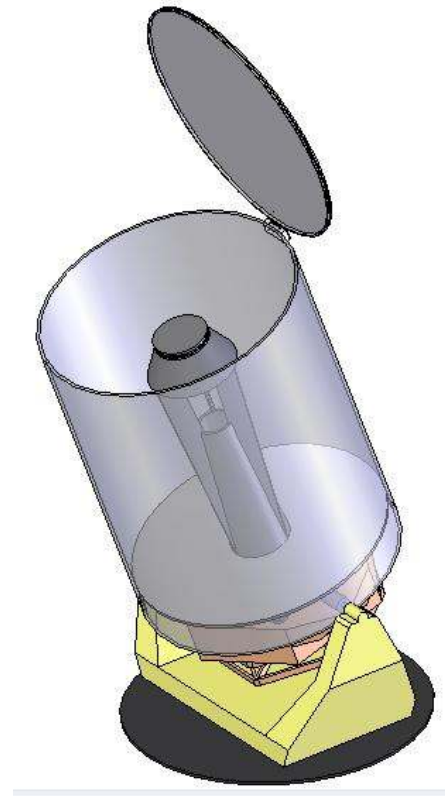


Figure 65. Conceptual design of LIMIT unit telescope.

The presence of a gravity field leads to a structure design resembling those of ground-based telescopes. Yet the need to launch the telescope to the Moon will drive the telescope towards a lightweight design, since launch mass has a significant impact on overall cost.

8.5.2 System definition and interfaces

The structure subsystem consists of the telescope mount needed to support the weight of the optics, the bearings and motor control to point the telescope. It contacts the lunar surface and allows the collecting telescope units to aim at astronomical targets.

8.5.3 Mount design description

The telescope mount supports the primary and secondary mirrors and the cylindrical shell, which serves to block stray light and create a thermal shield. With a U-shape, the mount provides a pivot point of rotation for elevation angle changes, while the entire mount is rotated about a zenith-pointing axis to give azimuth angle changes of up to 180 degrees in either direction.

For purposes of weight considerations, aluminum honeycomb is selected as a material that provides high stiffness- and strength-to-weight ratios. Its use in aerospace applications allows structure designs where weight is at a premium. Like other non-isotropic, composite materials, its properties vary with orientation within the material. Though detailed analysis techniques exist for composite layer analysis [61], this analysis uses the lower of the cited strength and stiffness values and then assumes isotropic behavior.

Figure 66 shows the structure mount design concept. The mount supports the weight of the optics, insulation, control mechanisms, and provides an anchor to the lunar surface. Since no mount structure was required for the free-flying Spitzer design, analysis was conducted to determine the size required for the LIMIT mount.

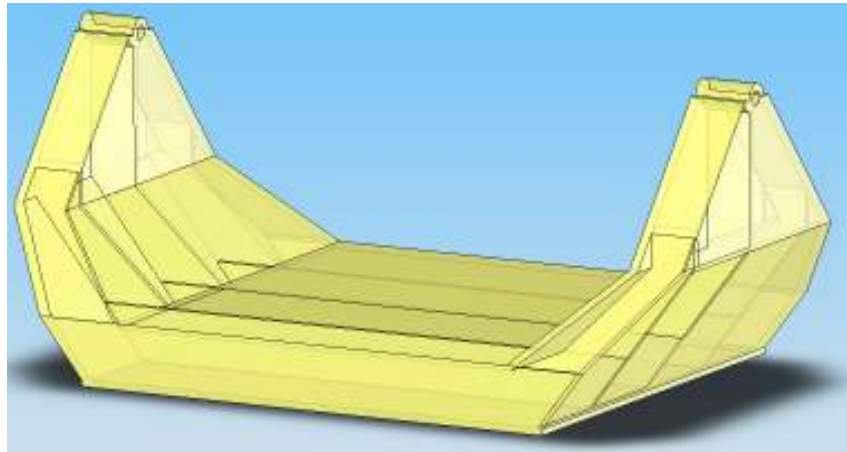


Figure 66. Mount concept consisting of hollow aluminum honeycomb structure with internal ribs.

8.5.4 Structural analysis

To conduct structural analysis, the structure is represented as a beam with a column on either end (see Figure 67). The structure is analyzed for the following: column buckling cross-section area, beam bending stress, and maximum beam deflection. Both column and beam cross sections are assumed to be square, and, with the lower strength (1150 psi) and stiffness (210 ksi) values of the aluminum honeycomb assumed, the required length dimension of each side is determined for the structure load. From the Spitzer design, it is known that the assembly comprising the primary and secondary mirrors has a mass of around 50 kg. The cylindrical shielding and components for optics and control bring the supported mass up to around 130 kg. This mass times the acceleration due to gravity on the Moon ($1/6$ that of Earth gravity) gives the total load the structure must support, which is divided by two to account for each column.

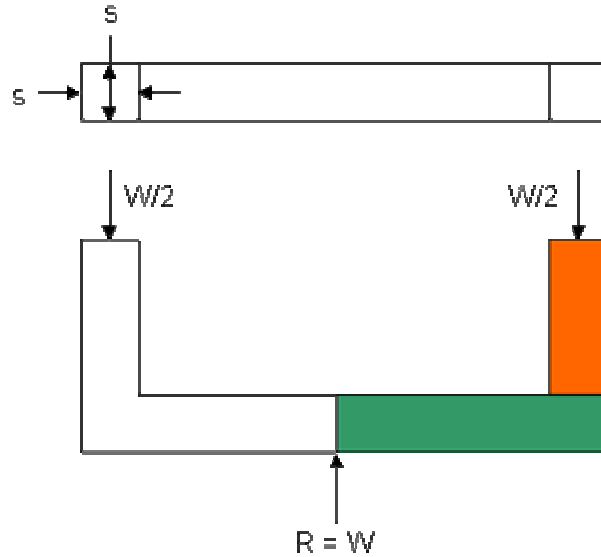


Figure 67. Simplified mount structure for analysis.

To determine the buckling load for a given modulus of elasticity, E , area moment of inertia, I , column length, l , and coefficient, K , that depends on the end conditions (for fixed-free conditions $k = 2$), the formula is:

$$F_{buckling} = \frac{k\pi EI}{l^2} \quad (\text{Eq. 22})$$

Given the load, and assuming a square cross section, the length of each side can be determined (where $I = s^3/12$). This calculation gives a column width of approximately 1 cm.

The horizontal portion of the mount is modeled as a cantilevered beam, with the two quantities of interest being the bending stress and maximum tip deflection. For a moment, M , given by $M = FL$, and side length, s , the bending stress is

$$\sigma_{bending} = \frac{Mc}{I} = \frac{6M}{s^3} \text{ (square)} \quad (\text{Eq. 23})$$

and the deflection at the end of the beam, the length of which is L , is given by

$$\delta = \frac{FL^3}{3EI}. \quad (\text{Eq. 24})$$

The bending stress limit puts the height of the beam at 5 cm, but a maximum deflection limit of 1 mm increases that to 10 cm.

Other components included in the structure are tapered roller bearings for elevation rotation, a needle thrust bearing for azimuth rotation, motors for pointing control (mass and power estimated from [37] based on telescope moment of inertia), and insulation.

Using the analytical structure results, the weight including other components is estimated to be 23.5 kg.

8.5.5 Finite element method analysis

Since an actual structure may not be a square column and beam design, a more detailed analysis was conducted. With potential horizontal loads present in deployment and handling, a mount with a wider base would be practical. This would also be stiffer with respect to vibrational modes. The U-shaped mount was analyzed using SolidWorks' CosmosExpress finite element solver. The refined design has panels of 1-cm thick aluminum honeycomb and a hollow core, except for 3 stiffening ribs which run internally between each column. Figure 68 shows the design analyzed for von Mises stress distribution.

The stress analysis revealed a roughly even stress distribution through the lower, horizontal structure, with peaks occurring near the internal ribs. The vertical column sections have lower stress throughout. Overall, the structure has a factor of safety of around 6, which indicates the design is overly conservative. Even so, the mass of this telescope design (including operating components) only comes to around 26 kg. For a more detailed study, this structure can be optimized to obtain a geometry that is between the analytical square column and beam analysis and that of the finite element analysis done here.

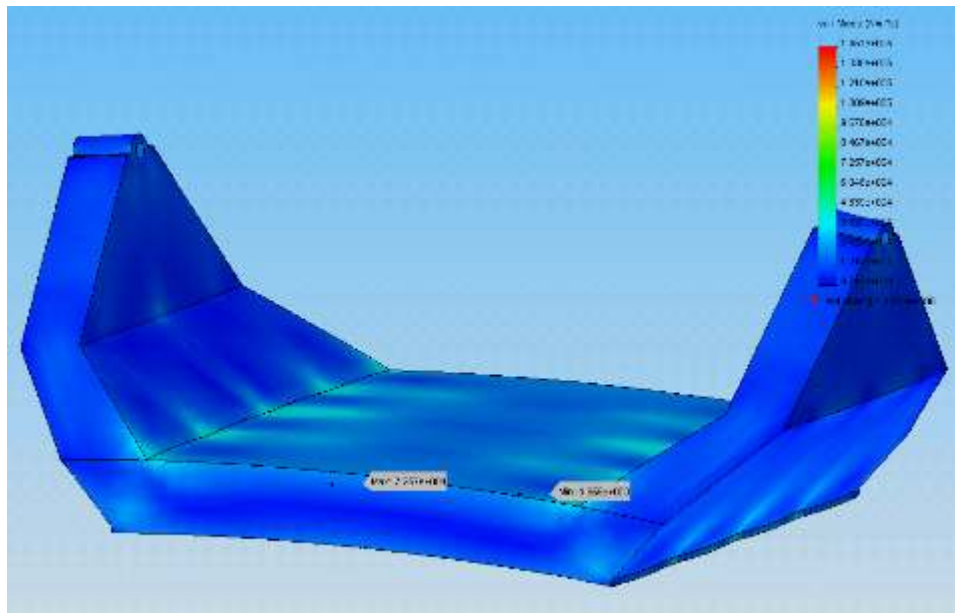


Figure 68. Finite element von Mises stress analysis for the telescope structure mount concept.

8.6 Thermal Control Subsystem

8.6.1 Introduction

The thermal control system (TCS) maintains the temperatures necessary for efficient operation of the telescope. The most important role of the TCS for the LIMIT observatory is to ensure that the IR optics and focal plane instrumentation are maintained at cryogenic temperatures to maximize sensitivity. Being located in a permanently shadowed crater offers ambient temperatures that are naturally cryogenic (< 120 K). Lester suggests that a crater floor at the lunar pole may be “the coldest place in the entire inner solar system [62].” To capitalize on the cold and stable environment, the TCS employs passive cooling to the greatest extent that

is feasible, reducing mass and design complexity. The active cooling design leverages advanced cryocoolers to sustain temperatures around 6 K, and loop heat pipes to facilitate heat rejection from the compressor and other electronics.

8.6.2 System definition and interfaces

The TCS is comprised of all the passive and active cooling elements, including multi-layer insulation (MLI), radiator panels, cryocoolers, and heat pipes. Each of the nine telescope collector units uses identical thermal control. The combiner unit, on the other hand, has a dedicated cooling system to achieve the required operating temperature for the IR detectors and instrumentation.

Cooling of combiner unit

The combiner unit is actively cooled through the use of a cryocooler, in addition to passive thermal shielding. The cooling requirement for IR detectors has been established at 6 K for JWST and TPF [63]. This design adopts the same detector operating temperature to ensure acceptable IR measurements. Several cryocooler architectures have been developed as part of the Advanced Cryocooler Technology Development Program (ACTDP), all of which have been designed to meet cooling requirements for JWST, TPF, and other NASA missions (in most cases, space telescopes at Earth-Sun L2 [64, 65, 66]). The LIMIT array intends to leverage these cryocooler concepts and eventual space-qualified hardware that arise from the ACTDP. Each design achieves two operating temperatures (18 K and 6 K) and employs a configuration that separates the cryogenic cold head from the compressor/electronic controller by several meters for thermal and vibrational isolation. For this combiner unit, the 18 K load is the combiner optics and the 6 K load is the IR detector and instrumentation. The cryocooler compressor and electronic are housed separately from (positioned adjacent to) the combiner unit. The input power for the compressor and electronic controller is supplied from the solar array and battery system.

Heat rejection system

A common heat rejection system removes internal heat arising from power dissipation in the cryocooler compressor/electronic controller and electronics units for other subsystems (command and data handling and communication). The system uses loop heat pipes to extract heat from the internal sources and remove it from the combiner unit to offboard radiator panels for rejection to the lunar sky. These panels are positioned to radiate waste heat in directions away from the telescope array.

Cooling of collector units

The goal for thermal control of the collector units is to passively cool the optics to around 10 K with adequate shielding from the surrounding crater. Further discussion on this idea is found later in the section.

8.6.3 Assumptions and ground rules

Since the lunar environment drives the TCS design, a detailed discussion of the assumptions about ambient conditions and external heat sources is presented here.

Lunar Polar Craters

Regions within the Shackleton crater remain in permanent darkness, and the absence the sun as a heat source keeps the ambient temperature below 100 K. Arnold identifies four heat sources that determine the temperature of permanently shadowed lunar regions [67].

1. Geothermal heat flow at 2×10^{-6} W/cm²
2. Solar wind at 9×10^{-8} W/cm²
3. Reradiation of solar flux from illuminated regions (e.g. crater rim)
4. Conduction from illuminated regions

The first two heat sources (geothermal heat flow and solar wind) result in the Moon's blackbody temperature of 24 K. The third heat source (reradiation) stands to be both the dominant source and the most variable, since it is highly dependent on line of sight geometry. Arnold gives the following equation to approximate the reradiation, as a function of the reradiating area/temperature, A_r/T_r , the angles between the reradiating/shadowed surface normals and the line connecting them, θ_r and θ_c , and the crater radius, R:

$$\frac{A_r}{\pi R^2} \cos \theta_r \cos \theta_c (\sigma T_r^4) = \sigma T^4. \quad (\text{Eq. 25})$$

For a band of reradiating area at the top of the inner rim of a small crater ($A_r \approx 0.1$ km² and $R = 1$ km), the resulting temperature in the shadowed region is about 40 K (including the first two heat sources). Note that the fourth heat source (conduction) is generally negligible. Vasavada confirms this result with a more detailed calculation [68]. Figure 69 (left) shows the predicted surface temperatures for a lunar crater at different latitudes. Figure 69 (right) is the estimated temperatures in the Shackleton crater. Polar lunar craters may achieve permanent surface temperatures below 80 K for most of the inner crater floor, possibly as low as 50 K.

Ultimately the actual temperatures reached at the Shackleton crater need to be studied experimentally. This uncertainty impacts design decisions for a telescope facility located there.

Surface temperature for lunar craters at three latitudes,
removed due to copyright restrictions.

Figure 69. Surface temperature for lunar craters at three latitudes;
(right) surface temperature for Shackleton crater at
89.7°S latitude (maximum temperature in left
column, average temperature in right column) [68].

Passive Thermal Control of Collecting Telescope Units

With crater temperatures potentially reaching as low as 40 K, a worthwhile goal of the thermal design of the LIMIT observatory is to take advantage of the low and stable temperatures. Furthermore, Lester indicates that with proper shielding, temperatures down to 7 K can be reached passively [62]. If so, this would be excellent conditions for an IR space telescope.

8.6.4 Temperature Goals

The question arises as to how cold the telescope must be. Because of the sensitive nature of IR photodetectors, the signal-collecting instruments must be maintained actively below 5 K. For the telescope optics and structure, though, the temperature must be such that its own thermal emission does not contribute to the signal that is being collected from astronomical objects. To get an idea of what telescope temperature is desirable, some insight can be obtained by comparison with other IR space telescopes.

For JWST, Spitzer, and Herschel, the longest observed wavelengths for each telescope, and the associated mirror temperatures are shown in Table 20. It can be seen that the product of these two values is roughly the same for all three telescopes. This is consistent with Wien's displacement law, which states that the wavelength of peak emission of a blackbody times the blackbody temperature is a constant, i.e.

$$\lambda_{\max} T_{\text{blackbody}} = 2897.7 \quad (\text{Eq. 26})$$

where λ is in μm and T is in K.

Comparing the product of wavelength and mirror temperature for the three space telescopes, the value is found to be approximately 3.7 times lower than Wien’s displacement constant. From this relationship between the observed wavelength and mirror temperature, *Figure 70* shows how the science requirements of the LIMIT observatory drive the desired mirror temperature.

Table 20. Space IR telescope wavelengths and temperatures.

Telescope	Longest wavelength observed, μm	Mirror Temperature, K
James Webb Space Telescope	28	18
Spitzer Space Telescope	128	5.5
Herschel Space Observatory	670	1.7

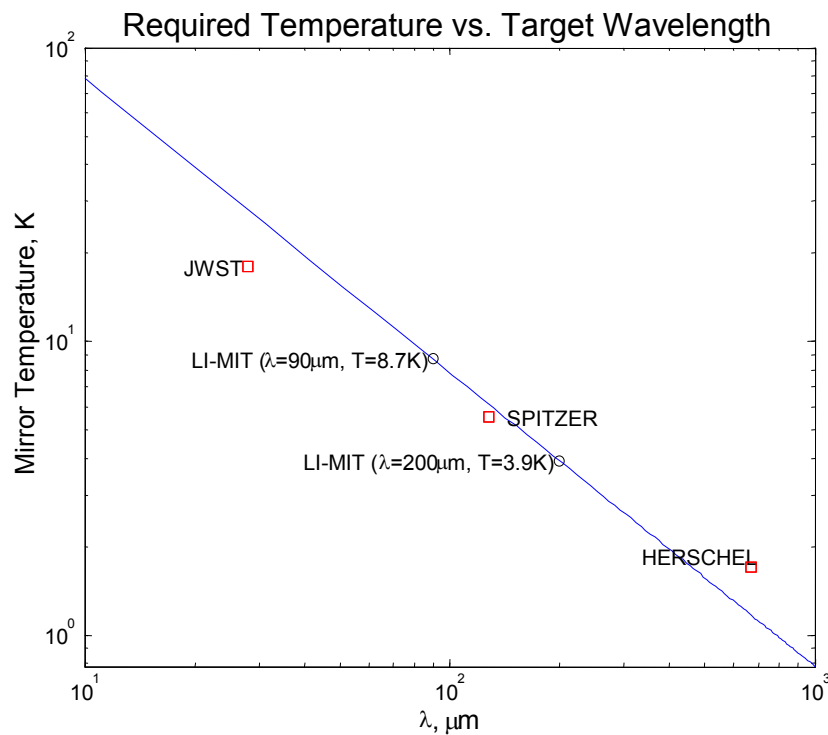


Figure 70. Mirror temperature and longest observed wavelength relationship for IR space telescopes.

For the goal of seeing out to 90 μm in the infrared, the mirror temperature goal should be about 9 K. Though longer wavelengths can be observed at the same temperature, this will be at the expense of increased noise in the signal.

8.6.5 Passively shielding, insulating

To analyze the conditions for passively cooling a telescope in Shackleton crater, the case of large, re-radiating shields is considered. The equation for heat transfer rate, q_{ij} , between large, adjacent layers, i and j , with absolute temperatures T_i and T_j , and area A , is given by

$$q_{ij} = \frac{\sigma A (T_i^4 - T_j^4)}{\frac{1}{\varepsilon_i} + \frac{1}{\varepsilon_j} - 1}, \quad (\text{Eq. 27})$$

where σ is the Stefan-Boltzmann constant, and $\varepsilon_{i,j}$ is the emissivity of layer i,j .

Figure 71 shows a radiation shield-based model to represent the telescope's radiation environment. Multi-layer insulation (MLI), commonly used in space missions as insulation in low-convection environments, serves as the insulating shield. Since the heat flux through each layer is the same, the mirror temperature can be calculated by comparing the temperatures and emissivities for the other known layers.

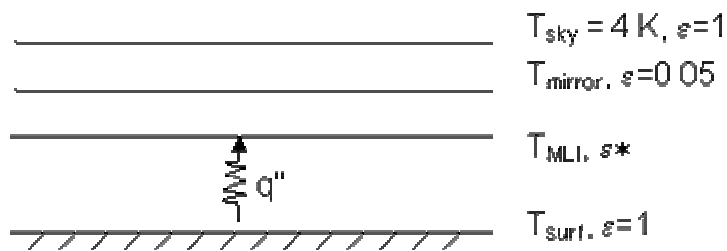


Figure 71. Radiation model for emissivity relationship to temperature.

Based on the assumptions of $T_{sky} = 4 \text{ K}$, $\varepsilon_{mirror} = 0.05$, $\varepsilon_{surf} = \varepsilon_{sky} = 1$, Figure 72 shows how the achievable temperature by passive radiation changes with the effective emittance, ε^* , of the multi-layer insulation. Since the lunar surface temperature is not known definitely, temperatures of 40 K, 55 K, and 70 K are plotted. Also, the effect of putting two more sheets of MLI as shielding is shown as dotted lines. Typical limitations of ε^* are shown as vertical lines in the plot, where 30-layer, medium-sized applications are usually around 0.005, and controlled testing of cryogen tanks have achieved values as low as 0.002.

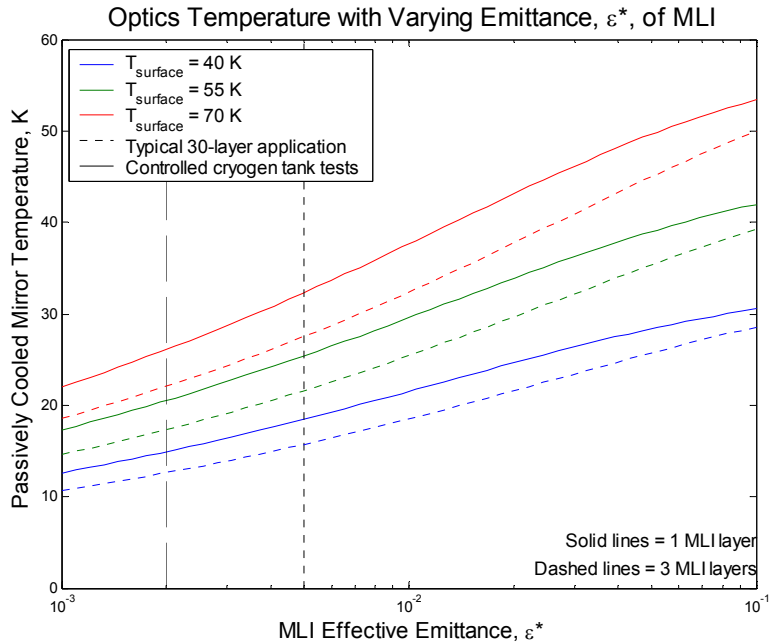


Figure 72. Temperature variation with effective MLI emittance for surface temperatures.

From this analysis, it seems unlikely that using only passive means of cooling the telescope optics and structure will allow temperatures below 10 K. The model studied is simplified, however, and more detailed analyses should be conducted to determine the feasibility of passively-cooled telescope collecting units. For the science goals of the LIMIT concept, it will be assumed that temperatures around 9 K can be achieved. The contingency scenario would be the deployment of cryocoolers with each telescope to cool it from ~20 K down to below 10 K for longer IR-wavelength exploration. This is obviously costly in terms of launch mass, development and testing cost, failure potential, and OTA design complexity.

8.6.6 Initial Deployment Cooling Requirement

Assuming the collecting telescopes will passively maintain temperatures around 10 K and arrive at the Moon fully insulated, there is a question regarding how long it would take to cool down before observations can be made. With Spitzer taking a couple months to cool to operational temperatures, it is worth looking at what could be expected for the LIMIT observatory.

A model was set up in which the multi-layer insulation surrounding the telescope (used to keep radiation energy out) was assumed to be perfectly insulating to keep energy in just after deployment, and the only means of energy loss is radiating to the sky (see Figure 73).

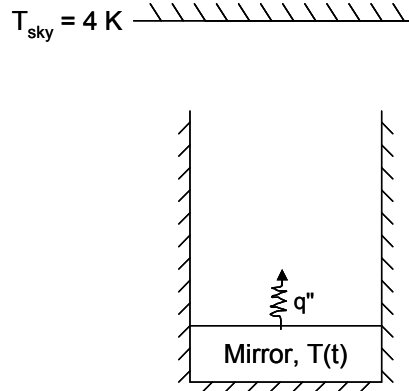


Figure 73. Model to determine the time required to initially cool the telescope after deployment.

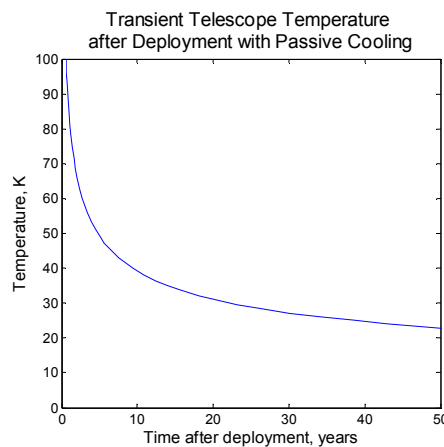


Figure 74. Transient results for radiative cooling to sky.

The results of this analysis, assuming a uniform temperature distribution throughout the mirror, shown in Figure 74, reveal that a very long time is required to cool the telescope if it is only radiating from the mirror to the sky.

A potential solution to this problem is to carry a tank of liquid helium on the telescope. After deploying the telescopes, a valve would open to release and carry the coolant over the telescope. A schematic of this concept is shown in Figure 75.

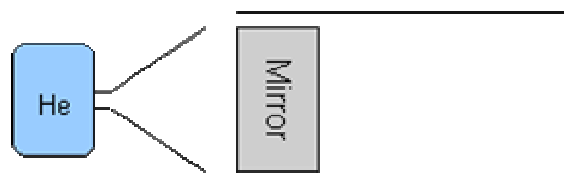


Figure 75. Helium cooling concept for initial deployment of telescopes.

For a first order analysis, a lumped capacitance transient heat transfer model using Equation 28 is used, where ρ is the density of the Beryllium mirror, V is the volume, c is the specific heat capacity, h is the convection coefficient, A_s is the surface area of the mirror, and T_∞ is the fluid

temperature (assumed to be liquid helium temperature of 4 K)

$$\rho V c \frac{dT}{dt} = -h A_s (T - T_\infty) \quad (\text{Eq. 28})$$

The convective heat transfer coefficient is approximated from an expression in [69] for fluid flow over a cylinder.

The results from this analysis are shown in Figure 76. Cooling from a temperature of 300 K requires about 400 seconds to get to ~20 K, and around 17 kg of helium is used. Due to the fidelity of this analysis, however, this is expected to be a moderately to highly conservative estimate, and more helium would likely be necessary.

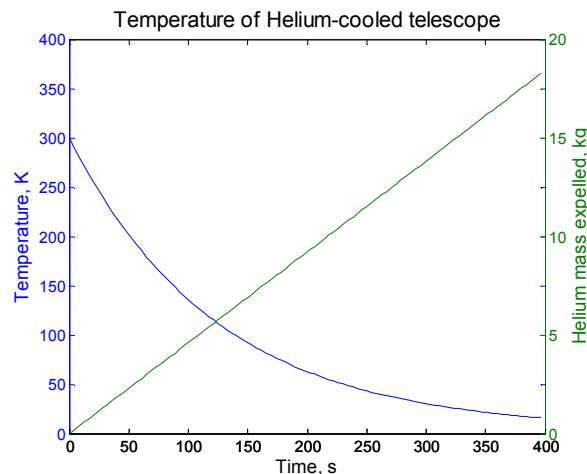


Figure 76. Transient temperature of He-cooled telescope and amount of He required.

If further analysis reveals prohibitively large quantities of helium are required for initial cooling, a couple of other cooling concepts are: 1) package a cryocooler on each telescope unit, or 2) have a central cooling system that works during transit or soon after landing when the telescopes can be cooled by a single system and then deployed to their positions, to save on many cooling units needing to be developed. If a cryocooler is required on each telescope, it can also be used to ensure low operating temperatures, where its size would probably not be too large, since passive cooling to 20 K to 30 K appears readily feasible. The initial cooling load and that operating requirement would be the main considerations for sizing the cryocooler for the collecting telescopes.

Advances in Cryocooler Technology

It is assumed that the development work under ACTDP will produce a family of mature cryocooler technologies that can be leveraged for the lunar IR telescope. For the preliminary design discussed here, it is also assumed that the refrigeration capacity requirements for the cryocooler to be used for the combiner unit are identical to those for the JWST and TPF missions. In particular, the design specifications call for a cold head performance of lifting 150 mW at 18 K and 30 mW at 6 K [63]. The heat dissipation requirements of the LIMIT array's combiner unit and IR detector are assumed to be the same 150 mW and 30 mW as seen on those missions.

8.6.7 Final subsystem design

The final estimates for the cryocooler design provide for a mass of 40 kg, a power output of 250 W, including the power required for the electronic controller, and a total cost of \$100,000.

8.7 Communications Subsystem

The communications system allows for the transmission of pre-processed data to a suitable downlink site, from which it will become accessible to ground-based researchers.

8.7.1 Introduction

The LIMIT communications system includes the necessary processors to control the interference of telescope signals, cables to transmit data, and the radio transmitter which downlinks the processed signal, either to the nearby human base or directly to Earth.

This architecture represents the simplest possible basic design. More complicated designs are not required, and would unnecessarily increase cost and risk.

8.7.2 System definition and interfaces

The system includes some basic electronic processing capability, for on-site data reduction, as well as the control cables connecting the outrigger elements to the main unit and the processor, and also includes the connections to the radio transmission station and the transmitter itself.

The mass needed is the mass required for the cables, processing equipment, and antenna/signal package. The power is the transmitting power plus the processing power. No power is specifically dedicated to dust mitigation, as a passive design may be used. The cost is the cost of the cable, antenna package, and processor hardware and software. No operating costs, satellite costs, or transportation costs are considered.

8.7.3 Assumptions and ground rules

Estimates of data rate taken from Spitzer and JWST [42, 43, 44] lead to 1 Gbps as an order-of-magnitude estimate for the downlink data rate, with 100-500 kbps as the uplink data rate. For transmission distances equal to or less than the distance to the Moon, a Ka-band radio will meet this data rate requirement [50].

The processor size, power, and mass are estimated according to [39], and it is assumed that the unit described is linearly scalable as a function of data throughput.

8.7.4 Development process, trade studies, and sensitivity

To develop the communications system architecture, a preliminary model of the system was constructed. It was designed to output estimated cost as a function of telescope outrigger distance, estimated data rate, and whether a radio link or a cable link was used. The communications architecture was designed to link to the human base, so that initial data analysis and later retransmission to Earth ground stations could be facilitated.

The preliminary model was used to compare data rates to costs for fiber optic cable links to the human base with costs for a radio link to the human base. The base distance to the human base was set to 5 km. This distance is dictated by the distance from the human base to the nearest permanently-shadowed cold trap, where the telescope will be placed. The distance is

estimated at between 3 and 20 km.

The preliminary model showed that a cable relay and a radio link break even in cost at about a distance of 2.34 km from the lunar base. Radio is thus selected as a preferred link method. The cable link scales up rapidly with distance, but not data rate, and the radio link scales up rapidly with data rate, but not with distance. Therefore, because distance will be driven by the location of cold traps, data rate is a more important variable in this trade.

Figure 77 and Figure 78 show the details of this trade, calculated from the first-order preliminary model. The breakeven points for cost and distance are approximately 5 km and 1 Gbps; these represent a low-end distance and a high-end data rate, so in both cases, a radio link is expected to be a cheaper option than a cable link for the most likely size and location of the final telescope design.

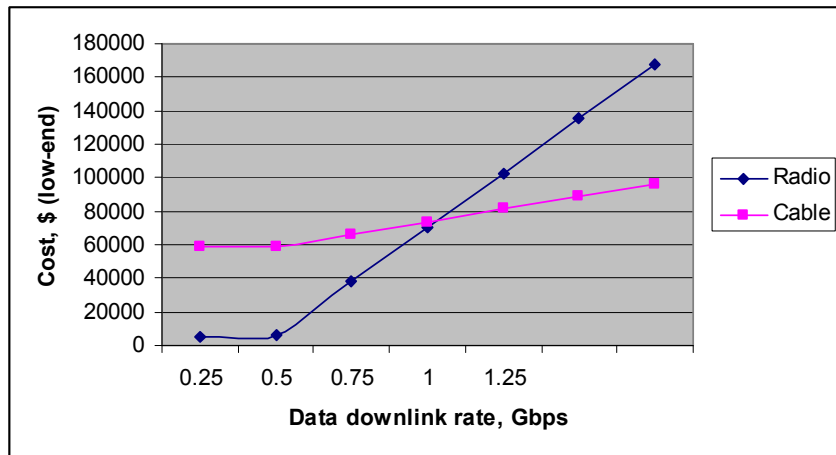


Figure 77. Cost versus downlink data rate.

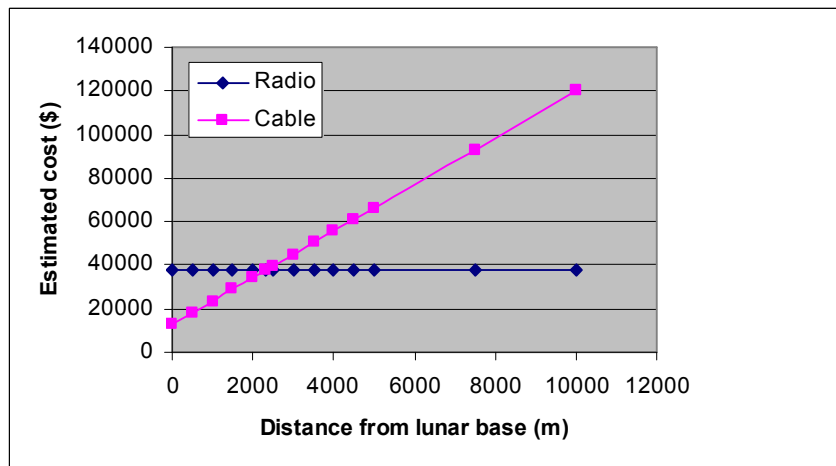


Figure 78. Cost versus distance from human base.

8.7.5 Final subsystem design

The final communications station will be a radio antenna operating in the 32-GHz Ka band, placed in the immediate vicinity of the telescope's central processor station but taking advantage of terrain features if possible.

According to [49], the link budget design for a short-range transmitter (to a nearby receiver

at the human base) is nearly the same as the link budget for a long-range transmitter (to Earth itself). This is probably because the receiving end is much more effective in the long-range link, which connects to the Deep Space Network. The power levels and dish sizes for a Ka-band antenna at 5.0 W are nearly exactly the same, with a 30-GHz carrier and SNRs of the same order of magnitude. Therefore it is assumed that the similarly-sized communications system for LIMIT can be designed to operate either as a point-to-point system, relaying data to the human base for retransmission to Earth, or as a direct downlink to the Deep Space Network. The final decision for this communications system architecture choice is left for future work.

Figure 79 shows the final telescope communications system architecture.

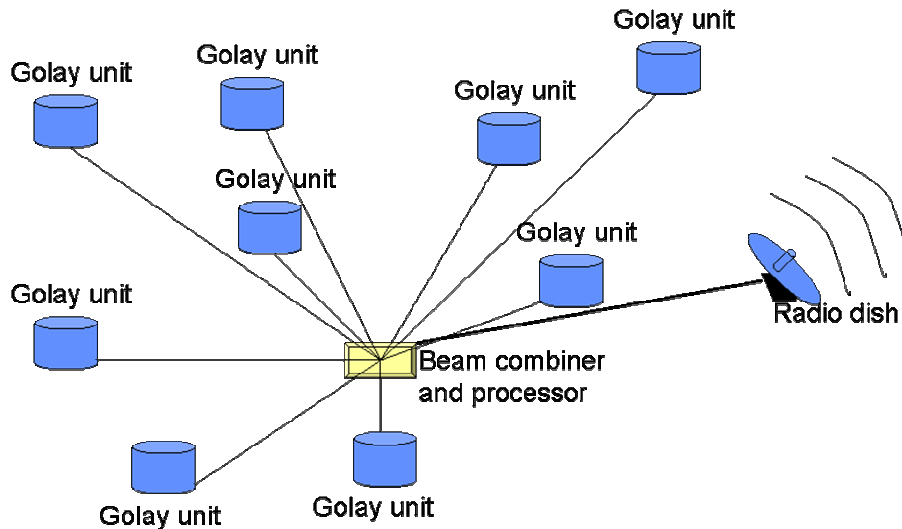


Figure 79. Communications system overview.

8.8 Transportation, Deployment, and Servicing Subsystems

8.8.1 Introduction

This subsystem consists of transportation, which is the launch, transportation, and landing of telescope elements from the Earth to the Moon, deployment, which is the deployment of the observatory on the lunar surface, and servicing, which is the activity to service the telescope elements. Servicing is included as a means of allowing sustained performance for LIMIT, including upgrades and repairs.

8.8.2 System definition and interfaces

Transportation

For LIMIT, the transportation system is mainly concerned with the transportation vehicle, the total mass of components to be transported, the launch cost estimate, and the landing site.

Deployment

The deployment system is mainly concerned with the assumption about human lunar outpost and rovers, the deployment process and configuration, and the extravehicular activity (EVA) and deployment time estimate.

Servicing

The servicing system is only concerned with the repair process when, for example, one telescope is malfunctioning and it has to be repaired at the lunar base. The inputs to the subsystem are the mass and location of each component and the distance from the telescope site to the lunar base.

8.8.3 Assumptions and ground rules

For LIMIT, it is assumed that, as shown in Figure 80, there is already a human lunar outpost at the Moon's south pole, and that rovers for operations on the lunar surface are present at the base. The location of the telescope site is assumed to be the Shackleton crater floor, at a distance of less than 10 km from the lunar base. Figure 81 shows a sketch of the location of telescopes and the lunar base.

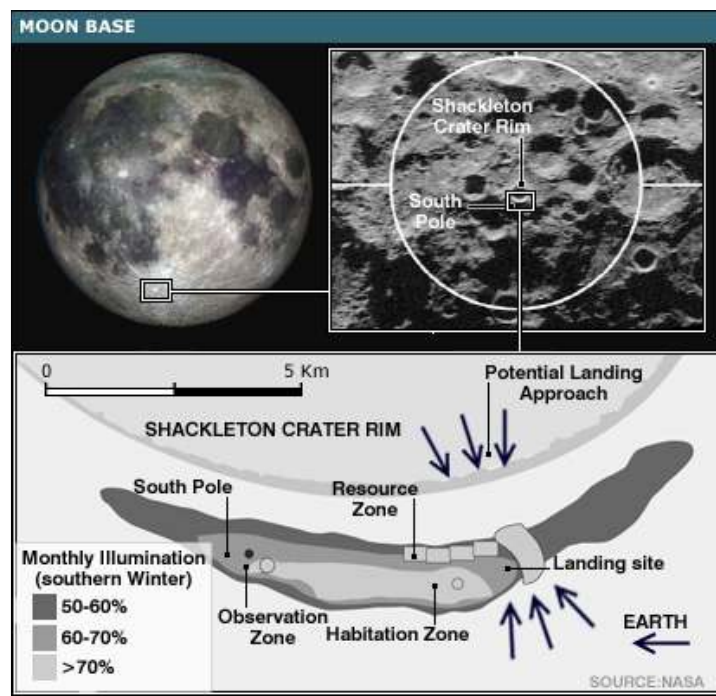


Figure 80. Moon base at the lunar south pole.

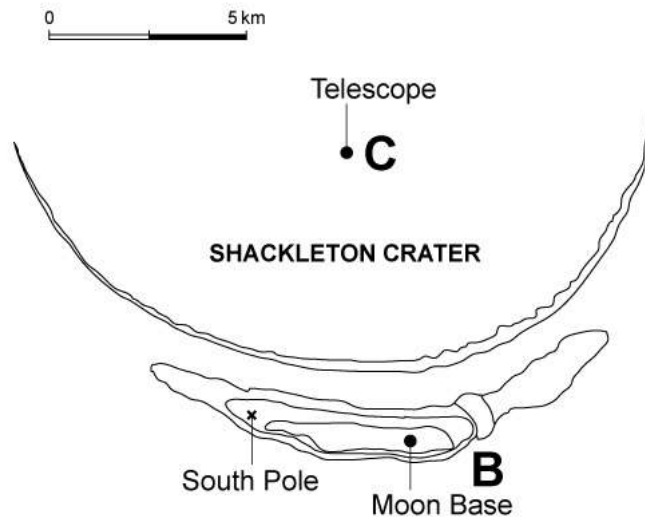


Figure 81. Telescope location.

Transportation

To leverage the vehicles under development for the Constellation program, the Ares V, also referred to as the Cargo Launch Vehicle (CaLV), is assumed as the launch vehicle for this project, as seen in Figure 82. The launch cost for the Ares V rocket is set at \$1.26 billion per launch. For the landing vehicle, NASA's currently planned Lunar Surface Access Module (LSAM), shown in Figure 83, is assumed. The landing site will be the Shackleton crater floor.



Figure 82. Ares V (CaLV).



Figure 83. Lunar Surface Access Module (LSAM).

Deployment

The deployment assumption for the IR concept is that the deployment will be carried out by astronauts and rovers (Figure 84), which is different from that for the LIRA concept, which operates autonomously. For a rover which will deploy the telescope elements, JPL's ATHLETE rover [70], as shown in Figure 85, is assumed as a reference. The ATHLETE rover is able to move at 10 km/h over Apollo-like terrain and its payload capacity is 450 kg per vehicle.



Figure 84. Crew/rover-assisted deployment.



Figure 85. ATHLETE rover.

8.8.4 System components to be transported

Table 21 shows a list of system components to be loaded onboard the Ares V and launched from the Earth. Location B corresponds to the lunar base and Location C corresponds to the telescopes on the crater floor (Figure 81). As shown in the table, much more mass must be landed at Location C than at Location B. Therefore, the landing site should be near Location C, on the crater floor. A non-dedicated Ares V launch would be enough for this mission, since the total mass that the Ares V can carry to the lunar surface is 18 mT, and the total system mass for this mission is approximately 4400 kg. The launch cost estimate would be about 25% of the \$1.26 billion cost for the Ares V, which is \$308 million.

Table 21. System components to be transported.

	Quantity	Mass of each [kg]	Area [m ²]	Volume of each [m ³]	Location
Telescopes					
Telescope + Insulation + Base structure	9	138	-	2.00	C
Fiber optic cabling	1	7.6	-	0.25	C
Beam Combiner					
Beam combining unit	1	300	-	3.75	C
Thermal cryocooler	1	40	-	0.25	C
Power					
Solar panels	1	27	2.25	-	B
Batteries	1	354	-	0.0052	C
Support equipment	1	27	-	-	B
Power cabling	1	1184	-	1.00	B-C
Power distribution box	2	50	-	0.25	B,C
Electronics & Communication					
Computer	1	9.7	-	0.01	C
Radio transmitter	1	3.6	-	0.28	C
TOTAL SYSTEM (plus integration)		4399			

8.8.5 Deployment process

Figure 86 shows the deployment process. After the lander lands near Location C on the crater floor, astronauts and rovers will arrive at the landing site. Using ATHLETE rovers, astronauts will unload the cargo and deploy and install all the telescope elements carefully and connect the cables between them. After all the installation is completed, astronauts and rovers will return to the lunar base and wait for a period long enough to allow any raised dust to settle. The mirror covers will then be opened to prepare for observation.

1. Lander landing (near C)
2. Cargo unloading
 - Staff/rover-assisted unloading
3. Operations by staff and ATHLETES
 - Deployment and installation
 - Telescopes (C)
 - Beam combiner (C)
 - Cry cooler (C)
 - Computer (C)
 - Radio transmitter (C)
 - Batteries (C)
 - Solar panels (B)
 - Cable connection
 - Fiber optic cables (C)
 - Power cables (B-C)
4. Prepare for observation
 - Dust settles down
 - Mirror covers open

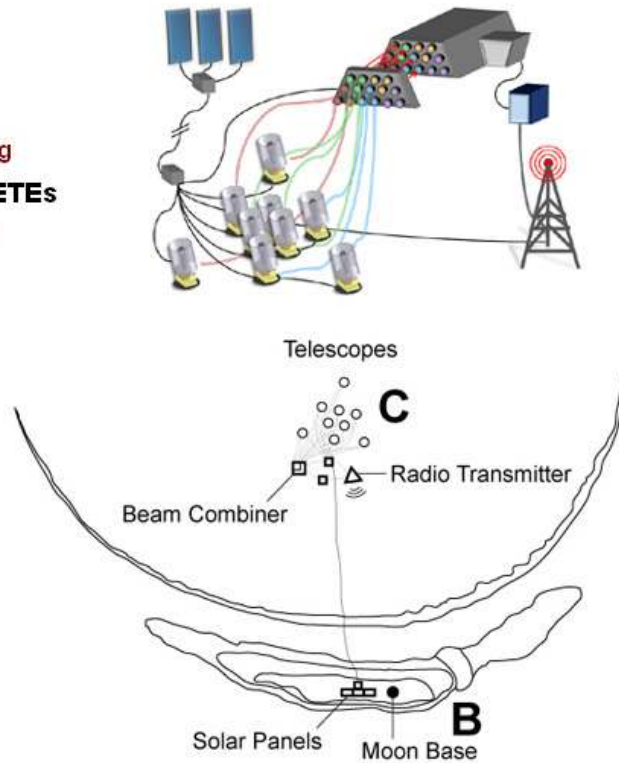


Figure 86. Deployment process.

8.8.6 Deployment time

It is assumed that 3 astronauts and 2 ATHLETE rovers will carry out the deployment operations. It is also assumed that 6-8 hours of extravehicular activity (EVA) will occur at one time, that is, during one operational day. Since the distance between the telescopes and the lunar base would be less than 10 km, and the ATHLETE rover moves at 10 km/h, it will take about 2 hours for the round trip from the lunar base to the telescopes during each EVA. Therefore, the operational time for one EVA is 4-6 hours. Table 22 shows the deployment time estimate needed for each component. The total operational time for the whole deployment would be around 68 hours, which means that 17 EVAs are needed for the deployment phase.

Therefore, the deployment operations will take approximately 2-3 weeks. For these calculations, however, operational time needed for each component was overestimated and operational time in one EVA was assumed to be 4 hours, so the deployment time of 2-3 weeks might be an overestimate and the actual deployment operation might not take more than 2 weeks.

Table 22. Deployment time estimate.

	Quantity	Operation Time of each [hrs]	Total Operation Time [hrs]	EVA # or Day [days]
Telescope	9	4	36	9
Fiber optic cabling	1	4	4	1
Beam combining unit	1	2	2	0.5
Thermal cryocooler	1	2	2	0.5
Solar panels	1	4	4	1
Batteries	1	4	4	1
Support equipment	1	2	2	0.5
Power cabling	1	4	4	1
Power distribution box	2	2	4	1
Computer	1	2	2	0.5
Radio transmitter	1	4	4	1
TOTAL EVA			68	17

8.8.7 Servicing telescope malfunction

When one telescope is malfunctioning, it can be repaired on site or at the lunar base. Figure 87 shows the repair process. Before retrieval, all the mirror covers on all the telescopes will be closed, so that the dust kicked up by the retrieval activity will not contaminate the mirrors. Astronauts and rovers will travel to the malfunctioning component, disconnect the cables, and then either make repairs or bring it back to the lunar base. After being repaired by astronauts or at the lunar base, the telescope will be brought back to the original position and reinstalled into the support structure. After sufficient time is allowed for any raised dust to settle, the mirror covers will be opened to resume observation. The same process can be applied in the case of system components being upgraded.

1. Servicing preparation
 - Mirror covers close
2. Retrieve malfunctioning component
3. Repair at lunar base
4. Reinstallation
5. Observation
 - Dust settles down
 - Mirror covers open

Image removed due to copyright restrictions.

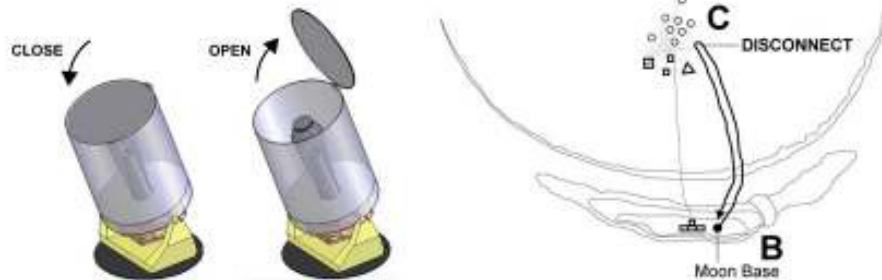


Figure 87. Repair process.

8.8.8 Final subsystem design

Transportation

System components to be transported, using the Ares V and the LSAM, are listed in

Table 21. The total mass to be launched from the Earth is 4400 kg, and therefore the launch cost is estimated to be around \$308 million. Considering the system mass distribution, the landing site would be near Location C on the crater floor.

Deployment

The deployment operation will be carried out by astronauts and JPL's ATHLETE rovers. The deployment process and configuration is shown in Figure 86, and the deployment time estimate is shown in Table 22. The total operation time is estimated to be 2-3 weeks (17 EVAs) or less.

Servicing

The repair process in the case of system component malfunction is shown in Figure 87. The same process can be applied in the case of system components being upgraded.

8.9 Dust Mitigation

The general problems of dust on the Moon pertain especially to the design and operations of LIMIT. Though the design of each piece of equipment sent to the Moon must consider the effects of lunar dust, particular issues arise in the context of an infrared telescope on the lunar surface, and these will be discussed in this section.

Infrared detectors are extremely sensitive to dust contamination. Any particles entering the detector can significantly degrade the performance of the whole telescope, if not disabling it completely. Because of this, much effort should be spent ensuring excellent sealing of these components. Redundant seals and layers would be wise for detector protection.

Optics

Another problem dust poses to a telescope observatory is the settling of dust on the mirrors. The three major issues are scattering, diffraction, and thermal emission. The first two would be related to the size of the dust particles that impinge on the optical surfaces. The average regolith grain size is about 70 μm , but Apollo samples have been measured as small as 0.01 μm , and between 10% and 20% of the regolith by weight is less than 20 μm [71].

Lunar dust grain, removed due to copyright restrictions.

Figure 88. Lunar dust grain.

Based on these sizes and the expected target IR wavelengths, there will be degradation of the observational capability of the telescopes. Unknown, however, is the amount of dust expected to be deposited on the mirror surface for a given amount of time. Tests of the reflectors placed on the Moon by Apollo astronauts indicate adequate reflective properties even after more than 30 years, but the data is not definitive due to incomplete knowledge of effects from surface EVAs versus subsequent obscuration.

Johnson [72] gives theoretical obscuration percentages for a typical Apollo 14 landing. Though this indicates that large amounts of dust would be deposited out to several kilometers from a landing site, the analysis does not consider how mitigation techniques such as landing site preparations or mirror covers would reduce the actual degree of obscuration. In addition, Hyatt [73] describes the complex plasma environment that exists near the terminator region on the Moon. A dust fountain model indicates charged dust particles can reach distances greater than 10 km from the surface; however, it is not clear to what extent these particles will obscure incoming astronomical signals, either above the lunar surface or in terms of the amount of dust

that falls on the mirror itself.

If direct dust settlement on the mirrors becomes a show-stopper, a few techniques are possible for improving the situation. First, the use of a non-stick coating on the mirror surfaces may reduce the adhering ability of dust. A low surface energy material such as polyimide would have a low susceptibility to couple with the primarily basaltic (SiO_2) Moon dust, increasing the success probability of other removal techniques. Thin films would not interfere with the optical surfaces. Though the coating would be exposed to bombardment from micrometeorites, a material such as polyimide is harder than something such as Teflon, which is easily scratched [74].

Calle has developed a means of moving electrostatically charged dust by using a timed sequence of electrodes to lift and push it away. While the experiment has not been verified for actual lunar dust, the concept is promising for keeping an optical surface clean [75].

Another method for the physical removal of dust from a mirror surface is the use of ultrasonic vibrations through the structure to induce migration of the particles off the optical surface. A low-amplitude, high-frequency excitement vibration could move dust either through the Cassegrain hold in the primary for a zenith-pointing angle, or off the edge for horizon-pointing angles. The experimental verification of this technique for use in telescope mirror cleaning has not been found, however, so tests proving the viability of such an approach are necessary [76].

The final means of dust cleaning from the mirrors is merely some brushing motion, probably robotically, but possibly by humans if the contamination is not greater than the decontamination. Reports from the Apollo missions indicate that the use of a lens brush was effective in cleaning the camera lenses. This should be contrasted, though, with the effect of trying to wipe dust off display windows, which rendered them unreadable due to scratches [73].

The last issue with dust on the optical surfaces is that of thermal emission. On JWST, for instance, dust grains sitting on the primary are thermally decoupled from the primary and heat up due to warmer surfaces that they see, due to a lower reflectivity than the primary [77]. To examine the problem for LIMIT, a transient heat transfer problem was modeled for a dust grain settling on the primary mirror surface, and isolated from view of anything outside the temperature other than the sky. The dust is assumed to be of average size ($70 \mu\text{m}$) in a disk shape with a height of $10 \mu\text{m}$. For an extreme case, the temperature of the grain is taken to be 396 K, the maximum expected temperature on the Moon, and the temperature distribution throughout the grain is assumed to be uniform throughout time. Figure 89 shows the transient dust grain temperature for a primary mirror temperature of 10 K. Since the time that is required to reach within 1°C of the mirror temperature is less than 5 seconds, the noise produced in the system by the settling dust particle is small. This result is also consistent with a conclusion given by Lester [62] that small amounts of dust on the mirror would not pose thermal problems. Not examined, however, is the case of dust on or near the secondary in the field of view that is possibly heated up by line of sight to re-radiating regions of the crater rim.

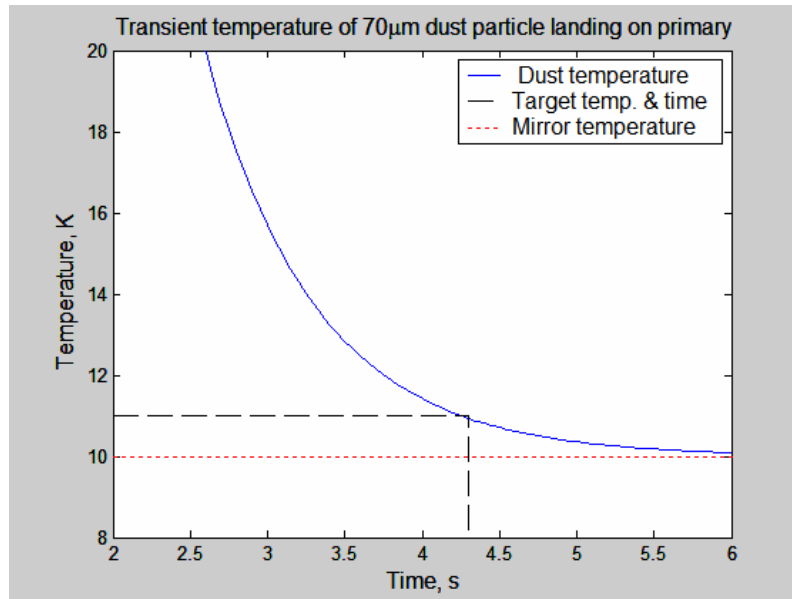


Figure 89. Transient temperature of dust grain incident on a LIMIT telescope mirror.

There is also the consideration of how much dust can potentially interfere with telescope operation. Because of the lack of atmosphere on the Moon, dust particles that are lofted off the surface travel in ballistic trajectories. Based on their initial velocities, the distances traveled by dust particles can be quite large for high-velocity departures. As given by [72], typical ejection speeds and range distances are shown in Table 23.

Table 23. Typical human activities and maximum ranges of particles ejected at speeds on the Moon.

Activity	Speed (m/s)	Horizontal Range (m)
Driving vehicle at 5 km/hr	1.38	1.17
Dropping a tool from 3 m	3.12	6.0
Throwing a major league fastball	40.7	1,023
Landing a rocket (rocket exhaust speed)	1,700	5,460,000

Locating the telescope at least 10 km away from a human outpost at the lunar south pole should prevent normal operations from sending dust as far away as the telescope. The dust kicked up by landings, however, is a concern. There are a number of possible mitigation techniques, including:

1. The construction of a retaining wall around the landing site would help prevent the wide dispersion of dust. Hardening of the surface around the landing site would also lessen the amount of escaping dust. This is beneficial for both the proposed observatory and a nearby human presence.
2. A cover for the telescope that shielded the optics during take-offs and landings would prevent dust from falling onto the primary mirror of each telescope. Since ejected dust particles would remain lofted for less than an hour, this would have little impact on the total observing schedule of the observatory [72].

Mechanisms

Another concern is the contamination of mechanisms by dust particles. The Apollo missions revealed numerous problems associated with contamination of tools and experiments, where unprotected mechanisms accumulated dust. One lesson learned is to ensure excellent sealing and covering of anything susceptible to dust accumulation. For the rotating telescope regions, i.e. bearings and motors, there could be a flexible material that allows relative movement between the stationary and rotating components while completely covering the moving surfaces from external dust contamination. Acting as a loose membrane, it would keep dust out without constraining the motion of the telescope during operation.

The modular telescope design concept of LIMIT refers to the possibility of deploying the individual apertures at different intervals, each time adding to the Golay configuration and obtaining a larger effective aperture diameter. Since it would be difficult to autonomously deploy each telescope due to the precise alignment required for interferometric observations, astronauts would necessarily be walking around, thus kicking up dust in the process. Two concepts stand out in terms of dust mitigation. The first is to close the telescope covers when astronauts are conducting EVAs around the sensitive equipment, as done during rocket take-offs and landings. Second, the potential for sintering of lunar regolith using microwave energy has been proposed by Taylor. As showed by a microwave experiment on Moon dust brought back from the Apollo missions, the lunar regolith quickly melts when exposed for just 30 seconds to microwave energy at 250 watts of power. The idea is to develop an instrument to sinter the lunar surface into a “glass road.” This would help reduce the amount of dust kicked up during astronaut-aided deployment [78].

Smoothed surface of sintered lunar dust,
removed due to copyright restrictions.

Figure 90. Smoothed surface of sintered lunar dust.

Concept for lunar lawn mower for microwave
regolith sintering, removed due to
copyright restrictions.

Figure 91. Concept for lunar lawn mower for microwave regolith sintering.

9. Cost Estimation and Spreading

9.1 Telescope Cost Estimation

When dealing with a space system as complex as a lunar observatory, accurate cost estimation is an important program driver. Accurate cost estimation is essential to the success of such a program. In both the LIRA and the LIMIT concept, an attempt is made to provide an accurate, yet conservative, estimate of the overall budget for all project phases. The processes used for estimating the costs of the two facilities are essentially parallel, but some differences exist because the respective design approaches were quite distinct. In both cases, an effort is made to keep the Technology Readiness Level (TRL) of all components as high as possible. Unless otherwise stated, all costs are provided in 2010 U.S. dollars.

For each concept, a conservative cost estimate, including a generous allocation for research and development (R&D), is formulated. In the case of the LIRA concept, these development costs are added to the cost of each component. For LIMIT, on the other hand, the development costs are added to the aggregate calculations since almost all components were previously flight tested and operationally employed so that prices are available for off-the-shelf components from previous missions.

9.2 LIRA Cost Estimation

The total cost of the LIRA telescope facility is estimated to be \$1.987 billion. The estimate for the system itself is \$726.2 million. For transportation costs, the current Ares V launch cost estimate of \$1.26 billion, as described in Section 9.5, is used. The details of the cost estimation are provided in Table 24 and

Table 25.

Table 24. Subsystem mass and cost breakdown for the LIRA concept over the entire development timeline.

LIRA Subsystem Mass and Cost Estimation		
	Mass (kg)	Component Cost (M\$)
Electronics	58.2	28.2
Communications	826.7	6.5
Power	4,546.1	1.7
Structures and Mechanisms	7,149.5	71.5
Deployment	1,007.3	256.6
Integration and Other	3,396.9	91.1
Software and Ground Segment	--	270.7
Subsystem Total	16,984.5	726.2 (M\$)

Table 25. Total transportation cost for the LIRA concept, based on the number of Ares V boosters required to transport all telescope subsystems.

LIRA Transportation Cost			
	Cost/Ares V (M\$/Launch)	Number of Launches Required	Cost (M\$)
Transportation	1,260	1	1,260
Total			1,260 (M\$)

The rationale for the cost estimates of the various subsystems are discussed in the following subsections.

9.2.1 Rationale for costing of computers and electronics

The cost estimate for the electronics subsystem is based on the actual costs of the command and data handling (C&DH) subsystem of the Solar and Interplanetary Radio Spectrometer (SIRA) telescope. Engineers at Broad Reach Engineering have verified that this estimate serves as a reasonable basis for costing the LIRA electronics subsystem [38].

9.2.2 Rationale for costing of communications

To estimate the cost of the communications subsystem for the LIRA telescope, the comparative costs for laser and radio communications equipment are estimated at \$5000 per kilogram and \$1000 per kilogram to reflect the relative difference in technological maturity between the two technologies. The relays are priced at \$10,000 per kilogram to reflect both their technology readiness level and the fact that more structure (as well as more miniaturized or carefully-scaled components) will likely be required for the relays than for the rest of the communications equipment. The costs for fiber-optic cable are based on current costs for commercial fiber optics.

9.2.3 Rationale for costing of power

Estimates for the solar and RTG power unit costs for the LIRA concept are derived from [79]. The numbers in this report represent the unit cost of technologies available to approximately 2012.

9.2.4 Rationale for costing of structures and mechanisms

SMAD estimates the uncrewed spacecraft structure system's theoretical first unit cost to be \$13,100 per kilogram in year 2000 dollars [37]. Adjusting this for inflation and adding a learning curve savings for production of 95%, the average cost per kilogram of cluster structure is approximately \$10,000 per kilogram in 2010 dollars.

9.2.5 Rationale for costing of deployment

Because the cost of deployment for the LIRA telescope is dominated by the development of the rover, the estimate is based entirely on the cost of that component of the deployment system. The closest past analogue to this system is the lunar rover used during the Apollo program. The rovers required for LIRA will have additional capabilities, including autonomous navigation and robotic loading/unloading of cargo. Nevertheless, the same level of development effort will not

be required for the structure, chassis, drivetrain, and other components as a result of experience from Apollo and other rovers. Assuming that these two factors roughly balance each other, the cost of the deployment system is taken to be the Apollo rover cost inflated to 2010 dollars plus 20 percent margin [80].

9.2.6 Rationale for integration and other costs

Integration costs and other space segment costs are anticipated during the implementation of the LIRA concept. To account for this, an additional mass and cost is added to the overall values for the various subsystems. This includes a conservative mass increase of 25 percent through the development and integration of the telescope architecture and a similar 25 percent increase in subsystem cost. This integration factor also contributes to higher transportation costs because of the increase in mass. The factor should account for any subsystems not included in the initial design and any increased complexity of current subsystems.

9.2.7 Effect of array design on cost estimation

As explained in Section 7.9.3, the number of dipoles used in the point design chosen for this study could be increased in future design iterations. Increasing the number of dipoles, however, will have a direct effect on the estimate for the total cost of the system. To account for this, Figure 92 shows the effect of the number of dipoles on overall system cost, indicating the location on the curve of the present design.

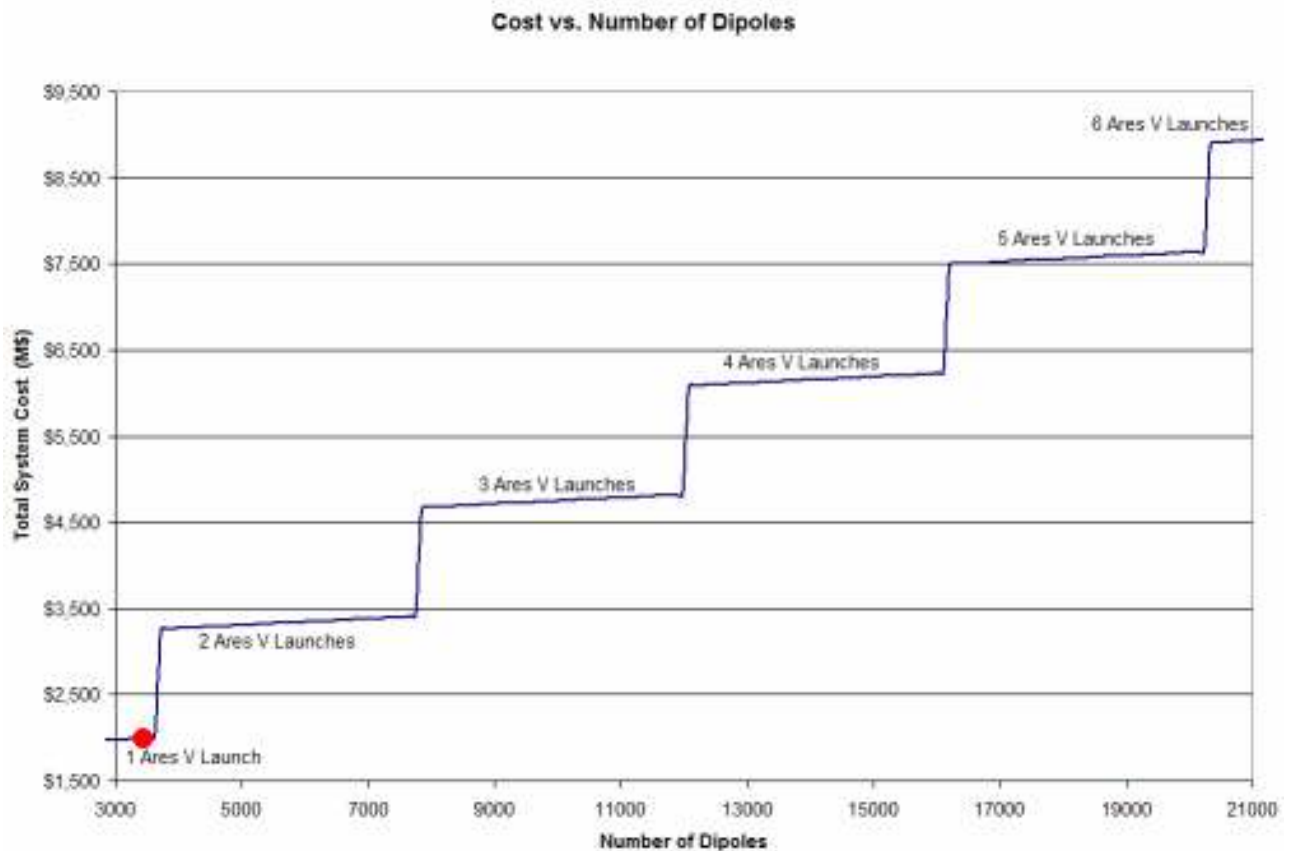


Figure 92. Effect of number of dipoles on total system cost. The steps in the graph result from the discontinuous cost increase that comes with each

additional launch needed as the total mass of all dipoles increases. The location of the point design discussed in this study is indicated by the red dot.

9.3 LIMIT Cost Estimation

The total cost of the LIMIT telescope facility is estimated to be \$1.631 billion. The system itself is estimated to cost \$1.322 billion. The transportation costs are taken to be approximately 25 percent of the current Ares V launch cost estimate of \$308 million (because it can be launched along with other systems, as described in Section 9.3.10). The details of the cost estimation are provided in Table 26 and Table 27.

Table 26. Subsystem mass and cost breakdown for the LIMIT concept over the entire development timeline.

LIMIT Subsystem Materials Cost and Mass Estimation		
	Mass (kg)	Component Cost (M\$)
Telescopes (9)	1027	45.1
External Optics	429	5.8
Structures and Mechanisms	212	2.9
Active Thermal Control	40	0.1
Electronics	10	4.7
Communications	13	0.2
Power	1789	0.3
Integration and Other	880	14.8
Subsystem Research & Development	--	977.8
Ground Segment Development	--	270.7
Total	4,399 (kg)	1.322 (B\$)

Table 27. Total transportation cost for the LIMIT concept, based on the number of Ares V boosters required to transport all telescope subsystems.

LIMIT Transportation Cost			
	Cost/Ares V (M\$/Launch)	Number of Launches Required	Cost (M\$)
Transportation	1260	>0.25	308
Total			308 (M\$)

The rationale for the cost estimates of the various subsystems are discussed in the following subsections.

9.3.1 Rationale for costing of primary optics and beam combining unit

The LIMIT telescope design is based largely on operationally tested hardware. This includes telescope optics and subassemblies from the Spitzer telescope, external combining optics from the Argos telescope array, and active thermal control architectures from NASA's Advanced Cryocooler Technology Development Program (ACTDP).

Due to the reuse of major telescope components, values for off-the-shelf costs of the various telescope components are based on previous program costs. For example, cost values for the

Argos beam combining optics and optics assemblies were determined from exact component costs of the Argos telescope itself. Due to the new application of these components, appropriate research and development costs were added to these component costs. Due to the new application and the additional hardware needed for the combining optics, the research and development costs was determined to be 20 times the cost of the components themselves. Similar R&D costs were calculated throughout the telescope design, valuing the component cost at 5 to 10 percent of the total component cost contribution.

It was more difficult to directly determine the cost of the individual telescope elements, as the Spitzer optical assembly cost was not directly available. Therefore, a Meinel relation was used based on estimations from SMAD [37]. The relationship used was

$$\text{Cost} = 356,851 * D^{0.562}, \quad (\text{Eq. 29})$$

where D is the diameter of the aperture. The result was then inflated to 2010 dollars. Since the Spitzer design is relatively complex, being composed of a single beryllium structural element, the above cost was multiplied by a factor of 10 to be conservative. In addition to this single element material cost, the research and development costs was determined to be 10 times the cost of the components themselves (telescope assembly equal to 10% of total contributing cost). This low number was used due to the similarity of this telescope to legacy designs. Also useful to note, this research and development cost was added to each of the 9 individual telescope elements, making the cost estimate still more conservative. Applying an appropriate learning curve to this technology development, research and development costs would realistically only be appropriate for the first element.

9.3.2 Rationale for costing of computers and electronics

As with LIRA, the cost estimate for the electronics subsystem of LIMIT is based on the actual costs of the command and data handling subsystem of the SIRA telescope, as verified by Broad Reach Engineering [38].

In addition to central processing, communication, and scheduling/pointing computer systems, the LIMIT concept uses similar charge-coupled devices (CCDs) and associated electronics from the Spitzer telescope. The collecting electronics are priced according to available information on Spitzer, with research and development costs added.

9.3.3 Rationale for costing of communications

The rationale for the LIMIT communications cost estimate is the same as for LIRA.

9.3.4 Rationale for costing of power

The rationale for the LIMIT power cost estimate is the same as for LIRA.

9.3.5 Rationale for costing of structures and mechanisms

The structure for supporting and pointing each telescope element is priced using commercially available, aerospace-grade aluminum honeycomb materials. Estimates of the cost of the movable parts and power systems for the supporting structure were also done using commercially available materials. In addition to the cost of material, a large research and development cost is added to account for the new technology development.

9.3.6 Rationale for costing of thermal control system

Cost estimates for the active thermal control of the beam combining unit are derived from the cost of various architectures from NASA's Advanced Cryocooler Technology Development Program (ACTDP). Estimates for the passive cooling of each telescope element were found using commercially available Multilayer Insulation.

9.3.7 Rationale for costing of deployment

The LIMIT telescope does not include deployment costs in the total for the telescope architecture. It is assumed that the human space flight program, including the south pole lunar base, will be heavily leveraged. This includes the use of two lunar base rovers for transportation and 2 to 3 astronauts for approximately 2 weeks. Due to the difficulty of assigning a value to this cost, it was left out of the cost estimation.

9.3.8 Rationale for integration and other costs

The rationale for integration and other costs for LIMIT is the same as for LIRA.

9.3.9 Research and development costs

Even though most of the LIMIT subsystems are designed to use operationally-tested technology, there is still a need for some new technology and integration and flight certification of legacy technology. In addition, it is estimated that there will be some subassemblies not included in the initial subsystem designs. To account for this, R&D cost multipliers ranging from 10 to 20 are used. This translates to an additional 90 to 95 percent of the subsystem cost as R&D-specific. The relative research and development multiplier costs for each telescope subsystem are shown in Table 28.

Table 28. Research and development cost multipliers for various LIMIT telescope subsystems.

LIMIT Research Development Cost Multipliers		
	Subsystem Cost (M\$)	R&D Multiplier
Telescopes	45.1	10
Supporting Structure / Mechanisms	2.9	20
External Optics	5.8	20
Active Thermal Control	0.1	20
Electronics / Computer	4.7	10
Communications	0.2	20
Power	0.3	15
Integration and Other	14.8	20

9.3.10 Rationale for costing of transportation

The transportation cost for the entire LIMIT concept is based on the number of Ares V booster vehicles necessary for launch. This number was calculated from the fraction of the total mass capability of an Ares V required for launch to the Moon. Because the LIMIT mass is less than the mass capability of a single Ares V launch, combined with the location of the LIMIT facility near the human base infrastructure, a decision was made to share the transportation with one or more other launches to the base. It is important to note, however, that the volume constraints for the Ares V were not known at the time of writing. For this reason, mass is used as the limiting factor in the estimation, though it could turn out that volume is the more important constraint.

9.3.11 Effect of number of elements on cost estimation

If it is decided in further design iterations that the number of Spitzer elements used in LIMIT should be increased beyond the number used in the point design chosen for this study, the modularity in the design of LIMIT provides an easy means of scaling the number of elements. Increasing the number of interferometer elements, however, will have a direct effect on the estimate for the total cost of the system. To account for this, Figure 93 shows the effect of the number of elements on overall system cost, indicating the location on the curve of the present design.

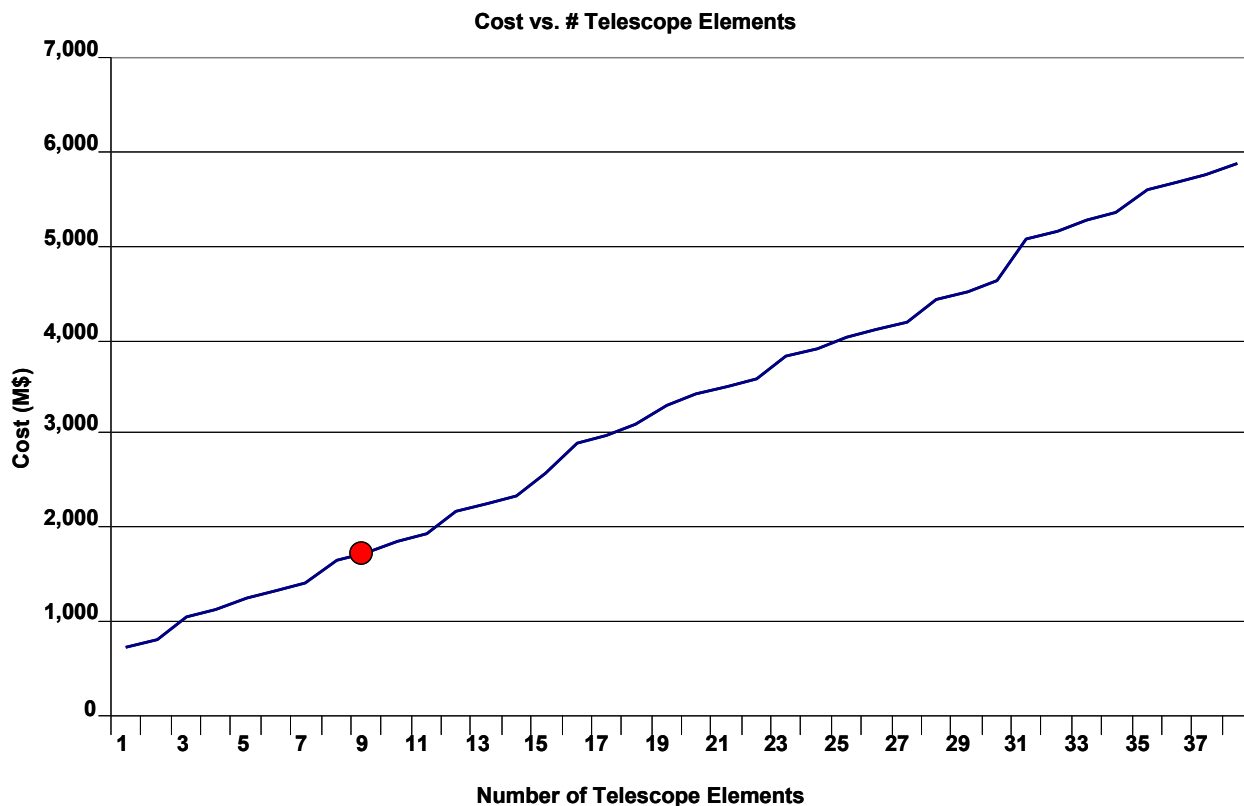


Figure 93. Effect of number of telescope elements on total system cost. The regular stepping behavior exhibited is indicative of the effects of increasing the number of elements past specific cost barriers, at increments of 10% of an Ares V launch

and increments of 15 elements per each beam-combining unit. The location of the point design discussed in this study is indicated by the red dot.

In this analysis, nothing was done to account for the learning curve for building in larger quantities. Thus, the actual total cost of the system would not increase as fast with increased number of elements as in Figure 93. The modular nature of the design, including beam-combining elements, leads to stepped cost increases due to the cost of adding 15-beam combining assemblies, as seen in Figure 93 at 16 and 31 elements.

9.4 Software and Ground Segment Development Cost

When dealing with a space flight program, it is often difficult to directly measure and calculate the cost of ground segment development. In principle, this can be done by estimating the square footage of operational facilities, the number of processors, or the amount of hardware needed. When the program is in the conceptual phases, however, there often is no reasonable basis for making such estimates. Thus, a useful heuristic for ground segment costs is to estimate the number of software lines of code (SLOC) required and then to estimate the relative weightings of software, facilities, equipment, and other ground segment factors. This type of estimation is fairly representative of what is typical of the conceptual phases of a major mission.

For the number of total lines of code on each of the lunar telescope concepts, it was assumed that the level of complexity of a lunar surface program would be approximately half that of a free space telescope program. While many subsets of software would be either reused or redeveloped for a Moon based telescope, no code would be needed for attitude control or orbital guidance. Also, the level of complexity of code will not need to be as high due to the relatively low impact of software failures on a surface telescope as compared to a space-based one. Both the LIRA and LIMIT concepts will need to contain software for field of view tools, pointing, scheduling, and various other functions.

To estimate the software lines of code for the LIRA and LIMIT concepts, the Hubble Space Telescope was used as a starting point. Due to the stable baseline, there will be no need for many space flight software functions, as previously mentioned. There will also be no need to keep all software space ready, as modifications to the code and re-uploading of software will only cost time, which is not as mission critical to a ground based system as to a free-flying one. Thus, the LIRA and LIMIT concepts were estimated to have approximately half the SLOC as HST. There will also not be a need to keep all software space-certified, resulting in lower complexity and cost. The HST has approximately 500 thousand lines of code (KLOC), so LIRA and LIMIT were estimated to have on the order of 250 KLOC, with only 1/3 of the code needing flight certification. From SMAD [37], this results in a software cost estimation of approximately \$80.2 million. Also from SMAD, this number can be used to calculate total ground segment cost as a function of KLOC. From this, the total ground segment development cost for both LIRA and LIMIT is estimated to be \$270.7 million.

9.5 Ares V Transportation Costs

It is assumed that the LIRA and LIMIT concepts will leverage the human space flight architecture currently under development, including the Ares V booster capabilities for transportation. At the time of this report, the Ares V has been estimated to have a capability of sending 126 metric tons to Low Earth Orbit (LEO). Using the cost of sending a single kilogram

of payload to LEO of \$10,000, it is determined that the cost of a single dedicated launch of an Areas V booster would be \$1.26 billion dollars. Also, the predicted payload capacity to the lunar surface is believed to be approximately 18 metric tons. From the cost and payload capacity of the Ares V, the transportation cost is estimated for both LIRA and LIMIT, using the required number of boosters to take the entire telescope payload to the lunar surface. It is assumed that this \$1.26 billion encapsulates the entire cost of landing payload on the lunar surface, including the cost of the landing vehicle (LSAM) and all other cost to the surface.

9.6 Operating Costs

From SMAD, the operating and maintenance costs for both LIRA and LIMIT were estimated on a per-year basis, assuming no major upgrade or servicing missions are performed. These costs will cover ground operations and support after the completion of the telescope. The day-to-day operations of both telescope facilities are expected to require approximately 25 government employees and 50 contractors. From SMAD, the FY2000 cost of a single government worker is \$110,000, and the cost of a single contractor is \$160,000. Inflated to 2010 dollars, this is equivalent to \$135,000 and \$196,000, respectively. Including a per year maintenance cost equivalent to 10% of the cost of software, equipment, and facilities, the total yearly operating cost of the telescope is estimated at \$31.03 million per year.

This cost is not included in the cost spreading sections to follow, as these costs will not be incurred until after the 15-year development window (or at least quite late in the timeline). If major servicing or upgrade missions are planned, the cost spreading section to follow can be updated to include such costs. This would help to illuminate how the budget for large-scale servicing mission could be spread beyond the 15-year initial project development timeline.

9.7 Cost Spreading

In the previous subsection, an estimate of the overall costs of the LIRA and LIMIT facilities is provided. These numbers, however, oversimplify the costing of a large-scale, long-term technology development program such as a lunar telescope. Space missions take several years to develop, so the costs must be spread across the entire development timeline. In this discussion, a notional timeline of 15 years is used to demonstrate the effect of cost spreading over the entire program. This choice is somewhat arbitrary. Nevertheless, changes in the actual development schedule will not affect the relative cost spreading timeline.

The cost spreading function in common use in the U.S. space program is:¹

$$F(S) = 10S^2(A + BS)(1 - S)^2 + S^4(5 - 4S), \quad (\text{Eq. 30})$$

where S is the elapsed fraction of the total development time, $F(S)$ is the fraction of the total cost spent after time fraction S , and A and B are coefficients that depend on the particular manner in which costs are split over the development time. In a typical program, about 60% of the costs are incurred by the midpoint of the development schedule. This split corresponds to values of A

¹ The form of this equation is algebraically simplified from that presented in SMAD.

= 0.32 and $B = 0.68$ [37]. These values of A and B were used for all major subsystems, R&D, integration, and ground segment development. For the transportation costs, however, it was assumed that the cost would be incurred at a later phase of development. Therefore, it was assumed that 20% of the transportation costs would be incurred by the midpoint of the development schedule. This split corresponds to values of $A = 0.00$ and $B = 0.04$ [37]. Using these parameters, we find the cost spreading functions shown in Figure 94 and Figure 95 for LIRA and LIMIT, respectively. According to these figures, it can be seen that the peak annual cost over the notional 15-year development timeline is about \$220 million for LIRA and about \$175 million for LIMIT.

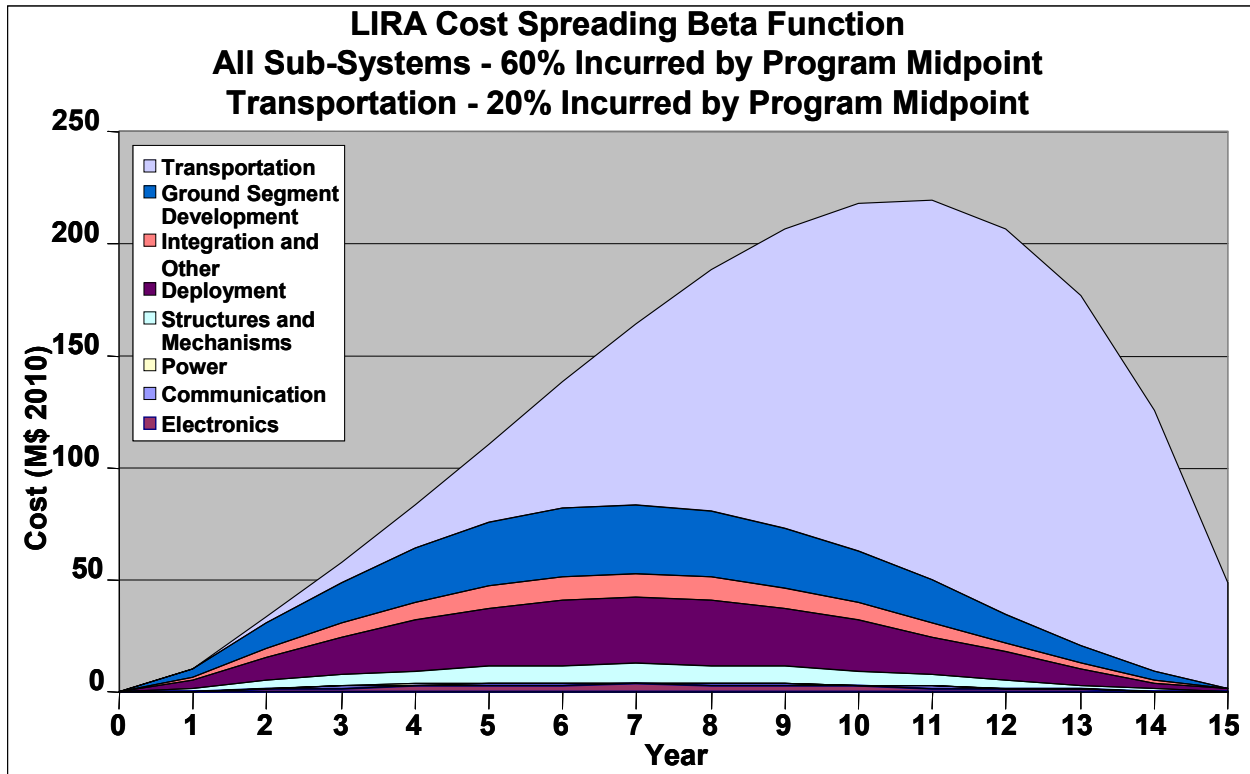


Figure 94. Spreading of the \$1.987 billion development cost for LIRA over a notional 15-year development timeline. The maximum annual development cost is about \$220 million.

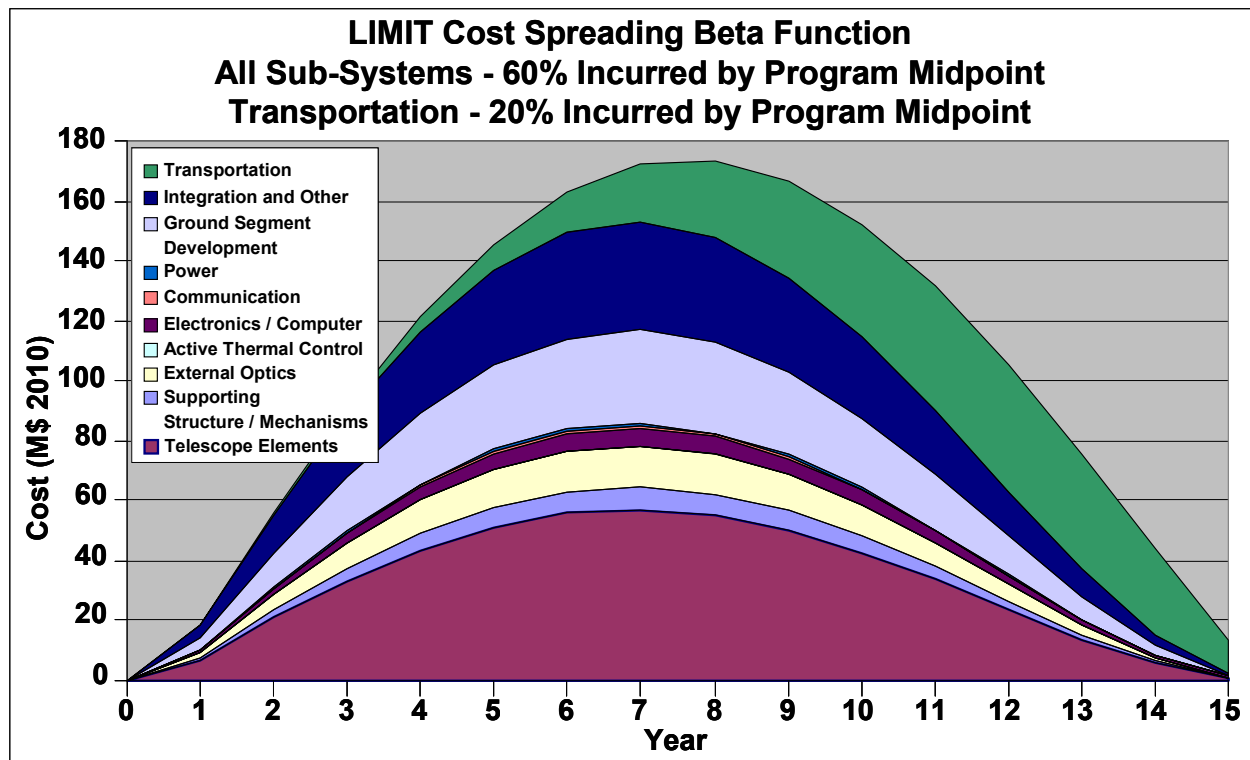


Figure 95. Spreading of the \$1.631 billion development cost for LIMIT over a notional 15-year development timeline. The maximum annual development cost is approximately \$175 million.

9.8 Cumulative Cost Spreading

Figure 96 and Figure 97 show the cumulative expenditure over the total development timeline for LIRA and LIMIT, respectively. In addition, these cumulative beta functions are augmented to provide a notional distribution of costs over various subsystems and other aspects of the program throughout the development timeline.

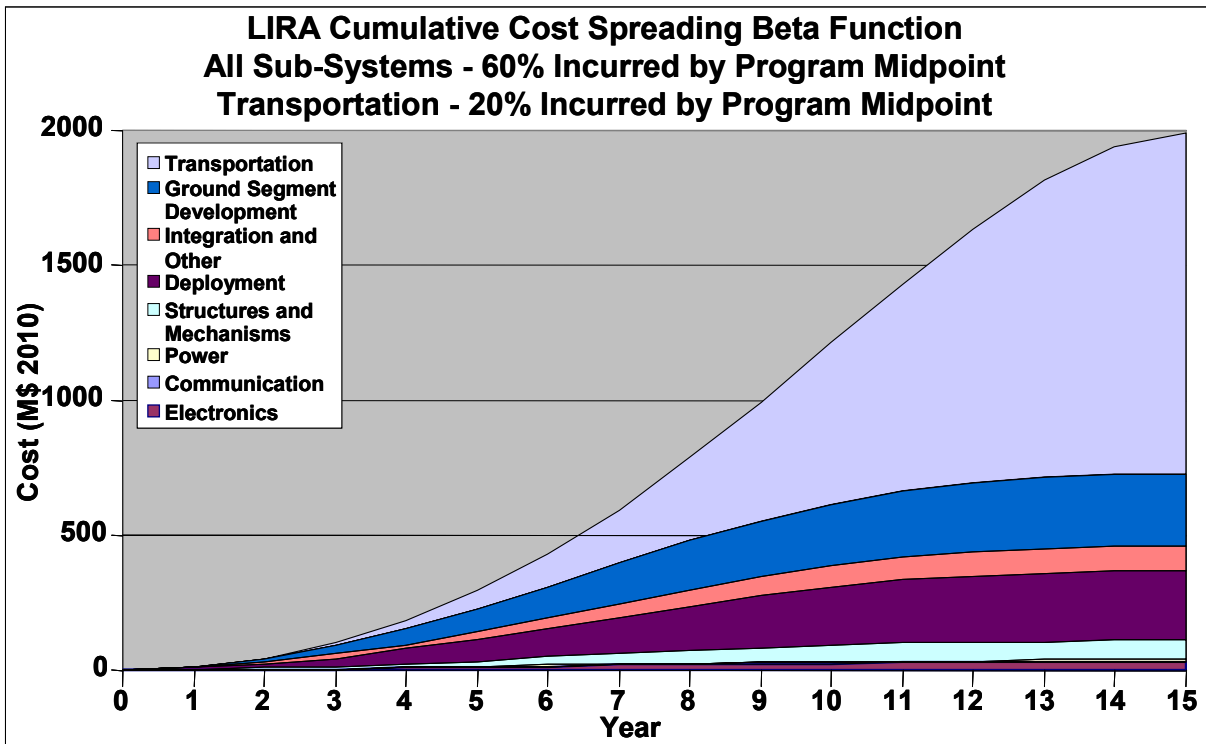


Figure 96. Cumulative cost spreading of \$1.987 billion development cost for LIRA over a notional 15-year timeline.

As can be seen in Figure 96, transportation comprises almost two thirds of the total cost of the LIRA architecture. Ground segment development and deployment on the lunar farside make up the majority of the remaining cost. At the end of the 15-year development timeline, the total cost of the LIRA concept is estimated to sum to \$1.987 billion. Also, the highest per-year expenditure is in year 11 (as can be seen in Figure 94), which is very late in the development timeline. This is due to the rightward shift (toward the out years) in transportation costs for LIRA development. This reduces the impact of the peak cost, as current year dollars are worth more than discounted future dollars.

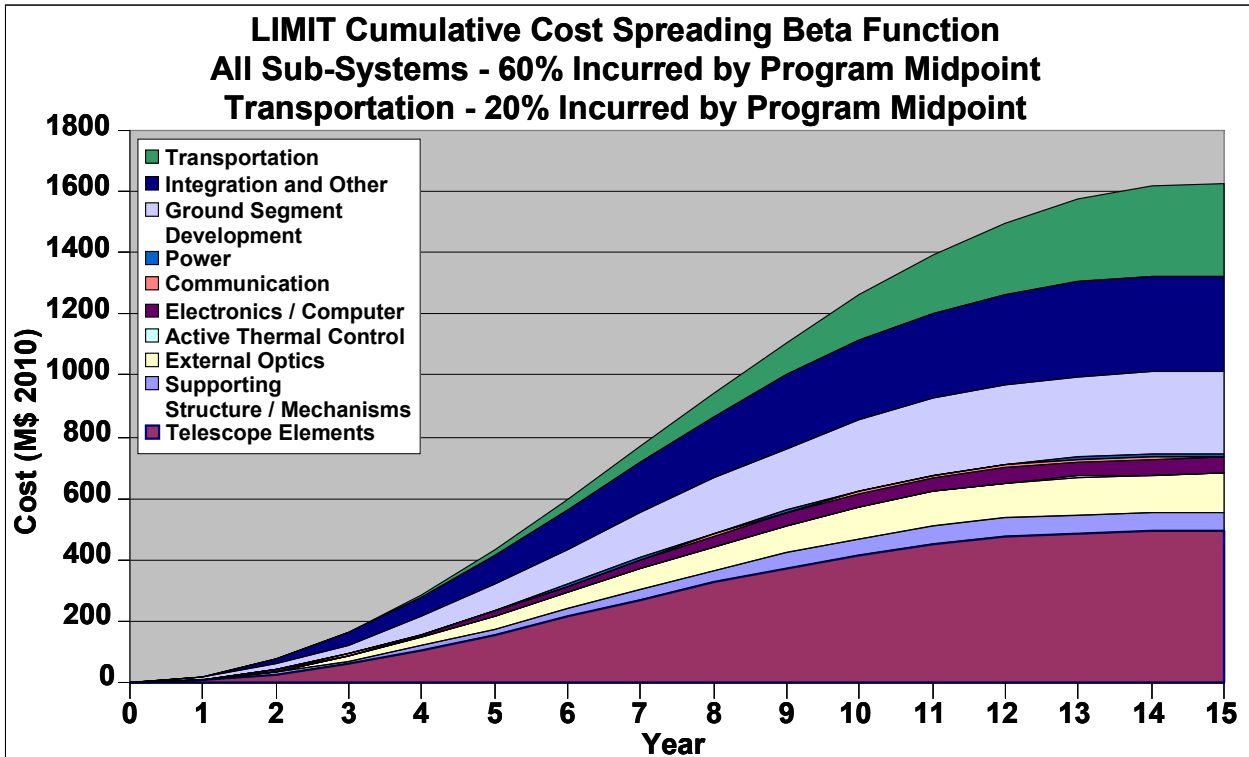


Figure 97. Cumulative cost spreading of \$1.631 billion development cost for LIMIT over a notional 15-year timeline.

In contrast to the LIRA concept, the cost of LIMIT is not dominated by transportation. For this reason, the highest per-year expenditure is in year 8, which is near the middle of the development timeline. At the end of the 15-year development timeline, the total cost of the LIMIT concept is estimated to sum to \$1.631 billion.

10. Future Work

The scope of this project enabled the generation of a multitude of possible architectures and the downselection to and maturing of two reference designs, which were explored in detail, although many important facets of each design were either left for future work or estimated. In some cases, insufficient data was available for detailed analysis; in other cases the reference designs required a higher level of maturity to define completely an aspect of the design. Continued work on these two reference designs is necessary for further maturity, and this section discusses certain areas which have been identified as meriting particular attention.

10.1 Further Design Trades

10.1.1 LIRA

The LIRA telescope has the potential for breakthrough astronomy, and its compact and lightweight design would allow it to be transported in the planned Constellation vehicle architecture. The concept, however, requires further analysis in three key areas.

Deployment

Autonomous deployment of 215 clusters of radio dipoles would require a sophisticated system of rovers, communications, and planning. Deployment by human power alone would likely strain the abilities and usefulness of astronauts on the Moon, and even automated deployment represents a stretch for existing capabilities. The design of a capable deployment rover, and the tradeoffs of complexity and cost between the rover and other elements of the telescope concept are important issues.

Optical communications

A second major consideration is the transmission of high data rates using laser relays on the far side of the Moon. The main objective is to avoid emitting radio waves, which may interfere with the astronomical measurements being done; it was deemed desirable to keep the far side of the Moon radio-quiet. This drove the design to include an optical relay system, the cost of which was found to be less than that of an orbiting satellite. However, the Technology Readiness Level of a laser-relay communications system such as this is still low, and further investigation into this problem is suggested to justify the choice or generate alternatives for the communications system.

Location

A significant driver in cost will be the determination of where to put the LIRA telescope. First, the attenuation of radio noise from Earth needs further study to determine the distance behind the limb necessary to achieve the sensitivity required for the primary science goal, observing the Epoch of Reionization. This choice impacts areas such as communications, power, and deployment, with the effects of location selection spiraling into the resultant cost.

10.1.2 LIMIT

The LIMIT array presents strengths in its modularity and evolutionary features. Building on the proven capabilities of the Spitzer optics, the telescope elements would be well suited for phased transportation to the facility site on the lunar surface, where growing array sizes allow increased performance with marginal costs. Some areas of remaining concern are:

Beam combination

Whereas other subsystems have had adequate development in other contexts, the system of beam combining for the Golan array would require further research and study. The need for an optical delay line on the same order as the array baseline implies the need for a system consisting of a moving trolley and/or an optical switchyard. If fiber optics are suitable for this use, a series of paths with different lengths and the ability to switch between them would allow the physical distance of trolley movement to be reduced to something on the order of a meter instead of tens of meters. This central beam combining unit is a primary area for additional work.

Final array configuration

The array configuration should be reassessed primarily in establishing its size and layout. The cost of building the array larger will limit the ultimate performance, but it is expected that effective diameters as large or larger than planned concepts can be achieved by the LIMIT observatory at a much lower cost. The flexibility in deployment allows for the incremental build up of performance over time. With this flexibility, it may be desirable to consider not a Fizeau interferometer design, but a long-baseline nulling interferometer design. While there are limitations to being on the lunar surface for something aimed at finding extrasolar planets (a space-based TPF mission would have several advantages), the stable surface allows precise metrology without the need for active station-keeping. The LIMIT concept as presented has focused on achieving numerous science goals with a Fizeau imaging array, but other configurations are possible, and this would depend heavily on the progress of the TPF and SAFIR missions. The development (or lack thereof) of TPF and SAFIR would then clarify the niche of the LIMIT concept.

Thermal and dust issues

The operation temperatures for particular wavelengths of interest should be considered more closely, particularly in determining the maximum allowable temperature for the telescope optics. It is desirable to allow for passive cooling of the mirrors, since that reduces weight, cost, complexity and risk. The permanently shadowed regions of the Shackleton Crater reach very cold temperatures, but the work done in this study has not been able to confirm that the design includes viable passive cooling to temperatures around 10 K. An unavoidable issue for Moon-related designs which is particularly relevant to a lunar telescope is dust, which will complicate the design of many components. Further means for mitigating the detrimental effects of moon dust should be considered in future work.

Other issues

Other work to be done would include optimizing the positioning of telescope elements to achieve the best performance over different viewing angles and for various targets (also with consideration of using the Moon's rotation to improve non-optimal configurations), improving the power transmission over about a 10 km distance to reduce the weight of the system, assessing future detector development for increased sensitivity, redesigning a more compact telescope support structure, and outlining the logistics of deployment with consideration of available human and robotic resources.

10.2 Other Future Development

10.2.1 Data gathering on the lunar environment

In order to conduct the detailed trade studies described in Section 10.1, more data on physical conditions prevalent on the lunar surface will be necessary. The manned lunar exploration program and the Lunar Reconnaissance Orbiter mission may provide key data that will be used to select exact locations for the proposed telescope reference design concepts, as well as to inform the proposed trade studies and allow for a better assessment of the detailed technical issues relevant to telescope design, such as dust mitigation.

10.2.2 Integration into planned science programs

Although there currently exist plans to carry scientific equipment to the Moon as part of the returned human presence there, the payloads are distributed between missions and do not include allowances for the placement of a major telescope on the lunar surface. However, the ability to place, maintain, and upgrade such a telescope, which will leverage the unique advantages of the lunar surface and deliver valuable information in previously-unexplored realms of astronomy, is itself a significant justification for the return to the Moon.

Evaluation of the astronomical targets which can be observed from given locations on the Moon, as well as assessment of the expected flows through the stakeholder value delivery network model developed in Section 3, will provide further weight to the case currently presented for returning to the Moon. Further detailed comparisons with other existing or planned space telescope programs may also be informative. If the case can be presented convincingly, the proposed telescope designs can be integrated into the overall plan and launch manifests for a lunar campaign.

11. Conclusion

This Final Design Review document summarized the results of the design process for a lunar telescope facility, motivated by plans for the return of a human presence on the Moon. The detailed consideration given to the Moon as the location for an astronomical observatory includes stakeholder analysis, a rigorous downselection methodology, and two matured reference designs for the proposed lunar telescope facility.

The Lunar Interferometric Radio Array (LIRA) reference design is an arrangement of 3440 simple radio dipoles with a maximum baseline of 62 km, with the goal of observing the Epoch of Reionization enabled by the radio-quiet environment on the far side of the Moon.

The Lunar Infrared Modular Interferometric Telescope reference design is a Golay-9 configuration of 0.85-m Spitzer-like units, relying on the operational heritage of many of its components and its location in a permanently-shadowed region of the Shackleton Crater, where the low ambient temperature and the stable baseline provided by the lunar surface uniquely enable the performance of its science goals.

Although the two reference designs operate in different regimes of the electromagnetic spectrum, both will use the unique properties of the lunar surface to deliver large gains in scientific knowledge of the universe, and advance human understanding of the stars.

Acknowledgments

The authors of this paper would like to acknowledge the following persons for their contributions to the design project, including delivering expert guest lectures on relevant topics and serving as external reviewers during key stages of the project.

Mr. Mark Baldesarra, of the MIT Department of Aeronautics and Astronautics
Professor Jacqueline Hewitt, of the Kavli Institute for Astrophysics and Space Research at MIT
Professor Jeffrey Hoffman, of the Space Systems Lab at MIT
Dr. Tupper Hyde, of NASA Goddard Space Flight Center
Dr. Gary Mosier, of NASA Goddard Space Flight Center
Ms. Sarah Shull, of the MIT Department of Aeronautics and Astronautics
Dr. Massimo Stiavelli, of the Space Telescope Science Institute

Special thanks are extended to Professor Edward Crawley and Professor Olivier de Weck, of the MIT Department of Aeronautics and Astronautics, for their inspiring guidance throughout the project and thoughtful reviews of the development process and resulting reference designs.

References

1. Lester, Daniel F. Testimony before the U. S. House of Representatives, April 1, 2004. URL: <http://gop.science.house.gov/hearings/space04/apr01/lester.pdf>. Accessed 5-20-2007.
2. Lester, Daniel F., Harold W. Yorke, and John C. Mather. "Does the lunar surface still offer value as a site for astronomical observatories?" *Space Policy* 20 (2004), pp. 99-107.
3. "Infrared Windows." Infrared Processing and Analysis Center website. URL: <http://www.ipac.caltech.edu/Outreach/Edu/Windows/irwindows.html>. Accessed 5-17-2007.
4. "Hubble Servicing Missions." URL: <http://hubble.nasa.gov/missions/intro.php>. Updated February 16, 2007. Accessed March 6, 2007.
5. "Space Station Expedition 14." URL: http://www.nasa.gov/mission_pages/station/expeditions/expedition14/exp14_evas.html. Updated February 16, 2007. Accessed March 6, 2007.
6. Akin, David L. "Robotic Servicing for Hubble Space Telescope and Beyond." Space 2004 Conference and Exhibition, 2004.
7. "NASA's Exploration Systems Architecture Study," National Aeronautics and Space Administration, 2005. URL: http://www.nasa.gov/mission_pages/exploration/news/ESAS_report.html.
8. "The Hubble Space Telescope." URL: <http://hubble.nasa.gov/index.php>. Updated February 22, 2007. Accessed March 6, 2007.
9. "The James Webb Space Telescope." URL: <http://www.jwst.nasa.gov/>. Accessed March 6, 2007.
10. "About Spitzer." Spitzer Science Center website. URL: <http://www.spitzer.caltech.edu/about/index.shtml>. Accessed 5-20-2007.
11. "Herschel Mission Homepage." Jet Propulsion Laboratory website. URL: <http://herschel.jpl.nasa.gov/mission.shtml>. Accessed 5-20-2007.
12. "What Is SAFIR?" Jet Propulsion Laboratory website. URL: <http://safir.jpl.nasa.gov/whatIs.shtml>. Accessed 5-20-2007.
13. "Terrestrial Planet Finder." Jet Propulsion Laboratory website. URL: http://planetquest.jpl.nasa.gov/TPF/tpf_index.cfm. Accessed 5-20-2007.
14. "HALCA [MUSES-B] Space VLBI." Institute of Space and Astronautical Science / JAXA website. URL: <http://www.isas.jaxa.jp/e/enterp/missions/halca/index.shtml>. Accessed 5-20-2007.
15. "LOFAR – General Information." URL: <http://www.lofar.org/p/geninfo.htm>. Accessed 5-20-2007.
16. Nein, Max E., and Billy Davis. "System concepts for a large UV/optical/IR telescope on the Moon." 98 / SPIE Vol. 1494, *Space Astronomical Telescopes and Instruments* (1991).
17. Angel, Roger. "Buyer's guide to telescopes at the best sites: Dome A, L2, and Shackleton Rim." SPIE Vol. 5487 (2004).
18. Universe Today website. URL: http://www.universetoday.com/am/publish/pristine_view_universe_Moon.html. Updated March 5, 2007.
19. Van Susante, P. J. "Study Towards Construction and Operations of Large Lunar Telescopes." Paper number COSPAR02-A-00327 / B0.3-F3.3-0030-02 in *Advances in*

- Space Research, by Elsevier.
20. Rayman, M. D., and Sanders, R. S. "Optical Interferometry from the lunar surface." In *Advances in Space Research* Vol. 18, Issue 11, pp. 45-48 (1996). URL: <http://adsabs.harvard.edu/abs/1996AdSpR..18...45R>.
 21. "181 Things to Do on the Moon." URL: http://www.moondaily.com/reports/181_Things_To_Do_On_The_Moon_999.html. Updated February 5, 2007.
 22. Meinel, Aden B. and Marjorie P. Meinel. "The Lunar Configurable Array Telescope (LCAT)." Presented at the Next Generation Space Telescope workshop, Baltimore, MD, September 13-15 1989.
 23. "The unfolding space telescope." URL: http://www.esa.int/esaCP/SEM5JA808BE_index_0.html. Accessed March 6, 2007.
 24. Beckwith, S.V.W. "The Hubble-JWST Transition: A Policy Synopsis Papers per year." SpaceRef.com, from Space Telescope Science Institute. URL: <http://www.spaceref.com/news/viewsr.html?pid=9910>. 2003.
 25. Office of Management and Budget, Executive Office of the President of the United States, "Budget of the United States Government, FY 2007," accessed March 15, 2007, <http://www.whitehouse.gov/omb/budget/fy2007/tables.html>.
 26. Office of Management and Budget, Executive Office of the President of the United States, "Budget of the United States Government, FY 2007," accessed March 15, 2007, <http://www.whitehouse.gov/omb/budget/fy2007/nasa.html>.
 27. Cameron, B.; Catanzaro, Sandro; and Crawley, Edward F. "Value Based Architecture Selection." IAC-06-D.3.1.3, 57th International Astronautical Conference, 2006.
 28. National Research Council. "Astronomy and Astrophysics in the New Millenium." National Academy Press, Washington D.C., 2001.
 29. National Research Council. "Connecting Quarks with the Cosmos." National Academy Press, Washington D.C., 2003.
 30. Lecture notes for Space Systems Engineering course (16.89). March 2, 2007, Massachusetts Institute of Technology.
 31. Stagney, D.B. and Massachusetts Institute of Technology Dept. of Aeronautics and Astronautics (2003). The Integrated Concurrent Enterprise.
 32. Lazio, J., Macdowall, R.J., Burns, J., Demaio, L., Jones, D.L., & Weiler, K.W., 2007, submitted to proceedings of the workshop Astrophysics Enabled by the Return to the Moon.
 33. Bussey, D. B. J., Spudis, P. D., and Robinson, M. S. "Illumination conditions at the lunar south pole." *Geophysical Research Letters*, Vol. 26, No. 9, pp. 1187-1190 (May 1999).
 34. Carilli, C. L., Hewitt, J. N., & Loeb, A., 2007, to appear in: "Astrophysics Enabled by the Return to the Moon," Cambridge University Press, ed. M. Livio.
 35. Wrobel, J.M and Walker, R.C. "Sensitivity". Synthesis Imaging in Radio Astronomy II. Taylor, Carilli, & Perley, eds. Astronomical Society of the Pacific Conference Series 180, 1998.
 36. Woan, G. 1996, Large Antennas in Radio Astronomy, 101.
 37. Wertz, J. R., and Larson, W. J., eds. *Space Mission Analysis and Design*, 3rd edition. Space Technology Library, 1999.
 38. Pala Manhas, Electrical Engineer, Broad Reach Engineering, Tempe (Arizona) Office, 2141 East Broadway Road #211, Tempe, AZ 85282, (480) 377-0400.

39. Smith, Terry, "Solar Imager Radio Array (SIRA) Command and Data Handling System", Presentation given at the Integrated Design Capability / Integrated Mission Design Center of NASA Goddard Space Flight Center, 25-28 August 2003.
40. Schmitz, Paul C., et al. "A Design of a Modular GPHS-Stirling Power System for a Lunar Habitation Module." NASA/TM—2005-213991, 2005, AIAA-2005-5716.
41. Lecture notes for Satellite Engineering course (16.851). Fall 2006, Massachusetts Institute of Technology.
42. Gal-Edd, J., Mooney, M., and Fatig, C. C. "L2-James Webb Space Telescope's Communication Challenges."
43. Isaacs, John C. "JWST Data Volume Analysis." Document JWST-STSci-000781, SM-12, released January 30, 2006.
44. "Spitzer Space Telescope." Lockheed Martin Corporation website. URL: <http://www.lockheedmartin.com/wms/findPage.do?dsp=fec&ci=14786&rsbci=0&fti=0&ti=0&sc=400>. Accessed 5-20-2007.
45. Hemmati, H., Wilson, K., Sue, M. K., Harcke, L. J., Wilhelm, M. Chen, C.-C., Lesh, J., Fera, Y., Rascoe, D., Lansing, F., and Layland, J.W. "Comparative Study of Optical and Radio-Frequency Communications Systems for a Deep-Space Mission." TDA Progress Report 42-128, February 15, 1997.
46. Marshalek, Robert G. "Laser Communication Requirements Drive Cost-Effective Solutions." Presentation given at the International Symposium on Advanced Radio Technologies, September 9, 1999.
47. "Antenna Factory Fiber Optic Cable." Antenna Systems and Solutions, Incorporated website. URL: <http://www.antennasystems.com/af-fiberopticcable.html>. Accessed 5-20-2007.
48. "Ultrahigh speed multi-gigabit wireless laser communication system with fully integrated high-speed microwave radio backup." MDA Technology website. URL: <http://www.mdatechnology.net/techsearch.asp?articleid=536>. Accessed 5-20-2007.
49. Abbott, J., Pixton, S., Roberts, C. J., and Reyhanoglu, M. "Lunar Interferometric Radio Array: L. I. R. A." Embry-Riddle Aeronautical University undergraduate team paper.
50. Geldzahler, B. "Deep Space Network Spectrum Management Issues." Presentation given to the NRC Committee on Radio Frequencies on May 14, 2003.
51. "Constellation Program: America's Fleet of Next-Generation Launch Vehicles – The Ares V Cargo Launch Vehicle." NASAfacts. URL: www.nasa.gov.
52. Lavoie, T. "Implementing the Vision – Lunar Architecture Overview", 2nd Space Exploration Conference, Houston, TX, Dec 2006.
53. Boeing, "Apollo 17 Lunar Roving Vehicle Technical Information", 1972. URL: http://www.history.nasa.gov/alsj/a17/A17_LunarRover2.pdf. Accessed 5-20-2007.
54. De Weck, O. Personal communication.
55. NASA MSFC Solicitation: Lunar Navigation and Communication Infrastructure (LNCI), URL: <http://www.spaceref.com/news/viewstr.html?pid=18894>. Accessed 5-20-2007.
56. Lecture notes for Satellite Engineering course (16.851). Fall 2006, Massachusetts Institute of Technology.
57. Larson, W. J., and Pranke, L. K., eds. *Human Spaceflight Mission Analysis and Design*, 1999.
58. Miller, D.W., "Adaptive Reconnaissance Golay-3 Optical Satellite."
59. R. L. Lucke, "Fundamentals of wide-field sparse-aperture imaging," in *Proc. 2001 IEEE*

- Aerospace Conf.*, vol. 3, pp. 1401–1419, Big Sky, MT (2001).
60. Kong, Edmund, *Optimal Trajectories and Orbit Design for Separated Spacecraft Interferometry*. Master's Thesis, Massachusetts Institute of Technology, 1998.
 61. Kaw, Autar K., *Mechanics of Composite Materials*, 2nd edition, Taylor & Francis, New York, 2006.
 62. Lester, Daniel F., Harold W. Yorke, and John C. Mather. "Does the lunar surface still offer value as a site for astronomical observatories?" *Space Policy* 20 (2004), pp. 99-107.
 63. Ross, R.G., Jr., and D.L. Johnson. "NASA's Advanced Cryocooler Technology Development Program (ACTDP)." *Advances in Cryogenic Engineering: Transactions of the Cryogenic Engineering Conference – CEC, Vol. 51*. American Institute of Physics, 2006.
 64. Glaister, D.S., W. Gully, et al. "Ball Aerospace 4-6 K Space Cryocooler." *Advances in Cryogenic Engineering: Transactions of the Cryogenic Engineering Conference – CEC, Vol. 51*. American Institute of Physics, 2006.
 65. Olson, J.R., M. Moore, et al. "Development of a Space-Type 4-Stage Pulse Tube Cryocooler for Very Low Temperature." *Advances in Cryogenic Engineering: Transactions of the Cryogenic Engineering Conference – CEC, Vol. 51*. American Institute of Physics, 2006.
 66. Durand, D., J. Raab, et al. "NGST Advanced Cryocooler Technology Development Program (ACTDP) Cooler System." *Advances in Cryogenic Engineering: Transactions of the Cryogenic Engineering Conference – CEC, Vol. 51*. American Institute of Physics, 2006.
 67. Arnold, James R. "Ice in the Lunar Polar Regions." *Journal of Geophysical Research*, Vol. 84, No. B10, September 10, 1979.
 68. Vasavada, Ashwin R. "Near-Surface Temperatures on Mercury and the Moon and the Stability of Polar Ice Deposits." *Icarus* 141, 179-193, 1999.
 69. Incropera, Frank P., DeWitt, David P., *Introduction to Heat Transfer 4th edition*, John Wiley & Sons, New York, 2002.
 70. "The ATHLETE Rover," Jet Propulsion Laboratory.
URL: <http://www-robotics.jpl.nasa.gov/systems/system.cfm?System=11>. Accessed 5-20-2007.
 71. Stubbs, Timothy J., Vondrak, Richard R., and Farrell, William M., "Impact of Dust on Lunar Exploration." URL:
<http://hefd.jsc.nasa.gov/files/StubbsImpactOnExploration.4075.pdf>. Accessed 5-20-2007.
 72. Johnson, Charles L., and Dietz, Kurtis L., "Effects of the lunar environment on optical telescopes and instruments," SPIE Vol. 1494 Space Astronomical Telescopes and Instruments, 1991.
 73. Hyatt, Mark, Greenberg, Paul, et. al, "Lunar and Martian Dust: Evaluation and Mitigation," AIAA Aerospace Sciences Meeting and Exhibit, 2007.
 74. Lee, A. Personal communication, 5-15-2007.
 75. Bell, Trudy E. "Lunar Dustbuster." April 19, 2006. URL:
http://science.nasa.gov/headlines/y2006/19apr_dustbuster.htm.
 76. Narula, B. Personal communication, 5-15-2007.
 77. Stiavelli, M. Personal communication.
 78. Bell, Trudy E. "Lunar Lawn Mower." November 9, 2005. URL:

- http://science.nasa.gov/headlines/y2005/09nov_lawnmower.htm.
79. Lecture notes for Satellite Engineering course (16.851). Fall 2006, Massachusetts Institute of Technology.
 80. Williams, D.R., "The Apollo Lunar Roving Vehicle," http://nssdc.gsfc.nasa.gov/planetary/lunar/apollo_lrv.html, 15 November 2005. Accessed on 5-2 2007.

Appendices

Appendix A: Contributors of new material by section

Section 1: Ryan Odegard, Phillip M. Cunio

Section 2: Ryan Odegard

Section 7: Mark Avnet, Chris Williams, Richard Jones, Jim Keller, Chris Tracy, Phillip M. Cunio, Zahra Khan

Section 8: Timothy Sutherland, Gautier Brunet, Jaime Ramirez, Bryan Gardner, Jeff Pasqual, Ryan Odegard, Phillip M. Cunio, Takuto Ishimatsu

Section 9: Mark Avnet, Justin Colson

Section 10: Phillip M. Cunio, Ryan Odegard

Section 11: Phillip M. Cunio, Ryan Odegard

Appendix B: An Analysis of Team Interactions (by Mark S. Avnet)

One of the unique aspects of the present study of two lunar telescope concepts is a meta-analysis on the interactions of the team itself. Over the course of the design study, each member of the LIRA/LIMIT design team completed a weekly survey logging their interactions (conversations, group discussions, and e-mails) with other team members. Based on these surveys, the team interactions during the preliminary and final design phases were analyzed.

B.1. Team Interactions in the Preliminary Design Phase

During the preliminary design phase, the team split into five subteams with the goal of downselecting to a few concepts. The subteams included one focused on Stakeholder Goals and Requirements (G), one whose purpose was the task of downselection (D), and three each analyzing one of the possible concepts considered – an IR interferometer (I), an IR segmented telescope (T), and RF dipoles (R). To retain anonymity, each member of each subteam is identified by a code consisting of the letter representing the subteam and a number between 1 and 3 assigned in no particular order.

The communications were coded by type and strength of interaction and were then organized in an N^2 diagram, shown in Figure B.1. A key is provided to show the meaning of each of the single-letter codes in the N^2 , and the weightings are provided on a 1-5 scale, which is represented by shading of the cells. The N^2 is similar to a design structure matrix (DSM) in that each cell represents the information obtained by the element in the corresponding row from the one in the corresponding column. Also, like a DSM, the matrix is partitioned, or ordered, in a meaningful way. Unlike a DSM, however, the rows and columns represent people rather than tasks, and the partitioning is done to group subteams rather than to represent chronological order. In a standard DSM, the goal of partitioning is to provide an order of tasks that minimizes interdependencies by reducing the number of marked cells above the diagonal [B1]. In the N^2 shown here, on the other hand, markings inside one of the boxes on the diagonal represent communication within a subteam, while markings outside the boxes (either above or below the diagonal) represent the passage of information from one subteam to another.

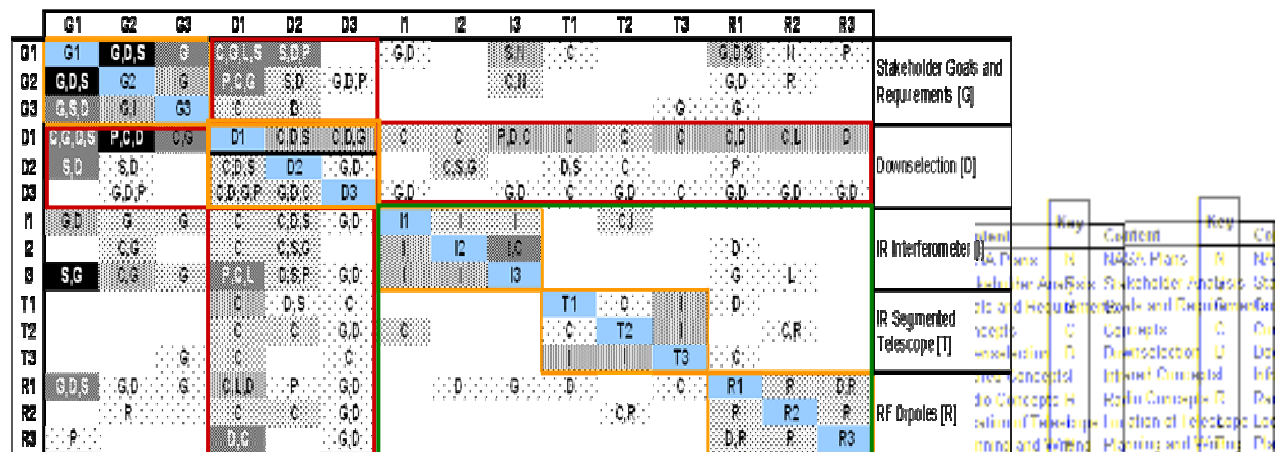


Figure B.1. N^2 representation of team interactions during the preliminary design phase. The figure demonstrates frequent communication internal to the Stakeholder Goals and Requirements subteam (upper left corner), strong interactions of the Downselection subteam with all other subteams (outlined in red), and the firewalling of the three concept subteams to ensure independence in developing each concept (outlined in green).

From the locations and weights of the interactions represented in the N^2 diagram, it can be seen that the strongest interactions within any given subteam occurred in Stakeholder Goals and Requirements. It was the Downselection team, however, that communicated most with all of the other subteams. This activity was important to the success of the downselection process, as this subteam needed to be aware of each of the three concepts under consideration, and it also needed to be able to relate those concepts to the results of the stakeholder analysis.

In addition, it can be seen that the intended firewalling of the concept subteams from one another (see Figure 22) was successfully implemented. The purpose of this firewalling was to ensure that the three concepts were developed independently. The sparseness of interactions between these three subteams demonstrates that the concepts were developed as intended – with little cross-fertilization between them.

B.2. Team Interactions in the Final Design Phase

In the final design, the LIRA/LIMIT team split into two separate teams to carry out the designs of the two lunar telescope concepts. In this appendix, the interactions of the team in Weeks 2 and 3 of the final design phase are presented. The results are organized in an N^2 format similar to that used for the preliminary design phase.

In the two N^2 diagrams shown in Figure B.2, the large box in the upper left of each represents the interactions within the LIMIT team, while the large box in the lower right represents interactions within the LIRA team (the small boxes at the upper left and lower right represent the Overall Systems Integrator and the Communications role, as their work cut across both teams). According to the figure, there were strong interactions within the LIRA team during both weeks, while the interactions within the LIMIT are relatively sparse, especially during Week 2. This, perhaps, can be attributed to the distinct design approaches taken for the respective telescope concepts. The LIRA team began defining the important relationships among parameters early in the final design process. Within a short amount of time, the team had developed a first-cut N^2 to represent the passing of parameters between subsystems and had begun to develop subsystem tools for an integrated model.

The LIMIT team, on the other hand, had to begin the process by completing the downselection between the two possible infrared concepts. Once the interferometer concept was selected, the team focused its effort on the modification of legacy systems for use on the lunar surface. Therefore, the low-level design interactions that occurred between subsystems for LIRA were not as necessary in the early stages of the design of LIMIT. As the design progressed from Week 2 to Week 3, however, the density of interactions increased as trades across subsystems became increasingly important. Although results of the survey data collected for Week 4 are not presented here, it is reasonable to posit that the interactions within the LIMIT team would appear denser during that week than in Week 3. The next step in the analysis, then, will be to use the survey data for Week 4 to determine if the prediction of a trend of increasing interaction density in the LIMIT team is supported.

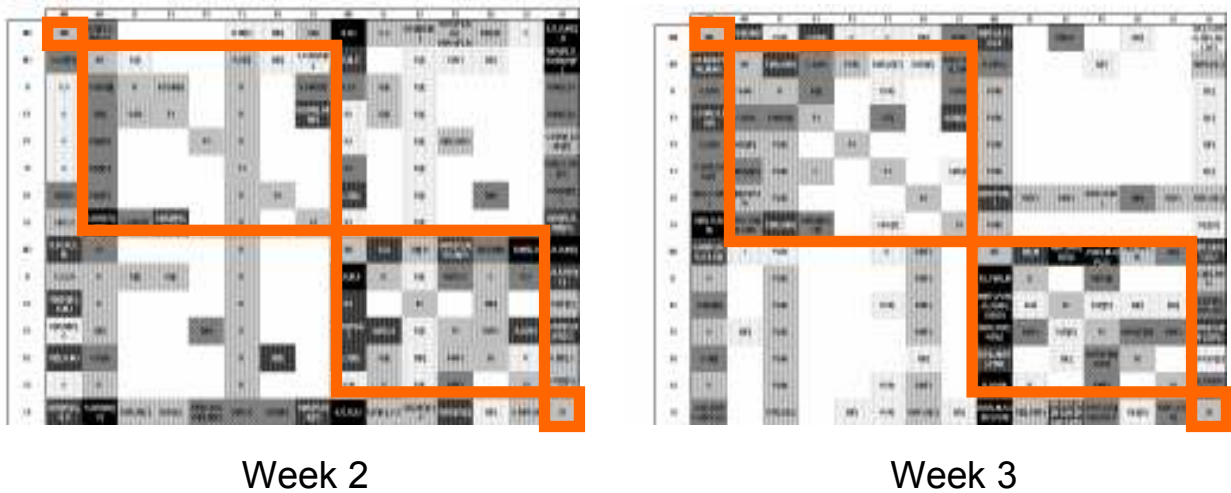


Figure B.2. N^2 representation of team interactions during Weeks 2 and 3 of the final design phase. According to these diagrams, the interactions within the LIRA team were frequent during both weeks, whereas the interactions within the LIMIT team were sparse in Week 2 and became somewhat denser during Week 3. (Note that the content codes in the cells are not discussed directly in this subsection, but the key containing the meanings of the codes used can be found in Table B.1.)

B.3. Future Work: Relating Team Interactions to the LIRA Design Outcome

Although the analysis of team interactions demonstrates some interesting phenomena regarding the work of the team, the real value of this analysis will come from relating the analysis to the technical design outcomes. Because the LIRA team organized its design through the use of an N^2 diagram of parameter relationships, the interactions of the LIRA team can be more readily analyzed in this way than can those of the LIMIT team.

To compare the parameter relationships to the LIRA team interactions, the first step was to examine only the LIRA interactions from the N^2 of Week 3 in Figure B.2. Although the team member in the role of Communications subsystem design performed this task for both the LIRA and LIMIT teams, that team member is considered to be part of the LIRA team for this purpose. The resulting LIRA-only N^2 diagram is shown on the left side of Figure B.3. Next, the relationships in the LIRA N^2 shown in Figure 26 were translated to a format equivalent to that of the team interaction N^2 , with the weighting of interactions determined by the number of parameters passed.¹ Although the parameters in Figure 26 flow in only one direction, the passing of a parameter from one subsystem to another often implies a two-way interaction between the two subsystems involved. Therefore, the translated parameter-based N^2 is constructed as a symmetric matrix. The resulting N^2 for LIRA is shown on the right side of Figure B.3.

¹ Presumably, some parameters are of greater importance than others and could be weighted differently here.

	M2	I2	E2	P2	D2	S2	C0
M2	M2	D[I],M	R(RF),M,D [E][D]	D(RF)[P] [V],P(RF), M,C(P),S	D[E], R(RF),M	D[V]	R(RF),M,D [C],S,I
I2	R,I,P(R), M	I2		D(RF)[E]			D[C][D],R, RF
E2	M(RF), P(R),R,I, R(RF),D [E][D]	R,M	E2	D(P)[E]	D[E]	D[V]	D(C)[P] E,I,R(RF), [E]
P2	R(RF), D(P), P(R),I	R(RF)	D(P)[E]	P2	D(RF)[P] [V]	R(RF)	D(RF)[C], R(RF), D[D],I
D2	D[D],I, M(RF), P(R)		D[E]	D(RF)[P] [V],R(RF)	D2		D(RF)[E] [C]
S2	R,I,P(R)	R		D(RF)		S2	D[C], R(RF),S, D[D]
C0	R(RF),M, S,I(RF),P IR	D[D], R(RF)	D[E][C] [P],R(RF), S[E][C]	D(RF)[C] [D],R(RF), P	D[C][E]	R(RF),S,D [E]	C0

	M2	I2	E2	P2	D2	S2	C0
M2	M2	D(RF)[E]	D(RF)[E], R(RF)[E]	D(RF)[P], R(RF)[P]	D(RF)[D], R(RF)[D]	D(RF)[S], R(RF)[S]	D(RF)[C], R(RF)[C]
I2	D(RF)[I]	I2	D(RF)[I] [C]	D(RF)[E] [P]	D(RF)[I]	D(RF)[E]	D(RF)[I] [C]
E2	D(RF)[E], R(RF)[E]	D(RF)[E] [C]	E2	D(RF)[E] [P]	D(RF)[E] [S]		D(RF)[E]
P2	D(RF)[P], R(RF)[P]	D(RF)[E] [P]	D(RF)[E] [P]	P2	D(RF)[P] [S]	D(RF)[P] [S]	D(RF)[C] [P],S
D2	D(RF)[D], R(RF)[D]	D(RF)[E] [S]	D(RF)[E] [S]	D(RF)[E] [S]	D2	D(RF)[S]	D(RF)[C] [S]
S2	D(RF)[S], R(RF)[S]	D(RF)[E]		D(RF)[P] [S]	D(RF)[S]	S2	D(RF)[C] [S]
C0	D(RF)[C], R(RF)[C]	D(RF)[E] [C]	D(RF)[E]	D(RF)[C] [P],S	D(RF)[C] [S]	D(RF)[C] [S]	C0

LIRA Team Interactions

LIRA N² of Design Parameters

Figure B.3. N² representation of LIRA team interactions during Week 3 of the final design phase (left) and technical parameter passing in the LIRA design (right). Comparisons of these matrices can lead to important insights regarding the relationship between communication among team members and the ultimate design outcome. The key containing the meanings of the codes used in the cells is shown in Table B.1.

Key			
O	Team Management Scheduling	(RF), (R)	<Type of Telescope>
S	Science Requirements (incl. Surveys)	[I]	Instrument
P	Comparison to Past Telescopes	[P]	Power
C	Concept Definition	[E]	Electronics
R	Telescope Relationships	[T]	Thermal
D	Design Issues	[D]	TDS
M	Model- and Tool-Building	[S]	Structures
I	Model Integration	[C]	Communications
\$	Cost	[V]	Environment

Table B.1. Key of content codes for interactions in Figures B.2 and B.3.

With a common format for the team interactions and parameter relationships established, it is then, in principle, possible to examine relationships between the two matrices. For example, statistical correlations and metrics of convergence can be calculated to understand the extent to which team interactions relate to the important design parameters. From this type of analysis, combined with a cell-by-cell content comparison of the two N² diagrams, it will be possible to provide the team with an understanding of the important relationships that were discussed among the team members, those that were not, and the issues that were discussed but that were not directly related to particular parameter relationships. This information, in turn, can be used to improve the team's process for future studies (or for refinement of the present study). This connection between team interactions and technical design outcomes is an important area of future work for the investigation of interactions in this and other design teams.

B1. Eppinger, S.D., D.E. Whitney, R.P. Smith, and D.A. Gebala. "A Model-Based Method for Organizing Tasks in Product Development." *Research in Engineering Design* 6(1): 1-13, 1994.